FACULTY OF SCIENCE, ENGINEERING AND COMPUTING

School of Pharmacy and Chemistry

Validation of novel HPLC methods to analyse metabolic reaction products catalysed by CYP450 enzymes and *in vitro* measurement of Drug-Drug Interactions

Submitted by

Amira HUSSAIN

This thesis is being submitted in partial fulfillment of the requirements of the university for the award of

Doctor of Philosophy

Kingston University London

May 2022

CONTENTS

ABSTRACT

Background: The inhibition of hepatic cytochrome P450 activity is one of the most significant mechanisms of a drug interaction which can result in a change in the pharmacokinetic behaviour of the drug. Severe adverse events have been associated with drug interactions caused during coadministration. COVID-19 infection has rapidly grown into a worldwide pandemic in 2020, and this has had a significant impact on human health. Dexamethasone, aspirin, ibuprofen, remdesivir, and omeprazole are some of the drugs being used in the treatment of COVID-19 during the pandemic.

Aim: This research aims to determine the inhibitory effects of aspirin, ibuprofen, remdesivir, and omeprazole on dexamethasone metabolism (CYP3A2 activity) and the effect of testosterone on Vitamin D metabolism (CYP2C11 activity) in rat liver microsomes using High-Performance Liquid chromatography.

Methods: A Dexamethasone and 6β-hydroxydexamethasone assay was developed and validated, and inhibition parameters were calculated using Lineweaver and Michaelis-Menten plots in Chapter 2. Using the previously developed HPLC assay, inhibition parameters were calculated using Lineweaver and Michaelis-Menten plots in Chapter 3. In chapter 4, a Vitamin D_3 and Vitamin D_2 and metabolites ($25(OH)D_3$ and $25(OH)D_2$) assay was developed and validated on HPLC using the isocratic mode of elution.

Results: The linearity ($r^2 > 0.99$), intra and interday precision (<15%), accuracy and recovery (80–120%), and stability study values of the newly developed methods for CYP3A2 and CYP2C11 substrates and metabolites were following International Conference on Harmonization (ICH) guidelines. Our inhibition study data showed that aspirin is a competitive inhibitor (weak) with the K_i = 95.46 ± 4.25 µM and IC_{50} = 190.92 ± 8.50 µM for the CYP3A2 assay. The results also showed that ibuprofen acts as a non-competitive inhibitor for CYP3A2 activity with K_i = 224.981 ± 1.854 µM and IC_{50} = 230.552 ± 2.020 µM although remdesivir showed a mixed inhibition pattern with a K_i = 22.504 ± 0.008 µM and IC_{50} = 45.007 ± 0.016 µM. Additionally, omeprazole uncompetitively inhibits dexamethasone metabolism by the CYP3A2 enzyme activity with a K_i = 39.175 ± 0.230 µM and IC_{50} = 78.351 ± 0.460 µM. Moreover, a study of inhibition parameters was not conducted due to the presence of interferences and extremely low concentrations of Vitamin D and metabolites.

Conclusion: The findings of this PhD research represent that there is a minimal risk of toxicity when dexamethasone is co-administrated with aspirin, ibuprofen, remdesivir, and omeprazole and a very low risk of toxicity and drug interaction with drugs that are a substrate for CYP3A2 in healthcare settings.

Keywords: cytochrome P450, dexamethasone, 6β-hydroxydexamethasone, types of inhibition, CYP3A2 activity, aspirin, ibuprofen, remdesivir, omeprazole, Vitamin D, testosterone

ACKNOWLEDGMENTS

This research project necessitated extensive dedication and determination and implementation of the project was not possible without the assistance of many people. Therefore, I would like to express my sincere gratitude to those who encouraged me throughout this journey.

The outcomes and research were not achievable without the support of my supervisors Prof. James Barker and Prof. Declan Naughton for their consistent support and academic guidance throughout the research project. I am thankful to have had the opportunity to develop my research skills and learn independently during my PhD project.

For technical assistance, I would also like to express my sincere appreciation to Dr. Siamak Soltani- Khankahdani for his help to encourage my practical skills and I would also like to thank Rizwan Meerali for continuous support throughout my PhD. Dr. Ian Beedham, thank you for your help and guidance.

I would also like to acknowledge my colleagues whom I cherish most for their support during the challenging and rewarding experiences of PhD: Sarah Fawaz, Carla Nassour, Sravani Emani, Chhayaben Patel, and Afshan Rafiq.

Finally, I would like to acknowledge my beloved family. Thank you, my beautiful daughter, Ayesha Shahid, and my amazing husband, Mohemmed Shahid who were always there when I was stressed over the last four years. Mohemmed Shahid, you have made this dream come true.

ABBREVIATIONS

ACE2	Angiotensin-converting enzyme 2
AML	Acute myeloid leukemia
APCI	Atmospheric pressure chemical ionization (APCI)
BzCl	Benzoyl chloride
NH_2	Amino
CAR	Constitutive androstane receptor
CDC	Center for disease control
CLD	Chronic liver disease
CL_{int}	Hepatic intrinsic clearance
COX-1	Cyclooxygenase-1
COX-2	Cyclooxygenase-2
COVID-19	Coronavirus
CYP450	Cytochrome P450
DDI	Drug-drug interaction
DMSO	Dimethyl sulfoxide
EDTA	Ethylenediaminetetraacetic acid
EMA	European medicines agency
EPH	Epoxide hydrolases
EPS	Extrapyramidal symptoms
FDA	Food and Drug Administration
FEL	Felodipine
GC	Gas chromatography
GSH	Glutathione
GST	Glutathione S-transferases
G6P	Glucose-6-phosphate
HPLC	High-Performance Liquid Chromatography
I	Concentration of inhibitor

IC_{50}	Inhibitor concentration required to inhibit 50% of the enzyme activity
ICH	International conference on harmonization
ICU	Intensive care unit
K_i	Inhibitory constant
K_m	Michaelis-Menten constant
LCMS	Liquid chromatography mass spectrometry
LOD	Limit of detection
LOQ	Limit of quantification
LPS	Lipopolysaccharide
MDZ	Midazolam
$MgCl_2$	Magnesium chloride
$NADP^+$	Nicotinamide adenine dinucleotide phosphate
NADPH	Nicotinamide adenine dinucleotide phosphate hydrogen
NAPA	*N*-acetylprocainamide
NAT	N-acetyltransferases
NIF	Nifedipine
NMO	NAD(P)H: menadione reductase
qNMR	Quantitative nuclear magnetic resonance
NQO	NAD(P)H: quinone oxidoreductase
NSAIDs	Nonsteroidal antiinflammatory drugs
OH	Hydroxyl
PA	Procainamide
PTAD	4-phenyl-1,2,4-triazoline-3,5-dione
PXR	Pregnane X receptor
RLMs	Rat liver microsomes
RNA	Ribonucleic acid
RSD	Relative standard deviation
S	Substrate

SNP	Single-nucleotide polymorphisms
SSRI	Selective-serotonin reuptake inhibitor
SULT	Sulfotransferases
TGA	Therapeutic goods administration of Australia
TSP	d_4-dimethylsilylpropionate
TST	Testosterone
UGT	Uridine 5'-diphospho-glucuronosyltransferase
V	Observed velocity
V_{max}	Maximum rate of the reaction

LIST OF FIGURES

LIST OF TABLES

CHAPTER 1

INTRODUCTION

1.1 Introduction to Cytochrome P450

Research on Cytochrome P450 began in the late 1950s and 1960s and the first report on the Cytochrome P450 (CYP) enzyme's existence was published in 1958 [1]. Formerly, it was thought that P-450 is a single cytochrome that could be detectable by spectrophotometry (450 nm) but when its hemoprotein nature was identified then it became known as Cytochrome P450 [1]. CYP is a superfamily of heme-containing enzymes accountable for the addition of molecular oxygen into inactivated C-H as well as C-C bonds. Fifty-seven genes that code for several CYP enzymes were also identified in humans [2]. In human tissues, CYPs are ubiquitous and are responsible for drugs as well as xenobiotic compound metabolism [2]. These CYPs are also essential for the peroxidative, oxidative, as well as reductive metabolism of a diverse group of compounds, such as bile acids, vitamins, fatty acids, prostaglandins, and leukotrienes.

There are plenty of substrates metabolised by CYPs and this is due to the abundance of P450 isoforms as well as to the broad substrate specificity of some CYP isoforms. CYP450 enzymes are present in all tissues with the exclusive existence of CYP450 in the liver [3]. CYP 450 is also found in the kidney, lungs, intestine, brain, heart, adrenal glands, skin, nasal, and tracheal mucosa.

Over 80% of marketed drugs are metabolised into relatively hydrophilic compounds by Cytochrome P450 enzymes in the liver which leads to their safe removal from the body [1]. CYP enzymes contain about 2% of the total microsomal protein in the human liver (0.3–0.6 nmol of total CYP per mg of microsomal protein). The content of the drug metabolising CYPs is much lower in other tissues as presented in Table 1 [4].

Table 1. The total content of CYPs in particular human organs tissues.

Tissue	CYP content (nmol/mg microsomal protein)
Liver	0.30–0.60
Small intestine	0.03–0.21
Adrenal	0.23–0.54
Testis	0.01
Kidney	0.03

Brain	0.10
Lung	0.01

Though 90% of drug oxidation appears to be associated with six main enzymes as CYP 3A4, 2D6, 1A2, 2E1, 2C9, and 2C19 [5], the most significant CYP450 enzymes are CYP2D6 and CYP3A4 (Figure 1). CYP3A4 is found in the liver and intestinal tissue. It also contributes to extrahepatic metabolism [5]. The human intestinal tissue helps in the absorption of nutrients, but it can also metabolise drugs.

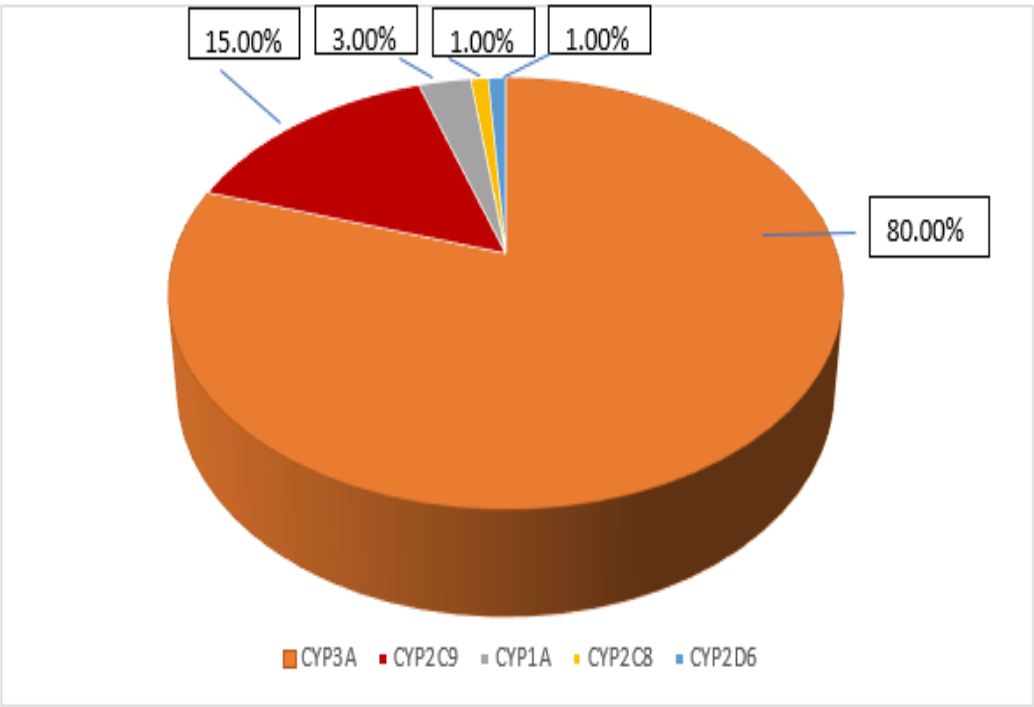

Figure 1. Occurrence of CYP450 enzymes (adapted from reference 5).

1.1.1 Classes

Almost in all living organisms, P450 enzymes are present in more than one form due to their diverse primary sequences, thus forming one of the biggest gene superfamilies depending on their identity of amino acid sequences [6]. The current Cytochrome P450 superfamily is believed to have been made by adaptive diversification and gene duplication. Moreover, the enzyme system is found in microsomes and comprises nonspecific NADPH-Cytochrome P450 oxidoreductase as well as some Cytochrome P450 isoforms. The

polymorphic CYP xenobiotic-metabolising enzymes can be primarily divided into two classes as well as the various local concentrations and sites of expression for the various P450 enzymes [6]. They are given a family number, such as CYP1, CYP2, as well as a subfamily letter such as CYP1A, CYP2D; then distinguished by a number for individual enzymes, such as CYP1A1, CYP2D6, etc.

Class I: Enzymes with 40 % identity of amino acid sequences or greater are categorised in the same family as CYP1, CYP2, and CYP3, which do not have significant functional polymorphisms, are well conserved and are active in drugs and procarcinogens xenobiotics metabolism [7]. The CYP3A4 family metabolises about two-thirds of all drugs as it is present in the human liver in the highest concentration and, it is also found in the gut wall where it might work as a primary defence mechanism [7], while CYP2D6 metabolises around one-quarter of all drugs, and other CYPs metabolise above one-tenth of all drugs.

Class II: The enzymes with 55 % amino acid sequence identity or greater are categorised in the same subfamily as CYP1A1, CYP1A2, etc. This nomenclature system is assigned based on the overall amino acid identity; in addition, alteration in a single amino acid may dramatically change the P450 substrate specificity [8],[1]. Thus, this classification system does not give information about P450 function, but the number of enzymes, as well as family, differs between different organisms.

1.1.2 Phases of CYP450

Drug metabolising enzymes such as CYPs play vital roles in the xenobiotics' metabolism, their elimination as well as their detoxification [9]. Generally, drug metabolising helps to protect the body against certain antibiotics as well as xenobiotics. Most of the tissues as well as organs in the body are well equipped with diverse and several drug metabolising enzymes to decrease the chances of possible injury triggered by these compounds. Drug metabolising enzymes comprise Phase I and Phase II enzymes and Phase III transporters, the later, after exposure to xenobiotics, are present in abundance, either inducible at higher levels or at the basal uninduced level [10].

Phase I: This includes mainly the CYP superfamily of microsomal enzymes found abundantly within the liver, lung, gastrointestinal tract, and the kidney, comprising enzyme families as well as subfamilies that are categorised based on identities of their amino acid sequence identities [11].

Above thirty-six gene families have been defined until now while twelve of them have a presence in all mammals and contain twenty-two subfamilies. Five CYP gene families in humans, for example, CYP1, CYP2, CYP3, CYP4, and CYP7 are supposed to play critical roles in the removal of drugs and xenobiotics as well as hepatic and extra-hepatic metabolism [12].

Phase II: The Phase II metabolising enzymes, contain many enzyme superfamilies comprising Uridine 5'-diphospho-glucuronosyltransferase (UGT) [13], sulfotransferases (SULT) [14], and NAD(P)H: menadione reductase (NMO) or NAD(P)H: quinone oxidoreductase (NQO) [15], glutathione S-transferases (GST), epoxide hydrolases (EPH), and N-acetyltransferases (NAT) [9]. Each Phase II drug-metabolising enzyme's superfamily contains gene families, as well as subfamilies, which encode the several isoforms with different specificity of substrates, developmental expression, and tissues, are inhibitory as well as inducible by xenobiotics [9]. Usually, conjugation by Phase II enzymes enhances hydrophilicity, and, thus excretion in the bile as well as urine. This, therefore, has a detoxification effect. While under some circumstances, conjugation by Phase II enzymes might produce activated metabolites as well as enhanced toxicity [16]. For instance, reactive electrophiles are usually conjugated by glutathione (GSH) catalysed by several GSTs, as well as when levels of GSH in the cells are decreased then they start forming reactive intermediates, therefore causing toxicological effects [17]. Also, the SULT, as well as UGT that are responsible for catalysing sulfation as well as glucuronidation, could play main roles in the conjugation, as well as eventual excretion and removal of xenobiotics and many drugs. These drugs comprise hydroxyl (OH) functional groups that may be formed after biotransformation by the Phase I enzymes (CYPs) or are present in the parent structure [14].

1.1.3 Mode of Action

Cytochrome P450's system comprises two functional classes, electron transfer as well as oxygenation. This system works with full catalytic competence and the consumption of reducing equivalents and O_2, produced stoichiometrically related hydroxy products [18] (Eq. 1).

$$RH + O_2 + H^+ + NADPH \rightarrow ROH + H_2O + NADP^+ \quad \text{Equation 1}$$

The basic reactions are spontaneous that produce the final product as metabolites (Figure 2).

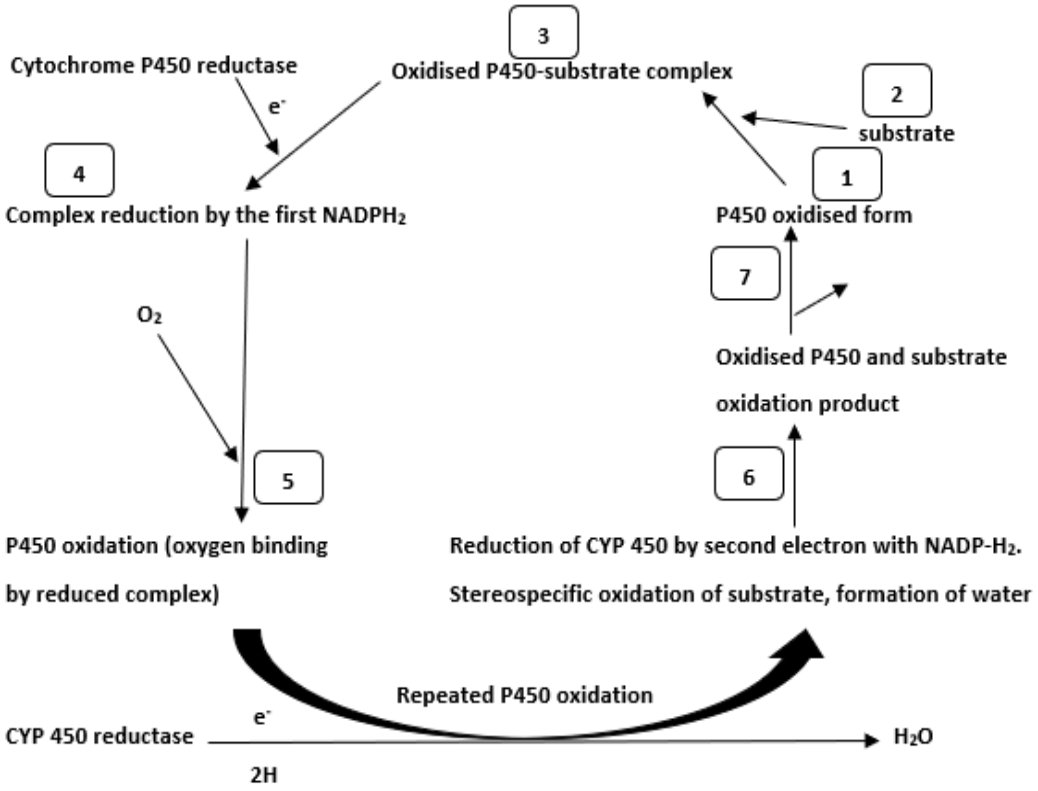

Figure 2. The common catalytic cycle of Cytochrome P450. (1) P450 oxidized form, (2) binds with substrate, (3) formation of P450-substrate-complex, (4) Further reduction with NADP-H_2 first electron, (5) oxygen molecules bind with reduced complexity and undergo oxidation, (6) NADP-H_2 second electron causes the oxidation of substrate and water molecules formation and (7) product (adapted from reference 18).

Briefly, the catalytic cycle of Cytochrome P450 is started by substrate binding, and usually, the reduction of heme iron occurs from the ferric to the ferrous state. Then, molecular oxygen temporarily binds at this site before being cleaved, transferring one oxygen atom

to the substrates R group, as well as the other oxygen atom to bind with two hydrogen atoms to form a water molecule [18].

1.1.4 Factors Affecting the Metabolism of Drugs

Some factors affect the metabolism of xenobiotic compounds such as hormonal changes in the body, disease states, sex, age, nutritional and dietary status, genetic and hereditary factors, and the activity of liver enzymes [19]. Environmental substances also influence liver enzymes activity such as foodstuffs, alcohol, medications, tobacco, and pollutants (household and atmosphere). The use of drugs as well as their distribution is related to gene polymorphisms that can either increase or decrease the individual enzymes' activities, with higher expression levels causing higher metabolic capacity, and that certain individuals are therefore called 'hyper' metabolisers [20]. Some environmental factors or xenobiotics are responsible for the induction of most of the drug-metabolising enzymes [21].

1.1.5 CYP Inhibition

When the particular CYP enzyme is impotent to effectively metabolise its substrate, because of interfering with another substance, the phenomenon is known as enzyme inhibition. Some substances (drugs) that inhibit the cytochrome action are known as enzyme inhibitors [20]. A phenomenon of enzyme inhibition is the direct effect on a specific enzyme e.g., naringin in grapefruit inhibits CYP3A4 [20]. Thus, inhibition is often a fast procedure and can commence as soon as adequate tissue concentration of inhibitor is attained. Several mechanisms are involved in the inhibition of metabolism such as competition as well as reversible binding to an enzyme (quinidine), enzyme destruction (vinyl chloride), inactive form of a complex with enzyme (macrolides), inhibition of enzyme molecule's synthesis of a particular isoform, or competing for the similar isoform.

Usually, P450-mediated reactions go along with simple Michaelis–Menten kinetics as shown in Figure 2. The Michaelis–Menten model is based on the fact that the enzyme has just one binding site for the particular substrate, as well as that the reaction velocity has a saturating hyperbolic profile. The maximum velocity of the reaction is usually called V_{max}. The amount of substrate required for a 50% optimal reaction between enzyme and substrate is called K_m [19]. In drug interaction studies, IC_{50} and K_i are used to measure the

potency of the inhibitor. Determination of IC_{50} is achieved at constant substrate concentration over various inhibitor concentrations [22]. K_i is the affinity constant of an inhibitor to the enzyme or the enzyme-substrate complex. The K_i is usually determined from *in vitro* experiments and units of expression are micromoles (µmol). The binding between enzyme and inhibitor is tight, if the value of K_i obtained is smaller, however, the large value of K_i represents strong binding between enzyme and inhibitor [22]. K_i is the same as IC_{50} value in the case of non-competitive inhibition, while the K_i is half of the IC_{50} value in the case of competitive and uncompetitive inhibition.

The categories of inhibitors are strong, moderate, or weak, dependent upon their influence on the substrate. Strong inhibitors cause more than 80% reduction in substrate clearance such as gemfibrozil (2C8), quinidine and fluoxetine (2D6), fluconazole (2C9), fluvoxamine and ciprofloxacin (1A2), and indinavir, ritonavir, and ketoconazole (3A4, 3A5, and 3A7) [19]. Moderate inhibitors cause a 50-80% reduction in substrate clearance e.g., trimethoprim (2C8), duloxetine, sertraline and terbinafine (all 2D6), amiodarone (2C9), erythromycin, fluconazole, verapamil, and diltiazem (all 3A4, 3A5, and 3A7) [19]. Weak inhibitors cause a 20-50% reduction in clearance. Cimetidine is a weak inhibitor at 1A2 (caffeine and theophylline), 3A4 (calcium channel blockers and benzodiazepines), and 2D6 (tricyclic antidepressants). Amiodarone is also a weak inhibitor at 2D6 [19].

1.1.5.1 The Usefulness of Lineweaver Burk Plot and Michaelis-Menten Plot

When compared to other models describing the energy of *in vitro* drug metabolism studies, the Michaelis-Menten technique stands out due to its fast response rate (V) to substrate fixation ([S]) as a result of the Michaelis steady-state (K_m) and the greatest response rate (V_{max}). On the other hand, there are two advantages of the Lineweaver-Burk plot over the Michaelis-Menten plot: it gives a more accurate estimation of V_{max} and more specific information regarding impediments (Figure 3). The accuracy of the measurements rises by linearising the information [23].

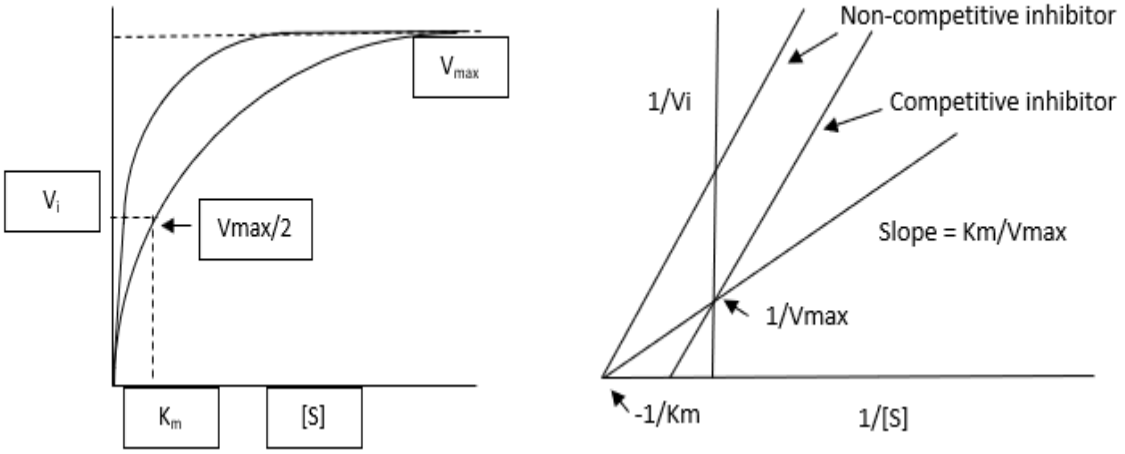

Figure 3. Michaelis–Menten (left) and Lineweaver–Burk (right) plots. The Michaelis–Menten equation defines the velocity of the reaction between substrate and enzyme. The addition of more substrate increases the reaction velocity until it reaches V_{max}. The amount of substrate that provides 50% reaction velocity is called K_m. The Lineweaver-Burk (double reciprocal plot) is used to quantify the unique potency of an inhibitor, where 1/V is plotted against 1/[S]. On the x-axis, the intercept is equal to $-1/K_m$ (adapted from reference 23).

1.1.5.2 Types of Inhibition

There are three main types of inhibition e.g., competitive, non-competitive, and uncompetitive.

(i) Competitive Inhibition

In competitive inhibition, substrate and inhibitor compete to bind to the same position on the enzyme active site [24]. In the case of competitive inhibition K_m increases and V_{max} remain unaffected (slope change, Y-intercept same) (Figure 4). As a result, it is frequently stated that competitive inhibition can be overcome by increasing substrate concentration which results in an increase in the apparent K_i value [25].

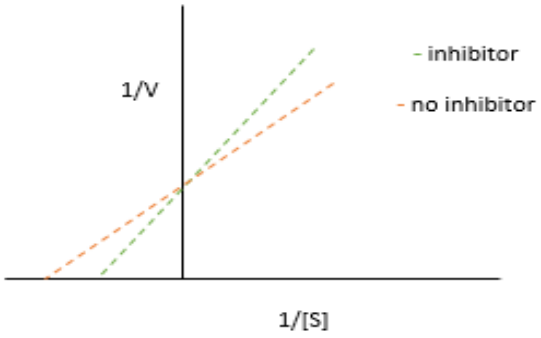

Figure 4. Lineweaver–Burk Plot represents competitive inhibition.

(ii) Non-competitive Inhibition

In non-competitive inhibition, the inhibitor binds equally well to the enzyme-substrate complex and free enzyme. The binding occurs entirely at a different site from the active site taken by the substrate. Figure 5 provides some illustrations of the more common non-competitive binding events. In the case of non-competitive inhibition, K_m remains unaffected, and V_{max} is reduced (slope change, Y-intercept change). The K_i of the non-competitive inhibitor does not change as a function of the concentration of substrate [25].

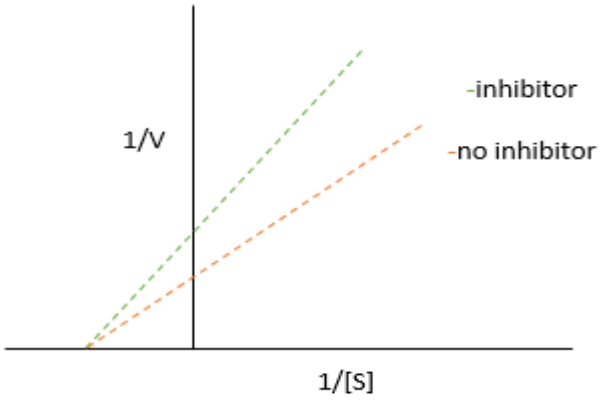

Figure 5. Lineweaver–Burk Plot represents non-competitive inhibition.

In some instances, an inhibitor may have an unequal affinity for both enzyme-substrate complex and free enzymes. This type of inhibition is called mixed inhibition (a mixture of non-competitive and competitive.

(iii) Uncompetitive Inhibition

In uncompetitive inhibition, the inhibitor binds completely to the enzyme-substrate complex resulting in an inactive enzyme-substrate-inhibitor complex. The V_{max} and a K_m both reduced in uncompetitive inhibition (slope same, Y-intercept change) (Figure 6). Uncompetitive inhibition is a rare phenomenon in drug discovery programmes, but these inhibitors could have dramatic physiological concerns. Uncompetitive inhibitor results in an increase in local substrate concentration as the inhibitor reduce the enzyme activity. There is no well-known mechanism to clear out the excessive substrate [25].

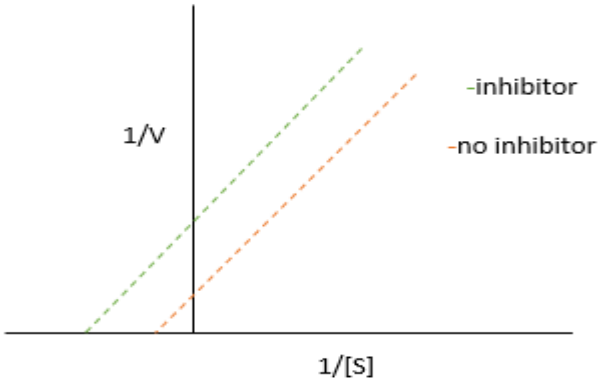

Figure 6. Lineweaver–Burk Plot represents uncompetitive inhibition.

Clinically, the importance of an inhibition interaction is determined by the relative concentration of the drug. Moreover, drugs could bind by the heme-binding site reversibly or irreversibly and this inhibits the other drugs from binding to them [24].

Some drugs undertake metabolic activation using the CYP450 system and, as a result, the stable complexes formed by CYP 450 could be generated using the metabolites, therefore the cytochrome is retained in an inactive state [26]. As it is a comparatively long duration process, there could be significant clinical importance to this interaction, but in the case of narrow-based therapeutic drugs, the chance of toxicity increases. Typically, the first dose of inhibitor is sufficient to start enzyme inhibition and when the inhibitor gets to a steady-state, the maximum inhibition is found as well. When the inhibited drug gets to a steady state at its new, longer half-life, the maximum inhibited drug concentration occurs. Also,

the time required for the interaction to resolve similarly depends on the involved drugs' half-lives (Figure 7) [26].

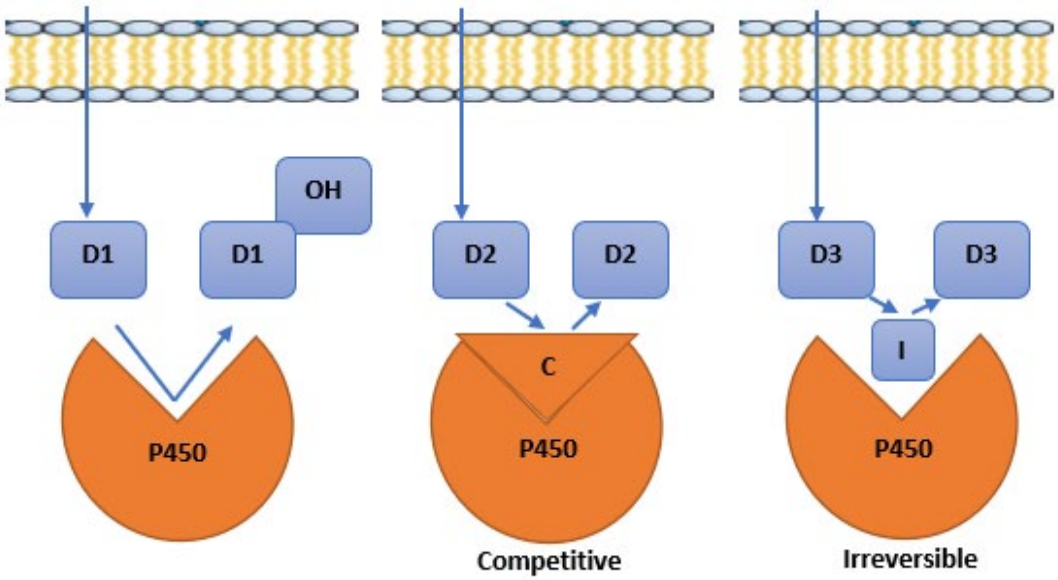

Figure 7. Diagrammatic illustration of inhibition of metabolism by P450 enzyme. D1: Drug entering nucleus, D2: P450 enzyme inhibited by a competitor drug, D3: Irreversible inhibitor drug, OH: Hydroxylation of the drug by P450 (adapted from reference 26).

1.1.6 CYP Induction

A particular CYP450 isoform is stimulated by an exogenous compound (drug) in a process called enzyme induction, and the numbers of molecules of drug-metabolising enzymes increase by gene mediation [4]. An inducer (drug) is a chemical substance that stimulates the enzyme. This complex phenomenon is related to the dose that is needed by the inducer to reach a critical concentration so that it can bind as well as activate the transcription factors at an intranuclear receptor, and then production of the protein increases by the up-regulation of messenger ribonucleic acid (RNA) [26]. The process of induction is relatively slow and could initiate after 3-4 days of an inducer exposure. Mostly, it typically occurs after 7-10 days and needs an equal or longer time to disintegrate when the inducer is stopped. The induction can take place when the co-administrated drugs' biotransformation is stimulated by a drug. This might happen via the same enzyme pathway or by another pathway. The two main concerns with CYP450 induction are: a decrease in the therapeutic effectiveness of co-medications such as the drug elimination would be increased for drugs

whose effect is created mainly by the parent drug and consequently lower the concentration of drug as well as reduce the pharmacological effect the drug. Moreover, induction might create a detrimental imbalance among detoxification as well as activation as an effect of enhanced reactive metabolites formation, leading to the risk of metabolite-related toxicity as well as potential drug-drug interactions [27].

Particular inducers are typically present for a specified CYP450 family, but occasionally a drug could induce its biotransformation and the induction effects could be seen in the first two days of treatment. The new enzyme synthesis commonly takes more than one week. Additionally, the inducers plasma concentration, the half-life of enzyme production as well as degradation are associated with the time progression of enzyme induction onset as well as an offset (Figure 8).

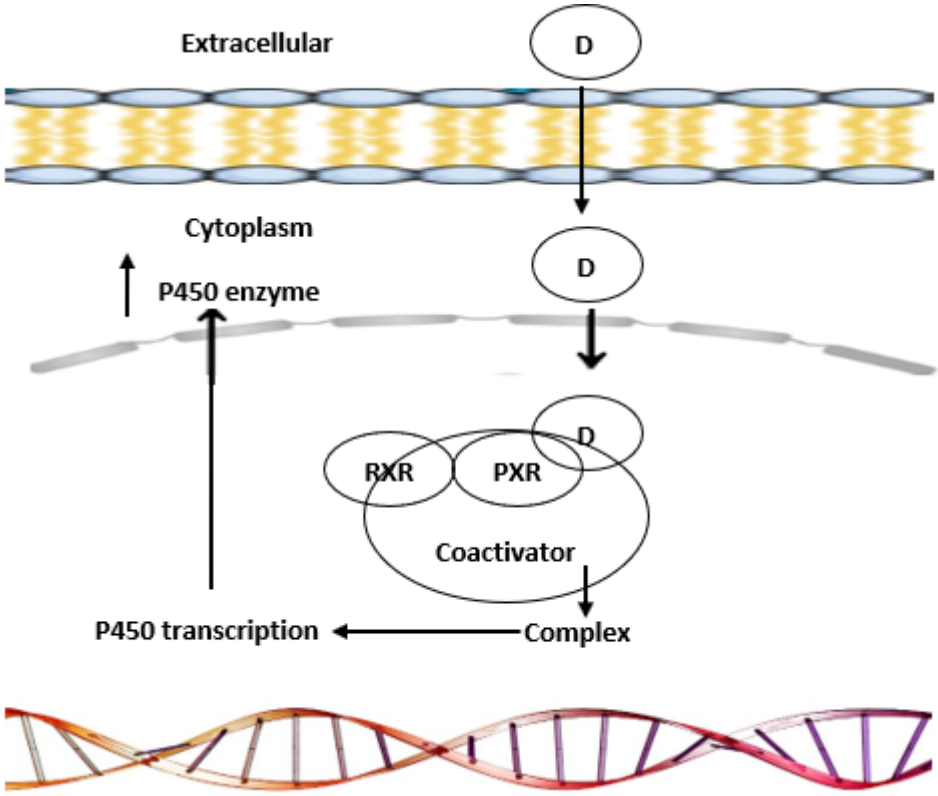

Figure 8. Diagram illustrating induction of CYP 450. D: Drug, PXR: Pregnane X Receptor, RXR: Retinoid X Receptor (adapted from reference 26).

Inducers are categorised on the basis of the percentage decrease in plasma area under curve (AUC) values of substrate drug. Strong inducers cause an 80% or more reduction in AUC of substrate e.g., rifampin, carbamazepine, phenytoin, and St. John's Wort (CYP3A4), while moderate inducers cause a 50% to 80% reduction in AUC of the substrate as well as

contain nevirapine, phenobarbitone, and efavirenz [26]. Weak inducers cause a 20% to 50% reduction in AUC substrate. However, interactions based on induction can lead to important manifestations, for example, estrogen metabolism induction could lead to a diminishment of the contraceptive effect as well as sudden pregnancy [28]. Also, therapeutic failure by digitoxin as well as digoxin is well-known. Moreover, the patients on enzyme inducer medication may show therapy failure to antimicrobial agents like doxycycline or metronidazole recommended for some infections. Thrombosis occurs due to the loss of warfarin anticoagulant effect, but when the induction decreases, failure to identify the requirement to decrease the warfarin dose might lead to bleeding. However, CYPs also show interaction with food and other substances e.g., CYP1A2 is identified to be induced through smoking [24].

1.1.7 Inducers and Inhibitors of Cytochrome 450

Table 2 presents data on inducers and inhibitors of the most important CYP enzymes responsible for xenobiotic metabolism. This table doesn't contain all the possible inducers and inhibitors of CYP enzymes due to the enormous literature available [29].

Table 2. Inducers and inhibitors of CYPs (adapted from reference 29).

CYP3A4/5 enzyme inhibitors		
Xenobiotic compounds	**Mode of inhibition**	**CYP selectivity (inhibition of other CYPs)**
Ketoconazole	Competitive	Moderate (2D6, 2C and 1A2)
Nelfinavir	Competitive	Moderate (2D6)
Ceritinib	Mechanism-based	Moderate (2C9)
Ciprofloxacin (CYP1A2 inhibitor)	Competitive	High
CYP2C8 enzyme inhibitors		
Dabrafenib	Competitive	Poor (3A4, 2C19, 2C9)

Trimethoprim	Competitive	High
Montelukast	Competitive	Moderate (CYP3A4 and 2C9)
CYP2C19 enzyme inhibitors		
Loratadine	Competitive	Poor (2E1, 3A4, 2D6)
Modafinil	Competitive	High
CYP2B6 enzyme inhibitors		
Sertraline (*in vivo*)	Competitive	Moderate
Clopidogrel (pro-drug)	Mechanism-based	Moderate (2C9, 2C19)
Voriconazole	Competitive	Poor (2C19, 3A and 2C9,)
CYP2D6 enzyme inhibitors		
Quinidine	Competitive	High
Stiripentol	Competitive	Poor
Bupropion	Competitive	High
Mirabegron *in vivo*	Mechanism-based	Moderate (CYP3A4)
CYP2E1 enzyme inhibitors		
Clomethiazole	Mechanism-based	Moderate (2A6)
4-Methylpyrazole	Competitive	High
CYP2C9 enzyme inhibitors		
Sulphaphenazole	Competitive	High
Vemurafenib	Competitive	Poor (1A2, 3A4)
Amiodarone	Non-competitive	Poor (3A4,2D6)
human cytochrome P450 enzymes inducer		
Drugs	**Receptor(s) implicated**	**Enzymes**

Rifampicin	PXR (pregnane X receptor)	CYP1A2
Carbamazepine	CAR (constitutive androstane receptor)/PXR	CYP2A6
Rifampicin	PXR	CYP2B6
Flucloxacillin	PXR	CYP2C8
Rifampicin	PXR	CYP2C9
Ritonavir (with lopinavir or tipranivir)	PXR	CYP2C19
Rifabutin	PXR	CYP3A4
Metamizole	Unknown	CYP3A4
Mitotane	PXR	CYP3A4
Carbamazepine	CAR/PXR	CYP3A7 and CYP3A43

1.2 Drug-Drug Interactions

Cytochrome P450s, as well as non-CYP450 enzyme systems, are incorporated in the xenobiotic metabolism as well as homeostasis. Ten isoforms of CYP450 are recognised to be included in the metabolism of the drug, specifically CYP1A1, CYP1A2, CYP2B6, CYP2E1, CYP2C8, CYP2C9, CYP2C19, CYP2D6, CYP3A4, and CYP3A5 [30]. CYP450s are involved in the metabolism of Phase I as well as UDP- glucuronosyltransferases (UGTs) which are involved in the metabolism of Phase II and catalyse many metabolic reactions. That might lead to drug-drug interactions, hepatotoxicity, formation of reactive metabolite (RM) as well as associated drug withdrawals [31].

A Drug-Drug Interaction (DDI) takes place when the pharmacologic effect of a specified drug is changed by another drug action which leads to unpredictable clinical outcomes. Moreover, this might decrease the effectiveness of the drug, cause unpredicted harmful side effects, or delay the absorption of the drug [32]. The co-administration of multiple medications (polypharmacy) usually increased the risk of DDIs. In the United States, a

report from the Center for Disease Control (CDC) mentioned that the percentage of the patient population using three or more prescribed drugs became higher from 11.8% in 1988–1994 to 20.8% in 2007–2010. Also, the number of people percentage using five or more medications has enhanced from 4.0% to 10.1% in the same era [33]. Thus, the risk of drug-drug interaction might increase with each novel drug added to an individual's system. Because of the common use of multiple drugs by people, the DDI is turning into a serious clinical safety matter. DDIs are the reason for more than 30% of entire adverse drug actions [34]. There is an annual increase in the costs of DDI-associated health care. Some drugs (e.g., astemizole, cisapride, as well as terfenadine) were withdrawn from the market because of late DDIs identification [34]. So, DDIs detection is important to drug regulatory agencies, the pharmaceutical industry, healthcare professionals as well as patients.

Drug interactions are also termed as either pharmacokinetic or pharmacodynamic. Pharmacodynamic drug interactions take place when drugs act at the same receptors, causing synergistic, additive, or antagonistic outcomes. Pharmacokinetic drug interactions define how one drug can affect the absorption, delivery, metabolism, or defecation of another drug [35]. Antidepressant drugs are mainly metabolised by the hepatic CYP450 enzymes. When this drug is used with strong inducers or inhibitors of CYP450, they act as a possible target for pharmacokinetic drug interactions.

1.2.1 Some Examples of Drug-drug Interactions

Fluoxetine (antidepressant), as well as its major metabolite norfluoxetine, are very strong inhibitors of CYP2D6 while moderate inhibitors of CYP2C9 and CYP3A4, however, sertraline causes dose-dependent CYP2D6 inhibition (at least 150 mg daily) [36]. Duloxetine is a moderate inhibitor of CYP2D6, and paroxetine is a very strong inhibitor of CYP2D6 while fluvoxamine is a strong CYP2C19 as well CYP1A2 inhibitor [37].

Recently, three antidepressants have come into the drug market in the US. The Food and Drug Administration (FDA) approved a drug in 2011 called vilazodone as the primary selective-serotonin reuptake inhibitor (SSRI) by serotonin (5HT)-1A partial agonist (Croft *et al.,* 2014). CYP3A4 is responsible for the primary metabolism of vilazodone, with minor metabolism by CYP2D6 as well as CYP2C19 [38]. Ketoconazole increases the concentration

of vilazodone by up to 50%. Consequently, the daily vilazodone dosage might need to be decreased when taken concomitantly with strong inhibitors of CYP3A4 such as ketoconazole [38], though dosage reduction is not required if patients are taking a short course of ketoconazole or erythromycin. A recent study of steady-state carbamazepine along with vilazodone 40 mg daily caused a reduction in exposure of vilazodone by up to 45% [38], but the choice to increase the vilazodone dosage must be patient-specific as well as depends on the patient's depressive signs.

FDA approved levomilnacipran in 2013 as a selective norepinephrine reuptake inhibitor by potent norepinephrine reuptake inhibition [39]. The CYP3A4 isoenzyme is responsible for the primary metabolism of levomilnacipran. Levomilnacipran interactions have been observed through *in vitro* studies with strong inhibitors of CYP3A4, e.g., ketoconazole, ritonavir, and clarithromycin. A substantial increase in the concentration of levomilnacipran has been observed in a recent *in vivo* study once co-administered with ketoconazole [39]. But the study did not demonstrate a major decrease in the concentration of levomilnacipran when co-administered with the strong inducer of CYP3A4 carbamazepine ketoconazole [39]. Because of the limited evidence, the manufacturer recommended the usage of a lower levomilnacipran dose with strong inhibitors of CYP3A4, especially 80 mg every day or less [39]. Levomilnacipran toxicity symptoms, comprising tachycardia, as well as hypertension, may be observed [39]. While there is no supportive evidence, levomilnacipran use with strong inducers of CYP3A4 requires closer checking for satisfactory management of depressive signs at the current dose [39].

The most commonly worldwide prescribed pharmaceutical drugs are nonsteroidal anti-inflammatory drugs (NSAIDs) and have extensive clinical value for fever, pain, inflammation as well as inflammatory disease management [40].

Lee and co-workers have studied the inhibitory effects on Cyclooxygenase-2 (COX-2) after administration of Nonsteroidal anti-inflammatory drugs (NSAIDs) using a lipopolysaccharide (LPS)-derived COX-2 induction model in samples of whole blood, in accordance with COX-2 single-nucleotide polymorphisms (SNPs) genotypes. COX is the key pharmacodynamic target of NSAIDs. In pharmacokinetic parameters' analysis, there was no significant difference observed in drug exposure for each SNP genotype while the

pharmacodynamic study showed that after a single oral dose of 200 mg celecoxib, the maximum influence of COX-2 inhibition was attained at 2.0 hours for all COX-2 SNPs genotypes. The inhibitory effects of celecoxib on COX-2 induction were changed in accordance with the COX-2 SNPs genotype and rs689466 is accountable for the inconsistency in response to celecoxib, thus proposing that in terms of COX-2 inhibition, an individual with the GG rs689466 genotype would be more responsive to celecoxib [40].

Warfarin is found to be generally co-prescribed with antibiotics such as ciprofloxacin, amoxicillin, clarithromycin, nevirapine, cotrimoxazole, norfloxacin, cloxacillin, erythromycin, metronidazole, cephalosporins, rifampin, ceftriaxone as well as isoniazid. One study in Norway revealed that drugs such as antibacterial, heparin, and NSAIDs were commonly interacting with other drugs [41]. In a similar retrospective cohort analysis, oral antibiotics such as Trimethoprim/sulphamethoxazole, azithromycin, and levofloxacin, were detected to increase the over anticoagulation degree and incidence [42]. Most antibiotics excluding rifampicin are liver enzyme inhibitors, thus their interaction with warfarin might cause over anticoagulation.

NSAIDs and corticosteroids were the other categories of drugs that have shown interactions with warfarin. To analyse the drug interaction severity, practitioners need to understand that a major form of interaction could produce negative consequences which consist of either over anticoagulation and bleeding risk or ineffectiveness.

Teklay and colleagues performed an analysis on the patients on warfarin therapy and checked interactions with each concurrent drug. They found that around 49.2% of patients had at least the main type of DDIs although 50.8% had modest DDIs. They also observed that drug-drug interactions were dominant. Generally, co-prescribed medications interacting with warfarin were anticoagulants, NSAIDs, diuretics as well as antibiotics [43]. They also found that bleeding difficulties were considerably related to increased INR value. Therefore, clinicians must consider possible drug interaction when prescribing drugs for patients with warfarin and regular monitoring of INR value is necessary to predict outcomes of treatment of patients on warfarin [43]. Patients must also be advised about drug interactions and bleeding complication symptoms related to warfarin.

Goswami and his coworkers designed a randomised, multiple-dose, open-label, parallel trial to assess the pharmacodynamic drug-drug interaction of lisinopril and concurrently administered diclofenac sodium. They performed this trial on osteoarthritic patients, non-diabetic and diabetic, and mild to moderate hypertensive. Patients were placed on a two-week washout period and this time is randomly given either 10 mg of lisinopril and 100 mg of diclofenac sodium treatments in combination or only 10 mg lisinopril for 8–12 weeks in patients with unhealthy states of osteoarthritis and hypertension with or without type 2 diabetes mellitus [44]. They found that the antihypertensive efficiency, as well as sensitivity of insulin in improving lisinopril action along with the renal function, may get poorer in hypertensive osteoarthritic patients getting parallel oral diclofenac sodium treatment with lisinopril. Furthermore, close monitoring of serum electrolytes is also recommended to rule out any long-term negative effects [44].

In the past 2 eras, statin utilisation has been increased much for their cholesterol-lowering as well as pleiotropic effects. After their increased use, arguments arose about their recommendation patterns because of some safety issues [45]. Usually, the side effects of statins comprise myalgia, dyspepsia, constipation, flatulence, elevated transaminase levels, generalised gastrointestinal discomfort, sleep disorders, headache, and central nervous system disorders [46]. The key safety issue associated with the statin's utilisation is the side effects related to the muscle that has variable intensity. Myalgia and limb weakness are comparatively common among statin users [47]. In observational factual research, the rate of myopathies is up to 10% [47]. The most serious statin-induced muscle condition is known as rhabdomyolysis, but it has a rare frequency (0.1-0.6%) [48]. The risk factors related to statin-induced myopathy consist of a history of muscle indications or increases in creatine kinase (CK), female sex, renal, hypothyroidism, older age, and hepatic insufficiency, excessive alcohol consumption, diabetes, and concomitant drug use that enhanced the serum concentration of statins [49]. Most statins are metabolised by CYP3A4 [50]. Their bioavailability increased when they are co-administrated with drugs that are either CYP3A4 inhibitors or substrates by inhibiting the hepatic first-pass metabolism [51]. In a study commenced in the United Kingdom, the concomitant treatment with CYP3A4 inhibitors or substrates was found in patients (up to 30%) recommended with CYP3A4 metabolised statins [52].

Bucsa and colleagues performed a study to determine the incidence of statins' potential DDIs in all hospitalised patients who had been given statins before or during hospitalisation. They also determined the frequency of muscle-related side effects. Consequently, they found statin-related DDIs in 27.5 % of patients (35 patients), most of which were under treatment before admittance [53]. The outcomes were moderate in 20 patients as well as major in 15 patients and of the total number of potential DDIs, 24 were affecting the muscular system [53]. Two drugs fenofibrate and amiodarone were found to be most often involved in the potential DDIs of statins. Therefore, the incidence of statins' potential DDIs was high, mostly in the therapy before admittance, while only a small number of potential DDIs caused clinical outcomes [53].

The most abundant P450 enzyme in humans is CYP3A4, and it metabolises a diverse range of structurally different therapeutic agents; therefore, it is the main target for several DDI. Recently, a report by Food and Drug Administration has revealed testosterone to be the most frequently utilised *in vitro* CYP3A4 analysis (50% of reported research) as compared to midazolam (15–20% of approximations of CYP3A4 activity *in vitro*) [53] while felodipine, nifedipine, as well as erythromycin were utilised in less than 10% of research studies [54]. Thus, CYP3A4 plays an active role in the metabolism of testosterone generating 6b-hydroxylation in humans.

There are diverse substrate subgroups for CYP3A4 based on relationship and cluster analysis of inhibition data of CYP3A4 for a variety of modifiers [55]. This was shown by others as well as further studied in a number of comprehensive mechanistic kinetic studies [55]which specified the presence of different and special binding domains for individual substrate subgroups, i.e., testosterone, midazolam, and nifedipine. Because of the substrate-specific response noticed for CYP3A4, the suggested method for a CYP3A4 DDI study is the usage of multiprobes where the lowest inhibition constant (K_i) attained shows the "worst-case scenario" for a possible interaction [55]. However, an unsuitable probe substrate selection might lead to a false positive or negative estimate of a DDI.

Galetin and coworkers have performed a set of *in vitro* interaction analyses in human lymphoblast expressed CYP3A4 including two CYP3A4 subclasses agents, testosterone (TST) as well as midazolam (MDZ); a specific subgroup, nifedipine (NIF); as well as its

structural analog, felodipine (FEL). They provided the mechanism of interaction of each substrates pair by using a variety of multisite kinetic models, mostly belonging to subtypes of a generic two-site model; however, a three-site model was necessary for TST interactions. Inhibition profiles complexity as well as the kinetic model selection with suitable interaction factors was contingent on the involved substrates kinetics such as hyperbolic substrate inhibition, or sigmoidal for NIF, TST and MDZ/FEL, correspondingly [55]. Simple reciprocity was not seen among substrates pairs. Several uncommon inhibition features were included in the observed interaction profiles between TST, NIF, MDZ, and FEL, also the pathway-differential properties reflecting an 80-fold variance in K_i values as well as a δ factor (describe the binding affinity alteration in a modifier presence) going from 0.04 to 2.3 [55]. They concluded that the performed multisite kinetic study supports the hypothesis of different binding domains for every substrate subgroup. Moreover, inter-substrate interactions analysis strongly specifies the presence of a mutual binding domain shared with each of the three subclasses of CYP3A4 substrate [55].

1.2.2 Psychotropic Drug Interactions

Antipsychotics are used to treat several psychiatric disorders and are usually performed by monotherapy or augmentation therapy in clinical settings. As a result, antipsychotics with concomitant therapy could result in pharmacokinetic interactions that cause adverse reactions. The metabolic clearance rate of most antipsychotic drugs is very low because of their lipophilicity, substantial volume of distribution, and extensive protein binding [56].

Phenothiazines which are first-generation antipsychotics undergo biotransformation mainly by CYP2D6 and from CYP3A4 and CYP1A2 with minor roles [56]. If a potent inhibitor of CYP2D6 such as paroxetine is administered in the body, then a significant increase in the concentration of antipsychotics can occur [57].

Several first generations of antipsychotic drugs such as haloperidol and phenothiazines have been found as P-gp inhibitors, though there is a lack of information showing clinically significant haloperidol P-gp interactions [58]. Concurrent administration of rifampin or verapamil (known inducers and inhibitors of P-gp) with first-generation antipsychotics may change the pharmacokinetic properties of these drugs.

CYP3A4 and UDP-glucuronosyltransferases (UGT) are responsible for butyrophenone, haloperidol metabolism, and are moderate inhibitors of CYP2D6 isoenzyme [59]. Clinically, there are limited drug-drug interactions involving haloperidol. The studies involving CYP3A4 inhibitors and haloperidol reported no adverse effects, as only a small increase in haloperidol plasma concentrations occurred [59]. But concurrent administration of CYP3A4 inducers and haloperidol has resulted in significantly lower haloperidol levels, leading to untoward clinical outcomes (relapse) [59].

Cigarette smoke triggers the induction of CYP1A2 by polycyclic aromatic hydrocarbons and can improve the clearance of a number of first-generation antipsychotic drugs, i.e., haloperidol, chlorpromazine, and fluphenazine [60]. Smoking interruption in patients taking first-generation antipsychotic drugs has been related to the development of extrapyramidal (EPS) related symptoms due to a reduced drug clearance [61]. The frequency of antipsychotic-associated EPS is substantially less in smokers taking antipsychotics than the non-smokers, but due to increased clearance of antipsychotic drugs related to CYP1A2 induction, the dose of the antipsychotic drug may need to be increased [61].

Most drug-drug interactions including second-generation antipsychotics take place at the metabolic level where CYP450s alter the biotransformation of the drug [62]. CYP1A2 primarily metabolised clozapine and nor-clozapine (active metabolite), while other CYPs have been involved in the biotransformation of drugs [63]. Patients taking fluvoxamine or fluoroquinolones (potent inhibitors of CYP1A2) have reported significant drug-drug interactions [64]. On the other hand, CYP1A2 induction has also been related to substantially lower serum levels of clozapine. In cigarette smokers, drugs such as carbamazepine, omeprazole, aryl-hydrocarbons, and rifampin can significantly lower olanzapine and clozapine levels, although discontinuation of these drugs may result in toxicity [65]. CYP3A4 and CYP2D6 are responsible for risperidone and aripiprazole metabolism and increased antipsychotic levels have been also observed in patients that exhibit poor metabolism characteristics of CYP2D6, i.e. polymorphisms [56]. Significant drug-drug interactions of risperidone with CYP3A4 and CYP2D6 inhibitors have been

reported clinically even though administration of traconazole (CYP34 inhibitor) failed to develop significant adverse reactions [66].

Paliperidone and ziprasidone via the CYP450 system are known to have the minimum chances for drug-drug interactions. The aldehyde oxidase system accounts for ziprasidone metabolism (non CYP450 mechanism), while 33% of ziprasidone metabolism involves CYP3A4. Paliperidone primarily undergoes Phase II metabolism, responsible for >60% of its metabolism, and is mostly lacking Phase I metabolism.

1.2.3 Antidepressants Drug Interactions

CYP 3A4, CYP1A2, CYP2D6, and CYP2C9/19 metabolise tricyclic antidepressants. Secondary tricyclic antidepressants such as nortriptyline and desipramine are weak inhibitors of CYP2D6 and have limited drug-drug interactions. Imipramine and amitriptyline (tertiary tricyclic antidepressants) have been reported as potent inhibitors of CYP2C19 [67]. Clinically, concurrent administration of other medications i.e., paroxetine (CYP450 inhibitor) with tricyclic antidepressants causes significant drug-drug interactions and often results in reduced tricyclic antidepressant clearance. Concurrent administration of tricyclic antidepressants and selective serotonin reuptake inhibitors causes severe adverse reactions, including fatality [68]. Reboxetine and mirtazapine, the newer antidepressants, have not been reported to involve clinically significant drug-drug interactions [69].

1.2.4 Anxiolytics Drug Interactions

Benzodiazepines are a class of psychoactive drugs prescribed to treat disorders, for example, insomnia, anxiety, and seizures. Benzodiazepines are involved in many drug-drug interactions via inhibition of CYP450 metabolism producing a high serum concentration of benzodiazepines. The majority of benzodiazepines metabolism primarily occurs through the CYP3A4 system followed by CYP2C19 [70]. Temazepam, lorazepam, and oxazepam metabolisms occur through Phase II conjugation reactions, hence lacking CYP450 interactions [71]. Many benzodiazepines are given along with antidepressants in the course of depression treatment or anxiety disorders, though many of these drugs inhibit CYP3A4, increasing serum concentrations of benzodiazepines. The metabolism of various benzodiazepines can be affected by potent inhibitors of CYP2C19 and CYP3A4

(fluvoxamine, fluoxetine, and paroxetine), which increased their serum levels by 30–100% [72]. Concurrent medications such as propofol and fentanyl (inhibitors of CYP3A4) to intensive care patients, reduced midazolam clearance [73].

Cimetidine, macrolide antibiotics, omeprazole, antiretrovirals, and azole antifungals are common CYP450 inhibitors and are involved in common drug-drug interactions. Consequently, primary care workers use caution while administering these drugs concurrently with benzodiazepines. Pharmacokinetics of benzodiazepines can also be affected by CYP2C19 or CYP3A4 inducers by increasing their metabolism and decreasing removal half-life. Decreased serum levels of benzodiazepines by drugs such as hypericum, rifampin, and rifampin have also been reported as these drugs increase the expression of CYP isoenzymes [70].

1.2.5 Flavonoids-drug Interactions

A large class of naturally existing compounds comprises the flavonoid group; they are usually present in the world of green plants, and 6,500 different compounds have been described. Generally, these compounds retain a skeleton of a chromane ring as well as an additional aromatic ring connected at positions 2, 3, or 4 (Figure 9). The classification of flavonoids into several subclasses is based on the oxidation status of ring C as well as different substitutions such as flavones, flavanols, chalcones, flavanones, and isoflavones (Figure 9). Fruits, vegetables, and plant-derived beverages are rich in flavonoids. For instance, almost 200–850 mg/L of total flavonoids have been found in grapefruit juice, amongst which the most abundant one is naringin (145– 638 mg/L), whereas orange juice mainly comprises hesperidin 200–450 mg/L [74].

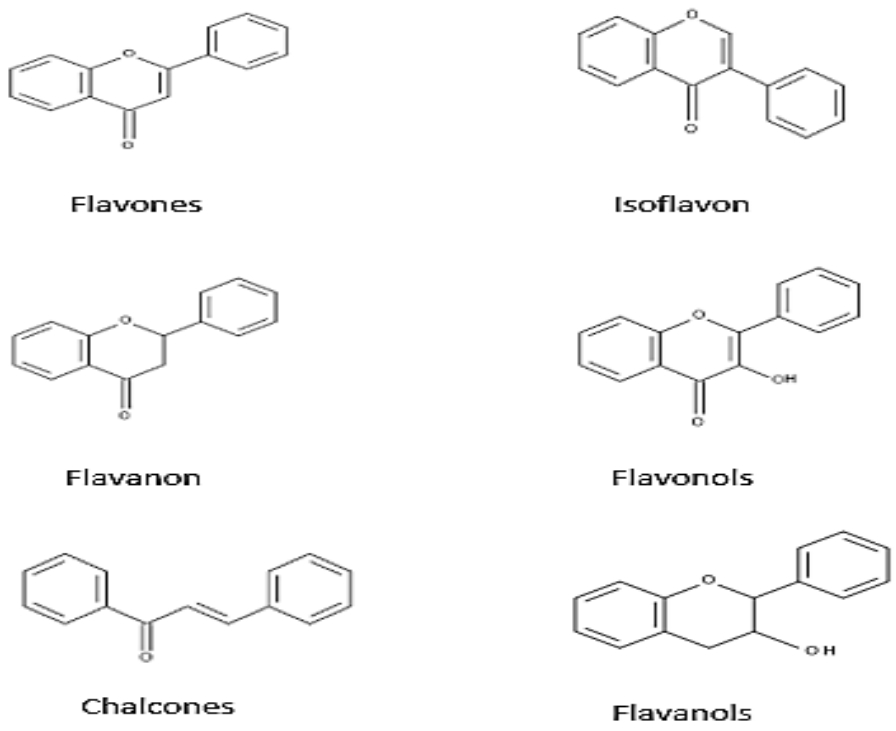

Figure 9. The chemical structure of flavonoids (adapted from reference 74).

There has been a resurrection of scientific attention to flavonoids in recent years because of the association of flavonoid compounds with diverse health benefits. Various studies have shown that flavonoids have anti-carcinogenic, anti-estrogenic, anti-viral, antioxidant, and anti-inflammatory activities [75]. Reduction in the risk of cancer osteoporosis, cardiovascular diseases, as well as other age-related degenerative diseases has been related to high flavonoid intake [75].

Absorption, distribution, metabolism as well as the elimination of endobiotic and xenobiotics agents occurred through several biological membrane systems. They also need these membrane systems to perform their biological functions by binding to their intracellular targets, for instance, enzymes or receptors. A lipid bilayer system that is embedded with several proteins containing many transporters is known as the biological membrane system. Therefore, these transporters' activities are anticipated to be key determinants of the pharmacodynamics and pharmacokinetics of many essential drugs, particularly those hydrophilic compounds.

Many flavonoids have been publicised for their interactions with the efflux transporters, particularly BCRP and P-glycoprotein *in vitro* studies, as well as the consequences of interactions of flavonoids and drugs due to flavonoid modulation of these efflux transporters have been described. Though, by pharmacokinetic interactions, the importance of these flavonoid–efflux transporter interactions have not yet been revealed. In addition, while sulfate conjugates and flavonoid glucuronides are anticipated to be the main circulating chemical species, research has not examined their interaction with these efflux transporters [74].

1.2.6 Herb-drug Interactions

The definition of herbal medicines is "finished, labeled medicinal products which involve as underground parts of plants, or active ingredients aerial or combinations thereof, even if as plant preparations or in the crude state" (World Health Organization). Plant material contains fatty oils, juices, essential oils, gums, and some other substances of this nature while herbal medicines might have excipients along with active ingredients. Herbal medicines comprise a combination of plant constituents that are pharmacologically active and claim to work independently to produce a greater effect than the sum of a single constituent's effects [76]. The public believes that herbal medicines are harmless as they are natural. But this is an unsafe oversimplification because many different side effects of herbal medicines have been described and recent studies include antagonistic events affected by herb-drug interactions [77].

As there are combinations of more than one active ingredient present in all herbal medicines, there is more possibility of herb-drug interactions than drug-drug interactions because synthetic drugs typically have single chemical entities.

According to clinical records, the interaction between herbal medicines and conventional drugs is obvious but although the clinical significance of the majority of such interactions is negligible, some of them may cause a serious risk to public health [78]. For instance, a combination of St. John's Wort and immunosuppressive, antiretroviral, or anticancer agents that are the substrates of P-glycoprotein and/or metabolised by CYP enzymes can cause the failure of the drug [78]. An herbal constituent (Hyperforin) present in St John's

Wort non-competitively inhibits the CYP2D6 isoform [79]. If herbal medicine is taken before surgery, it may cause serious health issues. Cases of cardiovascular collapse, delayed emergence, as well as blood loss have been reported. Recently, the Anesthesia Preoperative Evaluation Clinic at the University of Kansas Hospital described from a retrospective review of their surgery patients that about one-quarter of patients specified natural products' use before the surgery [80]. Therefore, before surgery, clinicians should screen their patients for the usage of these supplements.

If a drug and herbal constituent are both metabolised by the same CYP450 isoform, then mutual competitive inhibition may occur. For instance, garlic contains diallyl sulfide and it competitively inhibits the CYP2E1 isoform [79]. Herbal constituents with electrophilic groups (hydrazine group or imidazole) bind to the heme part of CYPs via non-competitive inhibition mechanisms. For instance, piperine inhibits CYP2A and CYP1A isoforms [79]. Diallyl sulfone is a component derived from diallyl sulfide and it acts as a suicide inhibitor of the CYP2E1 isoform. Diallyl sulfone formed a complex via an epoxide metabolite and starts/causes autocatalytic destruction of CYP2E1 [79]. Hence, caution is required for the patients taking concomitant drugs metabolised by CYP2E1 with garlic [79].

1.2.7 Food-drug Interactions

Drugs and food interaction are widely considered. Taking the drug after a meal or with food can affect some drug's pharmacokinetic parameters (rate as well as absorption, metabolism, bioavailability extent, etc.) [81]. To find out food drug administration timings and the influence of food intake on investigational drug pharmacokinetics, reference to the third phase development of drugs section within the European Medicines Agency (EMA) guidelines are recommended [82]. This is significant to decrease the inter-and intra-individual inconsistency of drug pharmacokinetics. Two varieties of the standard meal are suggested: high-fat and moderate meal in EMA recommendation in the food-drug interaction studies *in vivo* [82].

1.3 COVID-19

Across Europe, a pandemic began in late December 2019 and has later spread around the world, being established as a health emergency. On 11 February 2020, World Health Organization announced the disease as COVID- 19 [83]. The disease is identified and based on the similarities to the SARS epidemic in China in 2002, although SARS-CoV-2 is believed to be caused by a new and novel coronavirus that is severe acute respiratory syndrome coronavirus 2, SARS-CoV-2 [84].

Coronaviruses are known for their crown-like spikes present on their surface. Coronaviruses have four main genera: alpha, beta, delta, and gamma, where SARS-CoV-2 falls in the beta sub-category and is the source of mild to severe infection of the lower respiratory tract [84]. Till today 2022, there are 334,101,607 confirmed cases and 5,554,786 deaths of COVID-19 that have been reported.

30-50% of total COVID-19 patients may not show any symptoms, while mild forms of the disease have also been reported in most of the COVID-19 patients [85]. However, a significant percentage of COVID-19 patients develop moderate to severe symptoms, requiring ICU treatment and primary hospital care. The mortality rate among these patients is approximately 26.8 % [85]. The most common COVID-19 symptoms are dyspnea, fever, fatigue, cough, and myalgia. Hypogeusia, bilateral conjunctival injection without associated secretions, hyposmia, and skin rash are the other reported symptoms [85].

The treatment of coronavirus was based on previous experiences using pre-existing and marketed drugs because potential efficacy, characteristics, mechanisms, cytotoxicity, as well as dosages have been already approved. But these therapies cannot destroy the COVID-19 virus, particularly as it has a very broad symptoms spectrum [83].

1.3.1 Non-steroidal Anti-inflammatory Drugs (NSAIDs) and COVID-19

There were concerns about the usage of NSAIDs in the media, early in the COVID-19 pandemic, e.g. mifepristone, celecoxib, aspirin, ibuprofen, and dabigatran/warfarin may interact with drugs such as aldesleukin and can add to bleeding. Concerns particularly about ibuprofen

were based on unpublished data, and it led to guidance against the use of Ibuprofen as it might worsen COVID-19 symptoms. Several studies have been conducted to disapprove or prove a possible association. Theoretically, the NSAIDs could be harmful to COVID-19 patients by upregulation of angiotensin-converting enzyme 2 (ACE2) receptors in the arteries, lungs, intestines, heart, and kidney, which is an entry point into cells for SARS-CoV-2. Furthermore, NSAIDs could delay COVID-19 diagnosis by masking fever and inflammation [86].

A study conducted by Drake and colleagues evaluated the relationship between severe COVID-19 outcomes and NSAID exposure, involving mortality, need for invasive ventilation, critical care admission, acute kidney injury, and need for oxygen. The outcomes of the study were not associated with using NSAIDs in any exposure group as the distribution of NSAIDs was the same in those groups who survived and who died. A major subanalysis of the patients taking ibuprofen also did not show any increased mortality risk as compared with those who were not taking any NSAIDs [86].

1.3.2 Aspirin and COVID-19

Aspirin may affect the clearance of other medications from the body, for instance, some cancer medicines such as erlotinib, dasatinib, sunitinib, praziquantel, and rilpivirine [87]. Wijaya *et al.* provided evidence that among COVID-19 patients, the use of aspirin is substantially associated with reduced mortality risk [88]. The hospitalised COVID-19 patients indicate a reduced death rate in the aspirin-treated group as compared with the non-aspirin-treated group [89].

1.3.2.1 Metabolism of Aspirin

Aspirin was developed as a drug by Felix Hoffman in 1987. It was first synthesised by Frederich von Gerhardt in 1953. Aspirin is a commonly used anesthetic for the treatment of inflammation and arthritis. It also helps to decrease the risk of heart attacks. The metabolism of aspirin in humans is not completely understood yet. After oral ingestion, the acetyl group in aspirin is quickly hydrolysed, either non-enzymatically or enzymatically to form salicylic acid in the body (Figure 10). 1-31% of the compound can be directly excreted

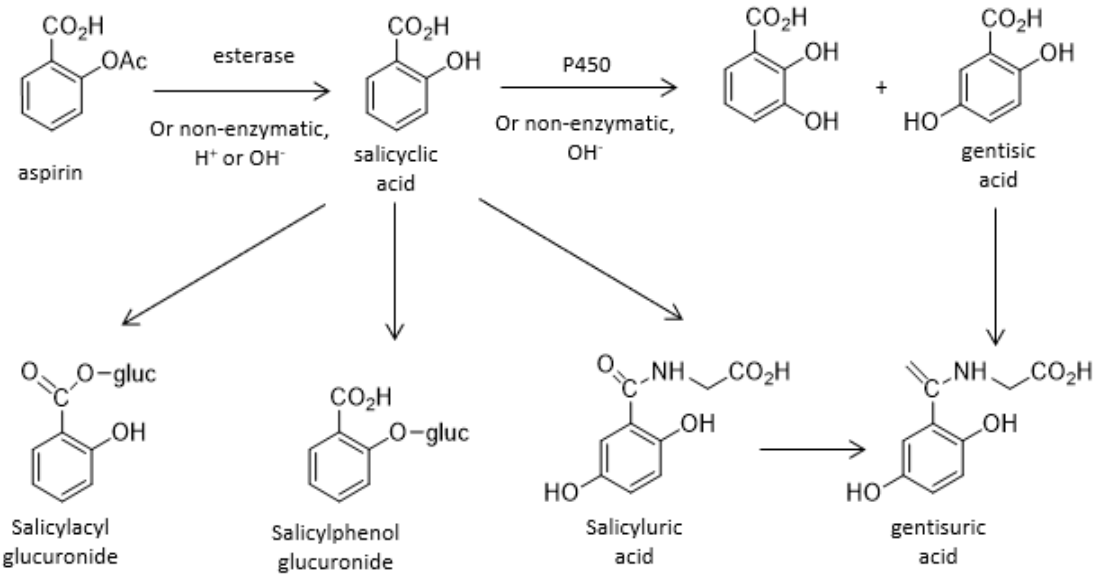

Figure 10. Metabolism of aspirin (adapted from reference 90).

The formation of salicyluric acid from the conjugation reaction of salicylic acid with glycine is a major route of metabolism of aspirin. This accounts for 20–65% of the products. Salicyclic acid conjugation with glucuronides results in the formation of other major metabolites (ester and ether, 1–42%) [90].

Glucuronidation comprises a wide range of uridine 50-diphosphoglucuronosyltransferases (UGTs), with UGT1A1, UGT1A3, UGT1A4, UGT1A6, UGT1A7, UGT1A8, UGT1A9, UGT1A10, UGT2B4, UGT2B7, UGT2B15, and UGT2B17 enzymes [90]. Different animals have different UGTS and thus have varying aspirin metabolism. For example, cats lack UGTs and show more toxicity to aspirin, and have a 22 h long half-life of aspirin when compared to dogs which have a half-life of 7.5 h [90]. The aspirin half-life has been reported to differ from 1 to 38 h in different animals. In humans, it is 6 hours [90]. 2,5-dihydroxybenzoic acid and 2,3-dihydroxybenzoic acid are two minor metabolites of salicylic acid. Oxidation of these products can be achieved by non-enzymatic Fenton-type reactions and CYPP450 enzymes. 2,5-dihydroxybenzoic acid further conjugates with glycine to produce gentisuric acid, which can also occur by salicyluric acid hydroxylation (Figure 10). Many studies support the P450 oxidation of aspirin and aspirin sensitivity because of polymorphisms in P450 2C9 (an enzyme suggested for aspirin oxidation) [90].

1.3.3 Ibuprofen and COVID-19

Ibuprofen is usually administered orally and is absorbed rapidly after oral administration (t_{max}, ~ 1–2 h varying on the particular oral formulation) [91]. At therapeutic concentrations, more than 98% of ibuprofen is bound to plasma proteins [91]. Ibuprofen may interfere with other highly protein-bound drugs (phenytoin and warfarin) and is unlikely to cause clinically significant drug-drug interactions [91]. The therapeutic concentration range of ibuprofen is wide for its anti-inflammatory, antipyretic, and analgesic effects (~10–50 mg/l) as well as having a comparatively short plasma half-life ($t_{1/2}$, ~ 1–3 h), thus frequent administration is required to maintain therapeutic concentrations in the plasma [91].

The pharmacokinetic profile of ibuprofen in adults has appeared to be the same in the young population, for instance, age > 0.5 years, while some findings have shown that ibuprofen clearance rates are higher in young children (0.5–5 years) [91]. Kragholm *et al.* conducted a study with 403 COVID-19 patients. Antipyretic drugs were given to 134 patients during the treatment period, ibuprofen was given to 49 patients and 85 were treated with paracetamol. Apparently, no adverse outcomes were shown by both treatment groups [86].

1.3.3.1 Metabolism of Ibuprofen

A racemic mixture of *R* and *S* enantiomers of ibuprofen is administered in the body like most NSAIDs while pharmacologic activity largely depends on *S*-ibuprofen. After oral administration, *R*-ibuprofen (50–65%) in the liver transforms into the *S*-enantiomer through an acyl-CoA thioester via the enzyme α-methylacyl-coenzyme A racemase [91].

The inactive metabolites of ibuprofen are formed by oxidative metabolism by CYP enzymes (Figure 11). Two major metabolites are ibuprofen 2-hydroxy-ibuprofen and carboxy-ibuprofen and are excreted through the urine, accounting for 25% and ~37% of an administered dose, respectively [91]. Other hydroxylated metabolites such as 3-hydroxy-ibuprofen and 1-hydroxy-ibuprofen have also been found in the urine in small amounts.

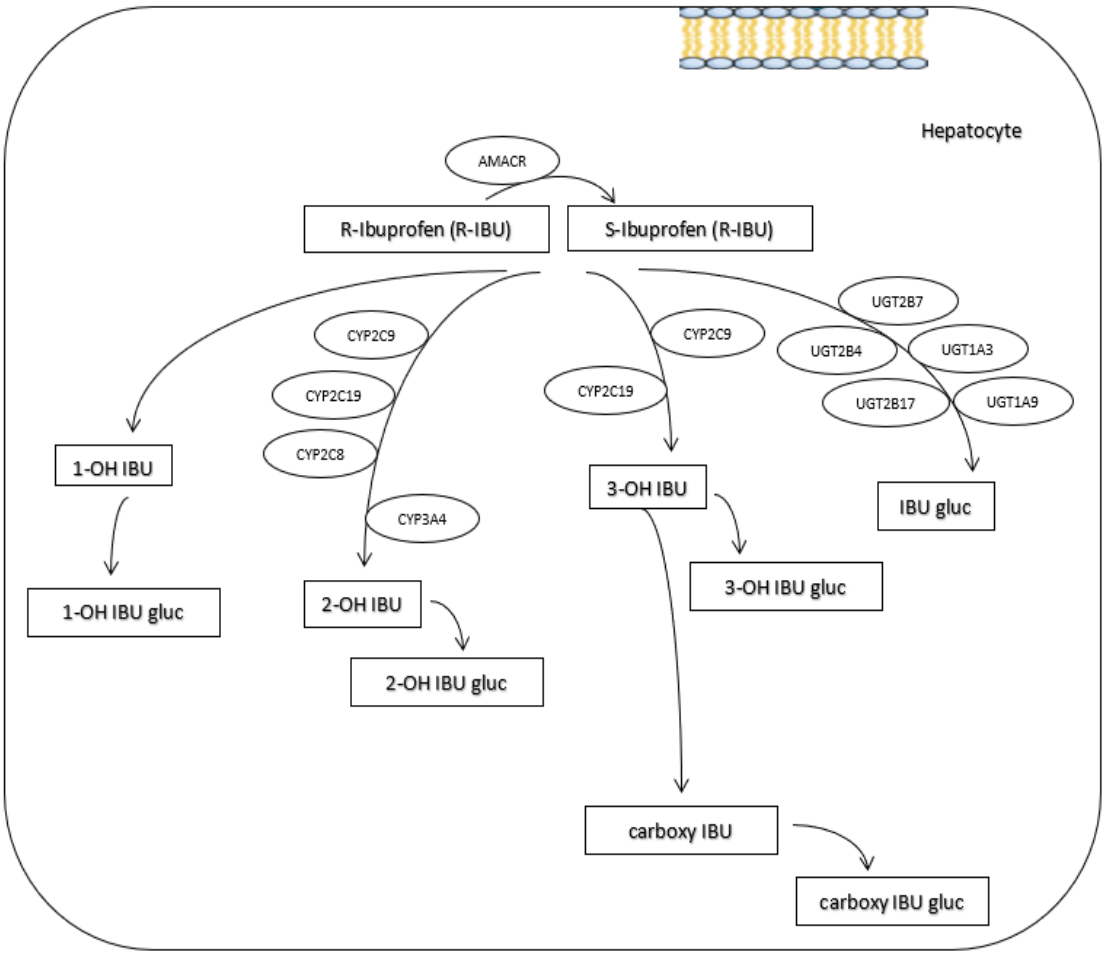

Figure 11. Metabolism of ibuprofen in the hepatocyte (adapted from reference 91).

The main clearance of ibuprofen is achieved by the CYP2C9 isoform which catalyses the formation of 3-hydroxy-ibuprofen (3-OH IBU), most of which is then converted to 2-hydroxy-ibuprofen (2-OH IBU) and carboxy-ibuprofen through cytosolic dehydrogenases [91]. Therefore, drug-drug interactions occur when ibuprofen is coadministered with CYP2C9 substrates (warfarin) or CYP2C9 inhibitors (selective serotonin-reuptake inhibitors) [91]. *In vitro*, the CYP2C9 isoform can easily metabolise both enantiomers of ibuprofen, whereas the CYP2C8 isoform displays stereoselectivity, preferably catalyses 2-hydroxylation of *R*-ibuprofen and plays a minimal role in the clearance of ibuprofen [91]. At high concentrations, the CYP3A4 isoform is responsible for ibuprofen clearance via 2-hydroxylation, although the CYP2C19 isoform shows a minor role in clearance [91].

Ibuprofen-acyl glucuronide is formed by direct glucuronidation of about 10–15% of an ibuprofen dose [91]. *In vitro* studies suggest that multiple uridine 5'diphosphoglucuronosyltransferases (UGTs) such as UGT1A3, UGT2B4, UGT2B7, UGT1A9,

and UGT2B17 are responsible for metabolising ibuprofen. UGT1A10, which is mainly expressed in the gut, can also produce ibuprofen-acyl glucuronide [91]. Carboxy and hydroxy metabolites derived from CYPs are metabolised to the subsequent acyl glucuronides, however, the phase II enzymes (UGTs) responsible for catalysing this reaction have not been examined.

Acyl glucuronides are possibly reactive metabolites while it is believed that glucuronidation is usually a detoxification pathway. These reactive metabolites have the potential to undergo intramolecular rearrangement as well as being able to covalently bind to macromolecules thus contributing to toxicity [91]. *In vitro* covalent binding of ibuprofen-acyl glucuronide to plasma proteins has been observed. This binding has also been observed *in vivo* in elderly individuals who were constantly treated with ibuprofen [91]. But the reactive potential of ibuprofen-acyl glucuronide was less than other compounds studied, indicating that in most individuals, ibuprofen-acyl glucuronide is not an important source of toxicity [91].

1.3.4 Dexamethasone and COVID 19

Dexamethasone is a corticosteroid that is thirty times more active than cortisone and has been in use since the 1960s to treat inflammatory disorders, inflammation, and even cancers to some extent. The higher potency of dexamethasone could be one of the reasons for its effectiveness in treating SARS-CoV-2 patients [92]. Additionally, dexamethasone is also stronger than NSAIDs like aspirin and ibuprofen. Dexamethasone is both immunosuppressive as well as anti-inflammatory, although NSAIDs only reduce inflammation of the vascular system [92].

However, still, there is no medicine (including remdesivir) that can be used to treat severe COVID-19 infection. Dexamethasone has been studied and proven with the potential to decrease death by 35%, and therefore, so far, dexamethasone is believed as the “breakthrough” medication for severe COVID-19 patients. Dexamethasone blocks antibody production and can indirectly inhibit the antibody-dependent entry of the virus, which eventually may reduce viral shedding. Moreover, it would be viable if the dexamethasone is co-administered with the luteolin: a natural flavonoid with anti-inflammatory and

antiviral properties, especially it can inhibit mast cells, which are the main sources of cytokines in the lungs. Nevertheless, further extended studies and clinical trials regarding dexamethasone action are required to resolve such controversy. However, ongoing clinical trials on hospitalised patients showed the desired effects of dexamethasone against severe cases of COVID-19 (i.e., lowering the mortality rate) [92].

Corticosteroids have been given in serious cases of coronavirus such as SARS-CoV-2, MERS, and SARS to monitor this immune-mediated lung tissue injury. Severe cases of COVID-19 patients with ventilator support have been treated with dexamethasone and shown a reduction in in-hospital deaths [92]. Corticosteroids used for COVID-19 treatment have lessened the ventilation need and have also reduced the hospital stay period in addition to better individual oxygenation status [92]. Dexamethasone also shows some side effects such as mood changes, an increase in appetite, headache, and agitation. Occasionally, it causes dizziness, and if it is in use for more than a week, it could lead to arrhythmias. So, heart and adiabatic patients use high doses with caution [92].

1.3.4.1 Metabolism of Dexamethasone

It is not clear if dexamethasone is an inducer or inhibitor of CYP 450. Several studies performed in that respect have had mixed results. Al Rhihani *et al.* studied the role of dexamethasone as an inducer and inhibitor of CYP 450 and observed that dexamethasone as an inducer significantly increases the expression of mRNA gene by initiating glucocorticoid receptors (GR). Also, a study found that incubation of liver enzyme CYP3A4 with dexamethasone results in the production of total cellular protein rich in dexamethasone compounds. Dexamethasone as an inhibitor was found to decrease the formation of 6α- and 6β-hydroxy dexamethasone in the liver [93]. Dexamethasone is metabolised to 6-hydroxydexamethasone and sidechain cleaved products in human liver microsomes *both in vitro* and *in vivo* by the CYP3A4 isoenzyme [94].

Tomlinson and their coworkers constructed the structural model for CYP3A4 based on amino acid sequence alignment between CYP3A4 [5] and a bacterial P450, CYP102 (of known crystal structure) [95]. To rationalise the known positions of metabolism, this model has been utilised for both substrates and inhibitors of CYP3A4 [95]. Residues in the putative

CYP3A4 active site seem to be involved in hydrogen bonding with CYP3A4-specific compounds. Testosterone, progesterone, gestodene, and cortisol (steroidal substrates) were examined in the model; and it was noticed in each case that hydrogen bond interactions in the active site of CYP3A4 were revealed to hold the steroid in an orientation where the 6β-position by the heme interaction might be responsible to hydroxylation (Figure 12) [95]. In dexamethasone, 6α and the 6β-hydroxylated metabolites may be formed by interaction with the heme proto-porphyrin. A human CYP17 model (responsible for site-directed mutagenesis experiments) [95] has also been utilised to investigate dexamethasone binding in an orientation in its active site, which may result in side-chain cleavage [95].

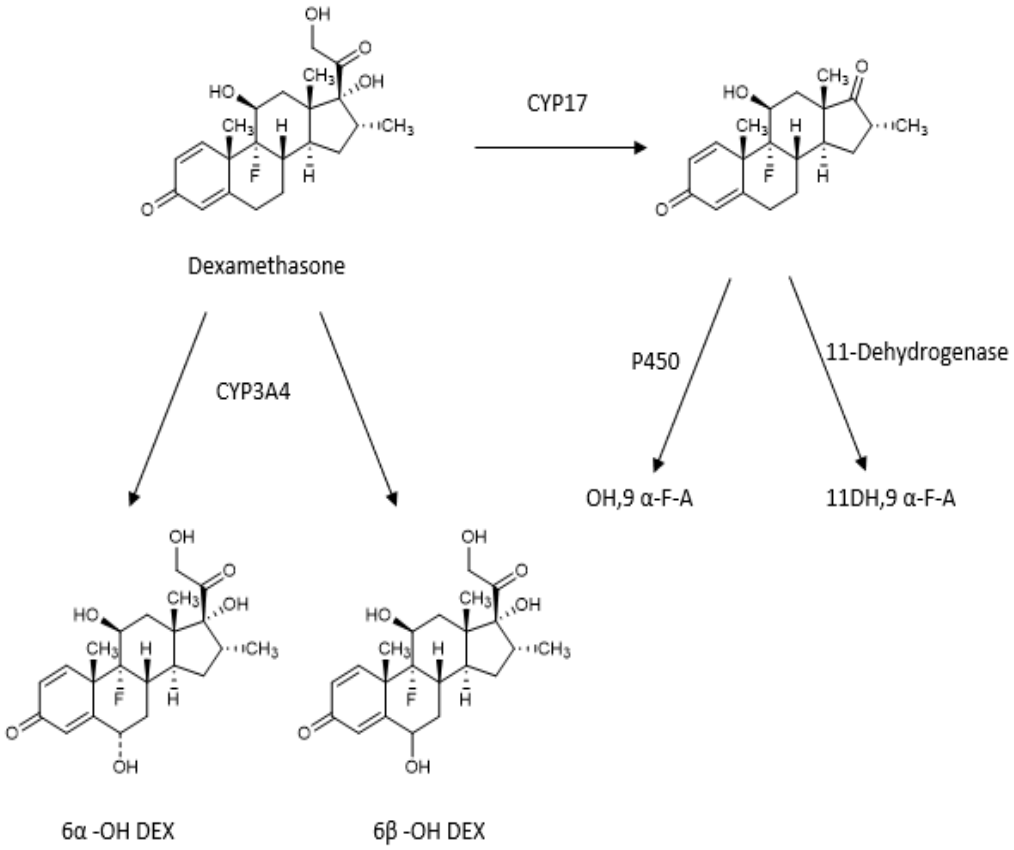

Figure 12. Dexamethasone metabolism *in vitro* (adapted from reference 95).

1.3.5 Remdesivir and COVID-19

As an antiviral medicine, remdesivir has the properties to reduce viral replication of SARS-CoV-2. There were some early shreds of evidence from positive research results on remdesivir that drew media attention and the US Food and Drug Administration (FDA) to allow the emergency use of remdesivir in COVID-19 treatment [96]. It has also been accepted by the Therapeutic Goods Administration of Australia (TGA) and by the European Medicines Agency (EMA). Remdesivir has also been commonly prescribed for COVID-19 patients in South Korea, India, and Japan [96].

Initial reports on the use of remdesivir for COVID-19 patients were lacking information on outcomes, but now there is knowledge about short-term outcomes such as for 53 of 61 patients with COVID-19 given remdesivir treatment in over 20 hospitals on three continents [96]. Patients with COVID-19 were given at least one dose of intravenous remdesivir and the duration of the treatment course was for 10 days as this was not a part of a clinical trial. At the start of remdesivir treatment, thirty were on ventilation support and four of them were treated with extracorporeal membrane oxygenation (ECMO). 47% of patients were discharged from the hospital and 13% died. The mortality rate was 5% among non-ventilated patients and the improvement rate by 18 days was 68%. Overall, in this study, 60% of patients had at least one adverse outcome while 23% of patients experienced serious adverse effects. Rashes, abnormal liver function, renal impairment, diarrhea, and hypotension were the most adverse outcomes. But this study has some limitations, such as the lack of a randomised control patients' group and the lack of information on initially treated patients, etc [97].

1.3.5.1 Mechanism of Action of Remdesivir

Knowledge about the mechanism of action of remdesivir makes it theoretically useful in COVID-19 treatment. Being a prodrug, remdesivir is formerly identified as GS-5734. Remdesivir is a monophosphate that is metabolised to an adenosine nucleoside triphosphate analog. This adenosine nucleoside triphosphate analog is then integrated into the viral RNA before its replication (Figure 13) [98] and consequently inhibits the RNA synthesis and function of RNA-dependent viral RNA polymerase [97]. Many validated studies on humans confirm the safety of the drug. In an *in vitro* study, the inhibition of

SARS-CoV-2 replication at a low EC_{50} value (0.77 µM) was evaluated [98]. In the randomised COVID-19 Treatment Trial (controlled and adaptive trial), remdesivir has proven to shorten the recovery time [99].

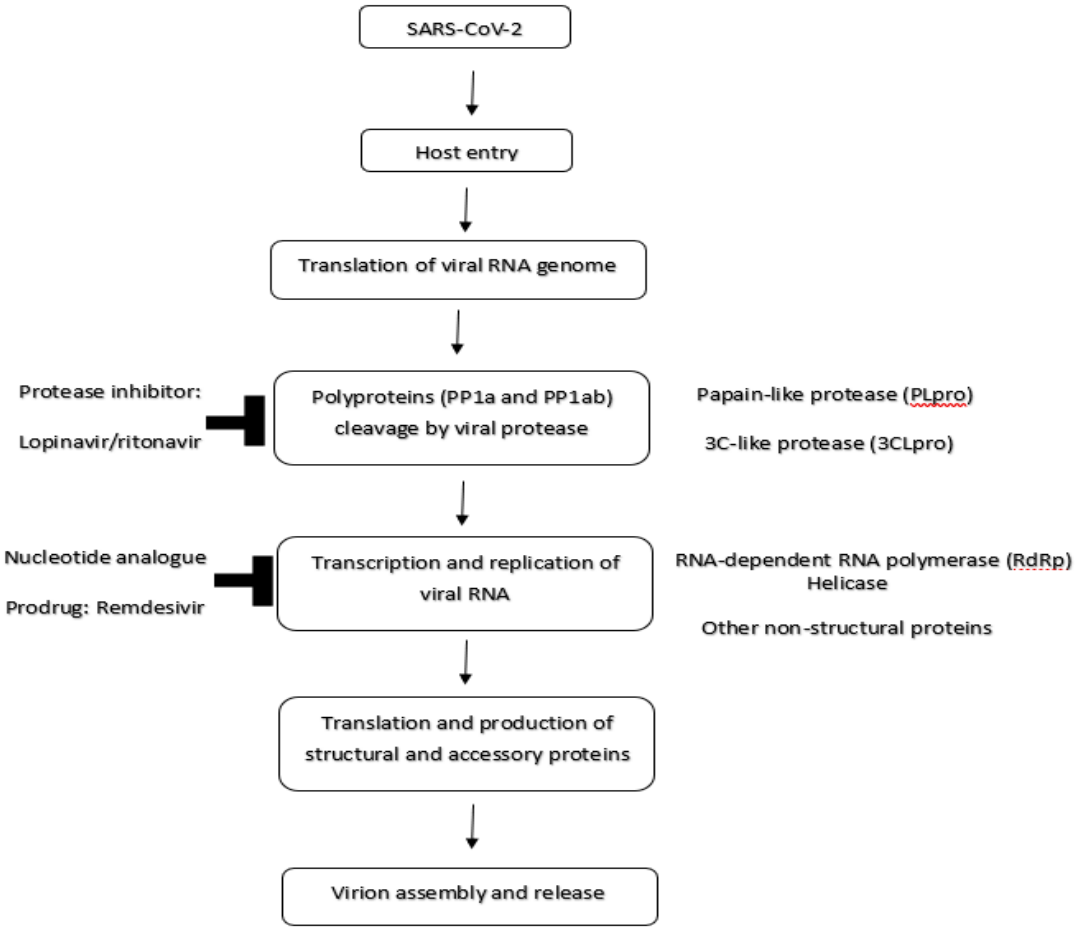

Figure 13. Inhibition of viral infection by lopinavir/ritonavir and remdesivir [adapted from reference 100].

1.3.6 Omeprazole and COVID-19

Acid-related disorders are treated by proton pump inhibitors (PPIs). Omeprazole is a proton pump inhibitor. PPIs have grown into one of the most usually prescribed agents because of their high effectiveness. Though, PPIs may possibly trigger pneumonia development because of the reduced production of gastric acid with microaspiration with subsequent colonisation of pneumonia as well as with consequent bacterial overgrowth within the upper part of the gastrointestinal tract [101].

Luxenburger *et al.* reported their findings that PPI-treated COVID-19 patients (treated with pantoprazole, esomeprazole, and omeprazole) showed more frequent symptoms of secondary infections when compared to non-PPI-treated patients [101]. They also mentioned that this effect stayed statistically important when adjusting for other potential risk factors. Additionally, there is a strong association between secondary infections and the development of acute respiratory distress syndrome suggesting an indirect negative effect of PPI treatment on the acute respiratory distress syndrome development. But this study required further validation to confirm these findings [101].

Previous studies on omeprazole have revealed that this drug may interfere with the lysosomes' acidification and inhibit replication of the virus [102]. In Germany, recent drug research has demonstrated that omeprazole inhibited SARS-CoV-2 formation beyond therapeutic concentrations of plasma at 8 µM [102]. But it also increased the anti-SARS-CoV-2 effects of remdesivir and aprotinin (protease inhibitor) by ten and 2.7-fold, respectively at therapeutic concentrations. Hence remdesivir or aprotinin along with omeprazole may be therapy candidates for COVID-19 treatment [102].

1.3.6.1 Metabolism of Omeprazole

There are two metabolites of omeprazole, 5-hydroxyomeprazole metabolised via CYP2C19 and omeprazole sulfone formed via CYP3A4, as presented in Figure 14. The principal route of omeprazole elimination from the body is through hydroxylation by CYP2C19. Therefore, the population studies results suggest that omeprazole is a probe drug used for phenotyping CYP2C19 [103]. Furthermore, omeprazole sulfone hydroxylation is also catalysed by CYP3A4 [103].

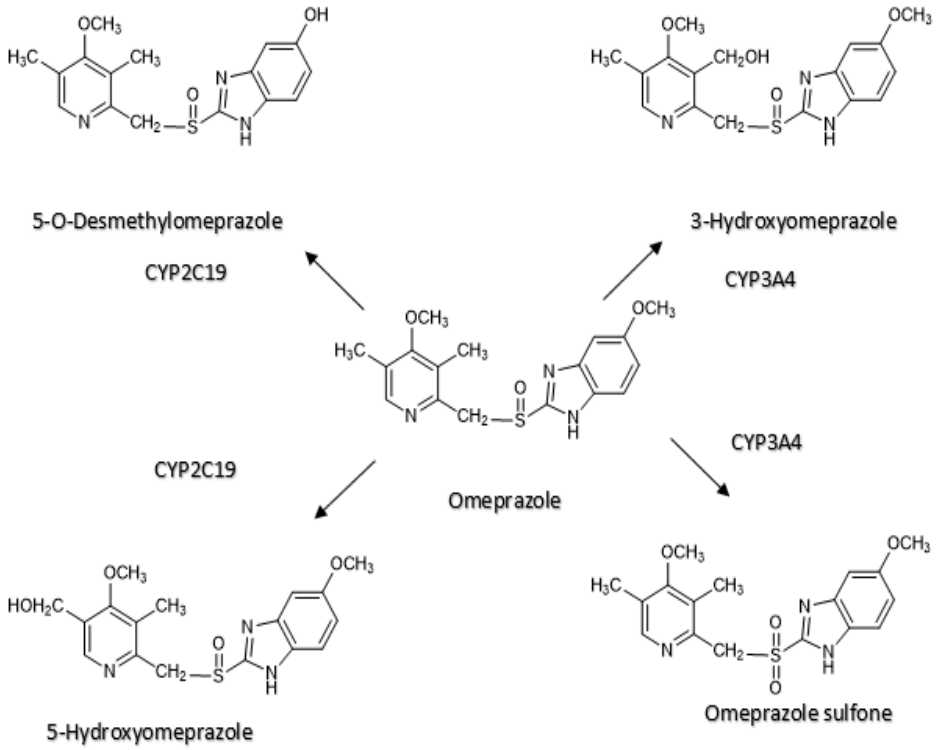

Figure 14. Metabolic pathways of omeprazole with metabolites structure [adapted from reference 103].

1.4 Vitamin D

Chronic liver disease (CLD) is described as the procedure of long-term progressive liver destruction as well as regeneration, and with progressing disease, cirrhosis, as well as hepatic fibrosis, occurs [104]. CLD progression, as well as deterioration of liver function, is related to several hepatic problems, for example, hepatocellular carcinoma, chronic liver failure, and infections. Another important extrahepatic sign of the advanced liver disease is called hepatic osteodystrophy which imitator features of traditional osteoporosis with an elevated risk for fractures [104]. In recent times, Vitamin D's role in CLD has obtained much consideration, particularly its process of inherent activation by the liver as well as the high frequency of deficiency of Vitamin D in this patient group [104]. Data is also under investigation to untangle potential direct therapeutic advantages of Vitamin D therapy. However, although clear evidence of a relationship between Vitamin D as well as liver

disease occurs, it remains unrevealed whether deficiency of Vitamin D causes a higher risk of liver infection or whether the liver infection causes deficiency of Vitamin D [104].

Vitamin D_3, as well as Vitamin D_2, are transformed into their active forms $1,25(OH)_2D_3$ as well as $1,25(OH)_2D_2$ individually in the body, while Vitamin D_3 has an extra active form as $1,24(OH)_2D_3$ that has been described to be physiologically less active [105]. In both compounds of Vitamin D, the side chain hydroxylation at C-25 or C-24 is a requirement for the succeeding 1α-hydroxylation regulated by physiological conditions [106].

The conventional synthetic pathway includes 25- as well as 1-α-hydroxylation of Vitamin D_2 as well as D_3 within the kidney and liver [107]. Primarily, hydroxylation ensues in the liver, and it produces $25(OH)D_3$; then $25(OH)D_3$ arrives in the systemic circulation, as well as it has a half-life of 12–19 days [107]. Secondly, hydroxylation ensues in the kidneys, where it organises a hormonal form of Vitamin D, which is most biologically active, i.e., $1,25(OH)_2D_3$ (calcitriol), as shown in Figure 15. The $25(OH)D_3$ serum levels are a reflection of total Vitamin D prominence in the body [107].

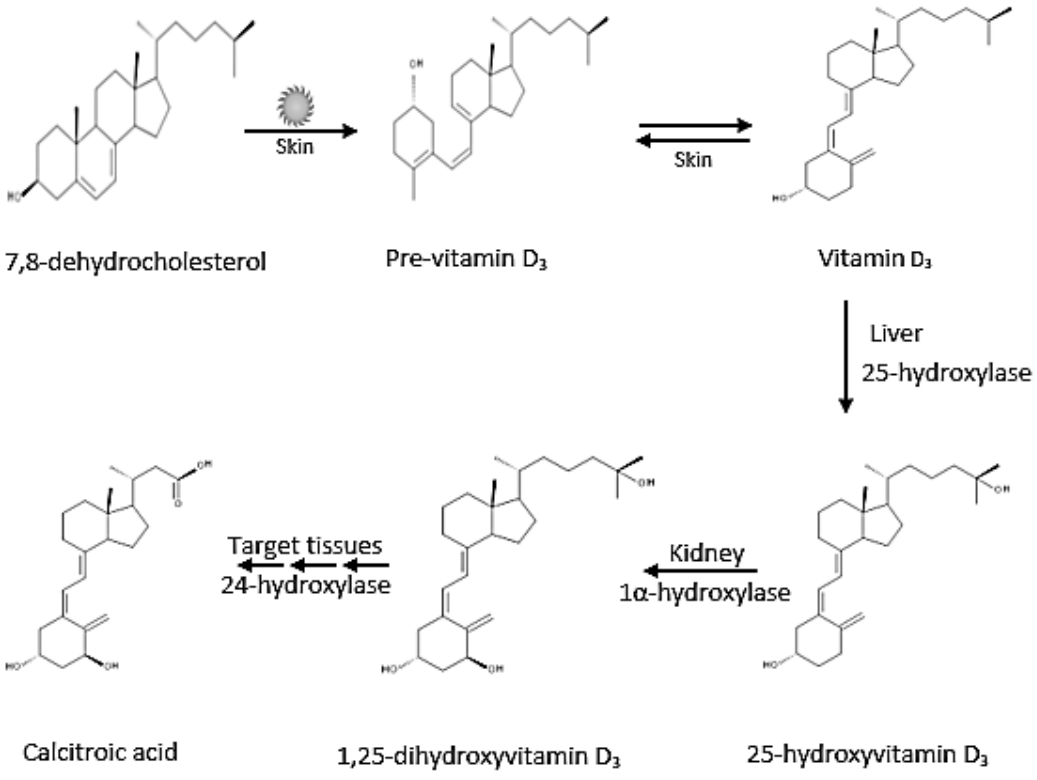

Figure 15. Vitamin D and its metabolites (adapted from reference 107).

So far, six Vitamin D 25-hydroxylases have been described e.g., CYP27A1, CYP2C11, CYP2J3, CYP2D25, CYP3A4 as well as CYP2R1 [108]. CYP27A1 is a mitochondrial p450 enzyme that undergoes hydroxylation at C-25 of Vitamin D_3 as well as at C-24 for Vitamin D_2 [109]. The gene of CYP450 is highly conserved in all vertebrates, however, the CYP450 gene of knockout mice shows no major changes in the metabolism of Vitamin D. CYP450 is believed to be critical for the synthesis of bile acid such as a sterol 27-hydroxylase. CYP2CD25, as well as CYP2D11, have been purified as main microsomal Vitamin D 25-hydroxylases in pigs and male rats, respectively [110] CYP2C11 is specifically related to male rats.

The drug–Vitamin D interaction's potential has hardly been considered. Robien and colleagues evaluated the amount to which drugs influence the status of Vitamin D or if Vitamin D supplementation changes the drug efficacy or toxicity within humans. They found that inadequate data were available to decide if antimicrobial agent lipase inhibitors, highly active antiretroviral agents, antiepileptic drugs, or H2 receptor antagonists change concentrations of serum 25(OH)D. Atorvastatin seems to elevate the concentrations of 25(OH)D, while concomitant supplementation of Vitamin D reduces atorvastatin concentrations [111]. Thiazide diuretics utilisation in combination with supplements of calcium as well as Vitamin D may become the reason for hypercalcemia in the old or those with hyperparathyroidism [111]. They concluded that larger analyses with stronger research designs are required to explain possible drug–Vitamin D interactions, particularly for Cytochrome P450 3A4 (CYP3A4) metabolised drugs. Healthcare workers must be aware of the possible interaction of the drug–Vitamin D [111].

1.5 Testosterone

Testosterone is an anabolic steroid and male sex hormone. It is an important provider of the healthy metabolic functioning of various biological systems. Over the past years, the misuse of anabolic steroids by athletes has been one of the most important detractors in the research and treatment of clinical states that could be affected by male hypogonadism [112]. CYP2C11 facilitates some endogenous steroids' hydroxylation e.g., testosterone and androstenedione, Vitamin D hydroxylation, and oxygenation of arachidonic acid [113]. The 2*α*- and 16*α*- testosterone hydroxylation is utilised as a marker reaction for analysing CYP2C11 activities in rats and this isoform of CYP (CYP2C11) is inhibited via diclofenac,

cimetidine, ethanol as well as inflammatory mediators [113]. CYP2C11 shows a 77% amino acid sequence homology, a functional analogy, and some substrate predilection with human CYP2C9, which is responsible for catalysing the metabolism of some clinically significant drugs such as S-warfarin, ibuprofen, phenytoin, diclofenac, antidepressant drugs, tolbutamide, arachidonic acid and steroids [113]. There are CYP2C11-particular reactions in rats such as the 2*α*- and 16*α*-hydroxylation of testosterone, while the reaction is catalysed by CYP3A4 in humans (16*α*-hydroxylation, Figure 16) [113].

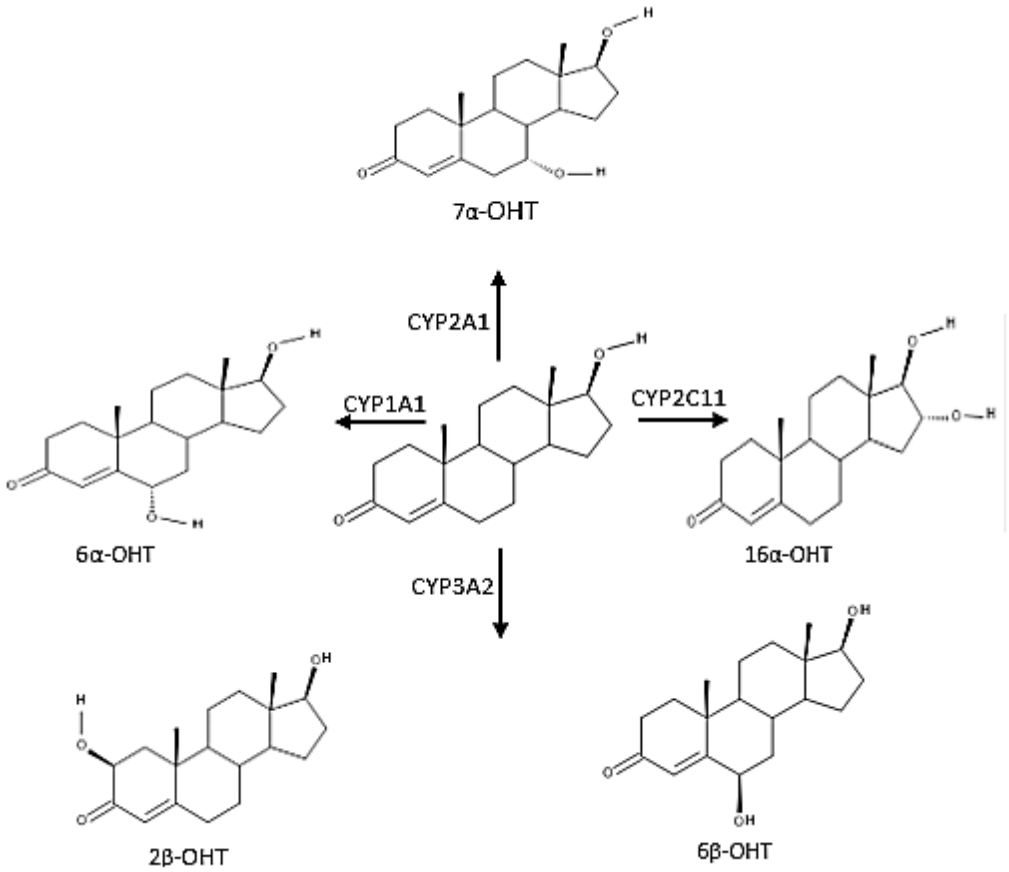

Figure 16. Testosterone and its metabolites (adapted from reference 113).

Chovan and colleagues have investigated the Cytochrome P450 (CYP) probe substrate's metabolism in liver microsomes of male Sprague Dawley rats and determined their substrate specificities. They varied the time and microsomal protein concentrations to regulate the linear conditions for each reaction. They tested 14 enzymes and 7 of them were perceived as the main rat CYP enzymes accountable for the majority of the metabolism of the substrate tested. Testosterone 2α- as well as 16α-hydroxylation reactions, were conducted mainly by CYP2C11, then triazolam 1'-hydroxylation and midazolam 4-hydroxylation were especially catalysed by CYP3A1/2, however, specificity

was normally poor [114]. They concluded that care needs to be taken in the understanding of metabolism results attained in rats using standard probe substrates, particularly in humans [114].

1.6 Chromatographic Techniques

Advancement in chromatographic techniques has stimulated the development of new methods in the pharmaceutical analysis field. More accurate testing of drugs is possible due to the newly developed methods, as well as by improved metrological parameters. It also allows the accurate testing between the composition of raw materials, intermediates, along with final products. Pharmaceuticals and para-pharmaceuticals present in the waste generated by research laboratories are also analysed by chromatographic techniques. Capillary analysis was the first chromatographic technique applied to pharmaceutical analysis. In 1930, it was applied to control the pharmaceutical formulation's identity. While chromatographic techniques were mainly a subject of review publications, their use was rare in experimental work in the 1940s and 1950s. In the 1960s and 1970s, thin layer chromatography and paper chromatography were introduced. Herbal medicine analysis and the field of phytochemistry research were developed due to these new analytical tools. At the end of the 20th century, the development of column chromatography-based techniques, such as high-performance liquid chromatography and gas chromatography were a major milestone. These techniques were widely applied in pharmaceutical analysis to test the impurities, assess the stability of drugs, pharmacokinetics studies, and test for degradation products. In the 21st Century, new detection techniques in liquid and gas chromatography were introduced [115].

1.6.1 High-Performance Liquid Chromatography (HPLC) Technique

HPLC is a kind of column chromatographic analysis technique used to separate, identify, as well as quantify the compounds in a mixture [116]. HPLC technique is mainly utilised for biological sample analysis. It mainly consists of a stationary phase (bound to silica particles in a column) and a mobile phase (solvent system). It depends on pumps to pass a pressurised mobile phase(s) through the column and a detector that shows the separation of components of the mixture (retention times of the molecules). The retention time of the

compounds depends on the interactions between the stationary phase and the mobile phase used [116]. A small volume of the sample of interest is introduced to the mobile phase stream and analytes are retarded by certain physical or chemical interactions with the stationary phase. The extent of retardation depends on the composition of both the mobile and stationary phases as well as on the nature of the analyte. Retention time is the time at which a specific analyte comes out of the end of the column. A miscible combination of organic solvents and water such as acetonitrile-water and methanol-water are common solvents used in reversed-phase HPLC [116]. Separation is achieved by an isocratic elution, where the mobile phase composition remains constant, or separation is achieved by gradient elution where the composition of the mobile phase change during the analysis. In gradient elution separation of the analyte, mixtures are based on the function of the analyte affinity for the current mobile phase [117]. After exiting the column, the mobile phase passes through a detector, e.g. a UV-absorbance detector. To optimise the sensitivity of HPLC detection, the selection of suitable detectors and wavelengths is crucial. The detector produces a signal relating to the amount of analyte present in the sample which is then amplified and recorded by an HPLC acquisition system [117]. There are two liquid chromatography techniques normal phase and reverse phase. The main difference between the two HPLC techniques is that the normal phase utilises a less polar mobile phase and polar stationary phase while the reverse phase utilises a polar mobile phase and a nonpolar stationary phase.

1.6.2 History of HPLC

Early LC systems/methods were not so efficient because the flow rate of solvents was reliant on gravity. Separations times were very long, and some analysis took days to finish. At this time, gas chromatography (GC) was more efficient than liquid chromatography; in any case, it was believed that gas stage partition, as well as analysis of highly polar biopolymers (high atomic weight), was not possible. GC separation was inadequate for some researchers due to the thermal instability of the solutes [118]. Therefore, alternative methods were hypothesised that would soon bring about the development of HPLC. In 1960, the original work of Martin and Synge was developed by Josef Huber, Cal Giddings, and others that showed liquid chromatography (LC) can be worked in a high-efficiency mode by reducing the particle size to 150 µm as well as using pressure to increase the linear

velocity. The early developmental evaluation started to improve LC particles, and the innovation of Zipax, a superficially permeable molecule, was promising for HPLC technology. There were numerous improvements in equipment and instrumentation in the 1970s. Experts started using injectors and pumps to make an easy configuration of an HPLC system. Gas amplifier pumps were introduced as they worked at a consistent pressure. After the appearance of permeable layer particles, the efficiency was enhanced by decreasing the molecule size. However, new concerns appeared, so another set of instrumental developments were needed to cope with the pressure [118].

1.6.3 Applications of HPLC

HPLC gives us information for the identification, quantification, as well as resolution of a compound. Preparative HPLC entails the process of compound isolation and purification, while analytical HPLC gives information about the sample compound [116].

The pharmaceutical applications of HPLC cover the shelf-life determinations of pharmaceutical products, the tablet dissolution study, and the identification of active ingredients of the pharmaceutical dosage form. Environmental applications include biomonitoring of pollutants, detection of phenolic compounds in drinking water as well as identification of diphenhydramine in sedimented samples [116]. HPLC is also widely used in forensics like analysis of textile dyes, identification of anabolic steroids in urine, hair, and sweat and quantification of drugs in biological samples. Clinically HPLC is used for the analysis of antibiotics in blood plasma, quantification of ions in human urine and estimation of bilirubin and biliverdin in blood plasma in hepatic patients. In food analysis, HPLC is used to ensure the quality of drinking water and soft drinks, sugar analysis in fruit juices, analysis of beer and analysis of polycyclic compounds in vegetables [116]. Some advantages and limitations of HPLC are summarised below in Table 3.

Table 3. Advantages and limitations of HPLC.

Advantages	Limitations
Precise and highly reproducible for quantitative analysis	Relatively difficult for inexperienced operators
Liquid Chromatography-Mass Spectrometry	Separation efficiency is less than capillary gas chromatography

Automated, flexible, customizable operation	Still difficult for regulatory testing
Sensitive detection with high separation power	Need for a standard universal detector
Responsive to the various sample types and analyte	-

Several biological samples are tested using ultraviolet spectroscopy together with the retention data of unknown drugs and metabolites. Due to the complex nature of the body fluid or biological samples, the extraction method must be performed to isolate the drugs of interest from co-extractives. The drugs of interest were further analysed by High-Performance Liquid Chromatography with the chosen stationary phase, eluents, detector, and software program during separation [119].

The 25(OH)D_2, as well as 25(OH)D_3 levels in plasma, are measured as the best indicator of the physiological status of Vitamin D; therefore, there is a great requirement for easy and precise techniques for pharmaceutical determinations as well as establishing plasma content of metabolites of Vitamin D in food [120]. Analytical techniques such as commercial immune binding assay kits (radioimmunoassay) and High-Performance Liquid Chromatography (HPLC) are useful for the analytical measurement. Unluckily, immune binding kits are incapable to differentiate among neighbouring metabolites of Vitamin (D(25(OH)D_2 and 25(OH)D_3) [120]. In most cases, the difficulty is also met in normal phase HPLC, whereas reverse phase HPLC with UV detection is the most suitable as well as easiest HPLC technique to work with. HPLC techniques offer the best method for the precise determination of pharmaceuticals and stability testing. Due to the lack of specificity, it is not always ideal for the resolution of the analyte. Though it has some advantages, such as it provides excellent linearity, as well as rapid quantitative analyses of the compounds of interest. HPLC instrument contains a high-pressure pump, an injector, a column, and a detector. The data is integrated through an acquisition system (Figure 17). The most important part of the instrument is the column where all the separation occurs.

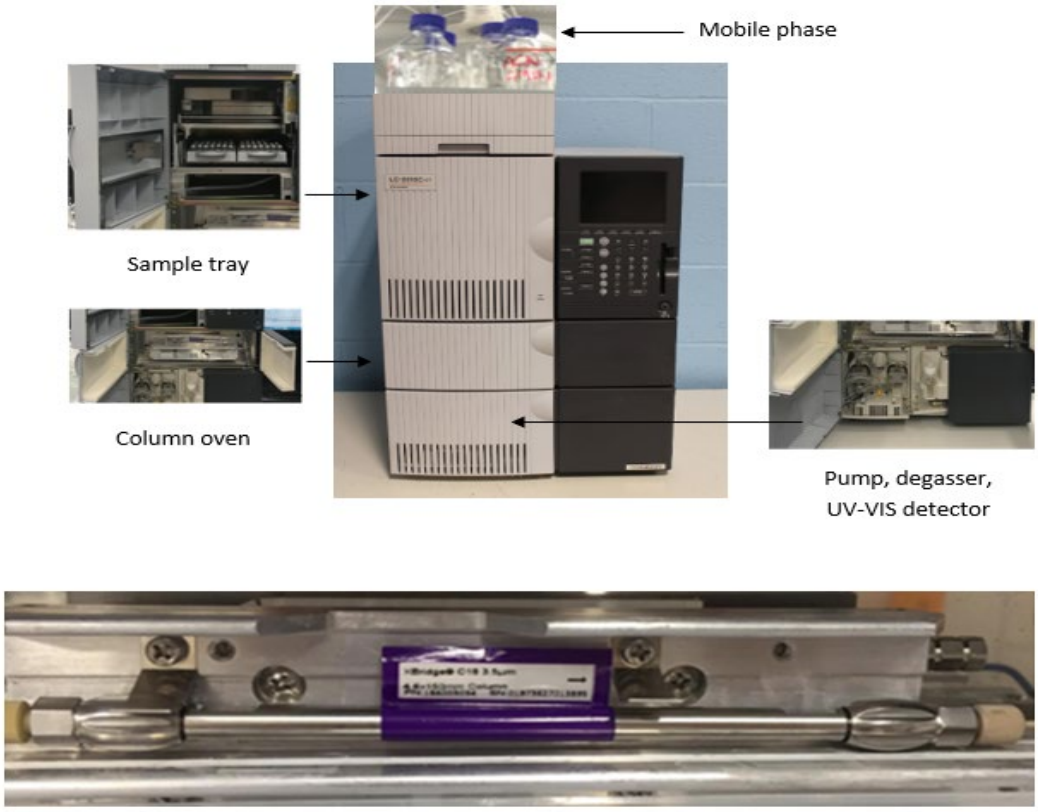

Figure 17. Illustration of the chromatographic system in HPLC.

1.6.4 Stability Studies using HPLC

The stability study in pharmaceuticals is important and the reason is to avoid any potentially toxic degradation products. The purpose of such studies is to demonstrate that the drug of interest has not changed over a specific period. In the case of degradation products formation, it is necessary to quantify them as well, because the formation of any degradation product from a formulation excipient may start an alteration in the drug release characteristics of the formulation, e.g., lactose, a commonly used excipient, can experience anomerisation in solution and converts to its α and β forms [119].

Today in the Pharmacopoeias of European, the USA, and UK, HPLC is used instead of other instrumental and chemical methods for the analysis of the drugs. As technology is emerging day by day, thus more efficient systems like HPLC-MS as well as HPLC-NMR (^{1}H NMR and ^{13}C NMR) are developed and their applications will have a huge potential in medical diagnostics. However, the utilisation of LC-MS/MS equipment is expensive and

needs a great deal of practical experience [120]. Systematic sample clean-up, as well as concentration, is typically accomplished via solid-phase extraction (SPE), liquid-liquid extraction with or without alkaline saponification, or preparative HPLC. Also, the addition of a suitable internal standard is a very effective way of lessening variation among samples and generating precise results [120].

1.7 *In vitro* analysis of substrates and metabolites

Identification of metabolites and profiling are important in several stages of drug discovery and development. To develop a new therapeutic agent, there is always a preclinical screening stage that requires research of the toxicological, pharmacodynamic, and pharmacokinetic properties of the drug. To investigate these properties, both *in vitro* and *in vivo* trials in different animal species are required [121]. Models of human drug metabolism are used to study *in vitro* drug metabolism and *in vitro* comparative studies are performed using tissue or enzymes from experimental species and humans and this provides a better estimation of the risk assessment gained from toxicology studies of the patient [121]. An essential issue in toxicology is that the information obtained from experimental animals should be suitable for human risk assessment. Still, the data acquired in animal studies can be better inferred for the patient by applying bridging studies with *in vitro* models of human drug metabolism. There are two basic categories of *in vitro* methods for the examination of human liver drug metabolism. The first group includes cell lines, primary hepatocytes, and liver slices while the second group includes the utilisation of the drug-metabolising enzyme preparations such as cytochrome P450, superasomes, S9 fraction, cytosolic fraction, rat and human liver microsomes. *In vitro* studies can distinguish the species-specific metabolic routes, as well as the experimental animal models which best indicate the possible human exposure to the drug (substrate) and its metabolites [121]

Identification of metabolite certainty can vary widely as the method of metabolite identification is complicated and generally depends on the robustness of the analytical techniques. In biological samples, direct quantification of metabolites is the most appropriate method, but similarly, other methods such as quantification supported by using response factors or indirect quantification of metabolite through parent drug (substrate) after metabolite hydrolysis may be used which mainly depends on the accessibility of suitable reliable standards. A typical identification method of Identification

of substrate and metabolites is using a radiolabelled parent drug (substrate). Different parameters can be calculated such as the percentage of the dose found in faeces and urine [121]. The primary detection method for the drug and metabolites' quantification was ultraviolet (UV) detection. It is simple to use, reliable and robust but has relatively poor sensitivity in the absence of a chromophore [122]. To determine drugs and their metabolites, electrochemical detectors, fluorescence, and UV are usually coupled with liquid chromatography (LC). LC ideally needs baseline separation for quantification purposes. HPLC coupled with UV is still extensively in use for the quantification of metabolites in biological samples [122]. Modern analytical approaches for metabolite quantification are based on liquid chromatography such as separation systems attached with several detector systems where LC-MS/MS plays a predominant role in bioassays for pharmacokinetic and metabolism studies due to its inherent specificity, sensitivity and speed.

David *et al.* have reported the *in vitro* impact of a medicinal plant *(Hyptis verticillate)* on a number of key CYP450 (CYPs 1A1, 1A2, 1B1, 3A4, and 2D6) enzymes. They determined its antioxidant properties (via 2,2-diphenyl- 1-picrylhydrazyl DPPH assays), chemical characterisation (utilising RP-HPLC and LC-MS) as well as its further effect on CYP1A2 [123]. They found that aqueous extract of dried plant showed potent inhibition of CYPs 1A1, 1A2, 3A4, and 1B1 activities. Further analysis demonstrated the identity of five lignans, seven phytochemicals, and two triterpenes [123]. These phytochemicals were individually screened against the CYP1A2 activity and yatein (phytochemical) was identified as a moderate inhibitor at 71.9 μM [123].

Yasuhiro *et al.* have performed an immunochemical study to examine the selectivity and ability of diclofenac to inhibit P450 enzymes via time-dependent loss of 2α and 16α hydroxylation activities of testosterone [124]. For this purpose, they preincubated diclofenac with the rat liver microsomes in the presence of NADPH while no effect of the preincubation was seen on activities of pentoxyresorufin *O*-dependentylase, ethoxyresorufin *O*-deethylase, and pentoxyresorufin *O*-dependentylase. The reaction followed pseudo-first-order kinetics for time-dependent decreases in 2α and 16α hydroxylation activities of testosterone as all the sites were saturable when the concentration of diclofenac was increased [124]. They concluded from the obtained data that a mechanism-based CYP2C11 inactivation occurs in the oxidative metabolism of diclofenac. On the other hand, in human liver microsomes, diclofenac metabolism did not cause CYP2C9 activation. Since the human

liver microsomes have got much less 5-hydroxylation activity and high diclofenac 4-hydroxylation activity, the latter pathway is suggested for inactivation [124].

Yoo-Seong *et al*. have proposed a physiologically based pharmacokinetic (PBPK) model that explains the procainamide (PA) and *N*-acetylprocainamide (NAPA) pharmacokinetics. NAPA is a primary metabolite of PA [125]. They studied PA and NAPA pharmacokinetics using the presence or absence of cimetidine in male rats and S9 fractions using UHPLC and LCMS [125]. Using their refined PBPK, they successfully predicted PA and NAPA interactions with cimetidine with respect to the urinary and plasma concentration excretion profiles of PA and NAPA. Their study also indicated that the cimetidine inhibitory effect via rMATE1 in rats may be significant in the renal elimination kinetics of PA and NAPA [125].

1.7 Aim of the Project

There are no previous studies that have been conducted to see the *in vitro* inhibition of CYP3A2 isoenzyme activity by aspirin, ibuprofen, remdesivir, and omeprazole using dexamethasone as a substrate (drugs often used together in COVID-19 treatment) and inhibition of CY2C11 by testosterone using Vitamin D_3 and D_2 as a substrate. Thus, this research project aims to develop and validate novel High-Performance Liquid Chromatography method (HPLC) methods for the simultaneous measurement of metabolic reactions products catalysed by hepatic CYP enzymes and study their kinetics in rat microsomes.

The specific objectives to achieve this aim are given below:

- Development and validation of an HPLC method to analyse metabolic reaction products catalysed by the CYP3A2 isoform to see inhibition of CYP3A2 enzyme activity by aspirin *in vitro*.
- Potential assessments of the effects of ibuprofen, remdesivir and omeprazole on dexamethasone metabolism (CYP3A2 enzyme activity) *in vitro*.
- Development and validation of an HPLC method for the quantitative determination of Vitamin D metabolites to see the effect of testosterone on CYP2C11 enzyme activity *in vitro.*

CHAPTER 2

DEVELOPMENT AND VALIDATION OF A NOVEL HPLC METHOD TO ANALYSE METABOLIC REACTION PRODUCTS CATALYSED BY CYP3A2 ISOFORM: *IN VITRO* INHIBITION OF DEXAMETHASONE METABOLISM (CYP3A2 ENZYME ACTIVITY) BY ASPIRIN (DRUGS OFTEN USED TOGETHER IN COVID-19 TREATMENT)

Publication

A. Hussain, D. P. Naughton, and J. Barker, "Development and Validation of a Novel HPLC Method to Analyse Metabolic Reaction Products Catalysed by the CYP3A2 Isoform: *In Vitro* Inhibition of CYP3A2 Enzyme Activity by Aspirin (Drugs Often Used Together in COVID-19 Treatment)," *Molecules*, vol. 27, no. 3, pp. 927, Jan. 2022.

Conference

A. Hussain, D. P. Naughton, and J. Barker. Inhibition of CYP3A2 enzyme activity by Aspirin in the Metabolism of Dexamethasone. The JPAG pharmaceutical analysis research awards, 2021. Poster presentation.

2.1 Introduction

Cytochrome P450 enzymes are responsible for the biotransformation of xenobiotics and the metabolism of endogenous compounds [126]. They are mainly found in the liver; however, a number of these enzymes are also expressed in the kidney, small intestine, placenta, and lungs [127]. The synthesis of these enzymes takes place endogenously, and both non-genetic and genetic factors could influence enzyme synthesis. Many drug–drug interactions of clinical interest change the pharmacokinetic behaviour of drugs due to changes in the hepatic metabolic pathway of drugs that are catalysed by CYP450 enzymes [128]. The drug interactions are caused by either CYP450 inhibition or induction. Enzyme induction or inhibition by food, drugs, and medicinal herbs, for instance, can be responsible for changes in the metabolic capacity of these enzymes [129], although inhibition is considered more important in terms of adverse clinical outcomes.

CYP450 enzyme inhibition by drugs could increase the concentration of other metabolising drugs and could result in drug toxicity issues [130]. CYP3A is the most important family among the identified families of CYP450 enzymes involved in biotransformation and metabolism in humans. The CYP3A family is responsible for the metabolism of 70 % of drugs as well as indicating broad substrate specificity [131]. CYP3A is frequently associated with most drug interactions because this isoform is highly inducible and could potentially be inhibited by other drugs and herbs [131]. Of the various isoforms, CYP3A4 is the most abundant isoform present in the human liver microsomes and responsible for the metabolism of various anticancer drugs [132]. Although CYP3A4 activity exhibits a 5-10-fold inter-individual variability, it still has substantial potential for clinical applications [132].

Dexamethasone is a steroidal anti-inflammatory drug that is widely used for the treatment of different conditions such as cancer, autoimmune diseases, and chronic inflammatory diseases [133]. The use of dexamethasone to treat multiple diseases significantly increases the risk of drug-drug interactions [134]. Tomlinson *et al.* (1997) stated that dexamethasone is metabolised into 6α as a minor metabolite and 6β-hydroxymethasone as a major metabolite through the CYP3A4 enzyme activity using human liver microsomes.

Previous studies have shown that ketoconazole, ellipticine, and gestodene cause inhibition of dexamethasone 6-hydroxylation [135]. Although many studies have been conducted on human liver microsomes, rats have the closest metabolic profile to humans and show 71% sequence homology [136]. The CYP3A2 isoform in male-specific rat liver microsomes (RLMs) is responsible for the 6-hydroxylation of dexamethasone (corticosteroid) [136]. Wang *et al.* [137] stated that codeine administration in male rats can inhibit the metabolism of midazolam (CYP3A2 activity).

COVID-19 infection has rapidly grown into a worldwide pandemic, and this has had a significant impact on human health. Dexamethasone and aspirin (Figure 18) are some of the drugs being used for the treatment of COVID-19 during the pandemic. The combined use of aspirin and dexamethasone has been shown to reduce the symptoms of moderate to severe COVID-19 infection [138]. A recent study has provided evidence in support of primary healthcare centres where they used aspirin and dexamethasone for the therapeutic management of severe COVID-19 patients [139]. Nonsteroidal anti-inflammatory drugs (NSAIDs) and aspirin are the most used therapeutic drugs worldwide [140]. Aspirin is an O-acetyl derivative of salicylic acid (acetylsalicylic acid). It is believed that it transfers this acetyl group to amino ($-NH_2$) and hydroxy (-OH) functionalities present in biological molecules [141]. Aspirin is also a prostaglandin synthase inhibitor that inhibits the production of prostaglandins. It has a non-selective effect on the cyclooxygenase-1 (COX-1) and cyclooxygenase-2 (COX-2) enzymes [142].

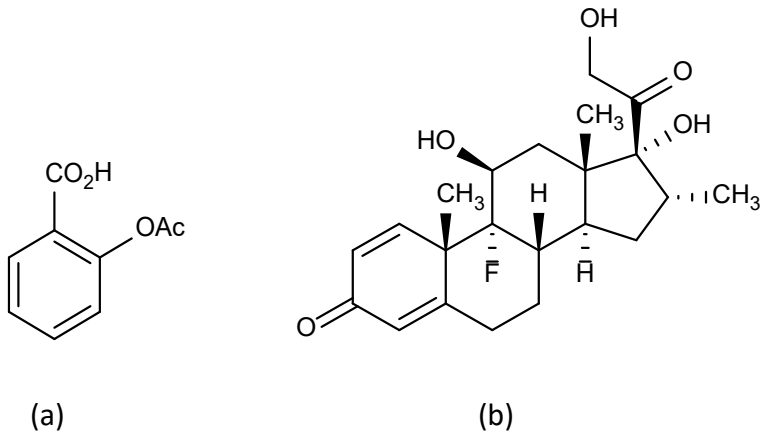

(a) (b)

Figure 18. (a) Aspirin (inhibitor), (b) Dexamethasone (substrate).

In this systematic study, a HPLC method has been developed and validated to investigate the impact of aspirin on the activity of the CYP3A2 enzyme in rat liver microsomes, whereby dexamethasone was the substrate. This study promotes the safe administration of Covid-19 drugs (dexamethasone and aspirin) in clinical practice.

2.2 Materials and Methods

2.2.1 Chemicals

6β-Hydroxydexamethasone was purchased from Cayman Chemical Company (East Ellsworth Road, Ann Arbor, Michigan, USA). Dexamethasone was obtained from Tokyo Chemical Industry CO.LTD Japan and 4'- hydroxyoctanophenone with purity greater than 99% was obtained from Alfa Aesar (A Johnson Matthey company, UK). Potassium phosphate monobasic, potassium phosphate dibasic, glucose-6-phosphate (G-6-P), glucose-6-phosphate dehydrogenase (G-6-PDH), phosphoric acid (85% w/w), $NADP^+$ (nicotinamide adenine dinucleotide phosphate), EDTA (ethylenediaminetetraacetic acid), magnesium chloride ($MgCl_2$) were purchased from Merck. Diethyl ether was purchased from Fischer Scientific (UK) and ethyl acetate from VWR chemicals (France). HPLC grade acetonitrile and water were obtained from Merck, Co. (UK).
The pooled liver microsomes from male rats (Sprague-Dawley) were purchased from Merck (UK) and stored at -80^oC.

2.2.2 Instruments

A 570-pH meter from JANEWAY Limited (UK) was purchased. A high-performance liquid chromatographic system (LC-2010A HT Shimadzu Corporation from Japan) was used for the analysis equipped with a degasser, a UV detector, a low-pressure quaternary pump, a LC column oven, and an autosampler. A WATERS (Waters Corporation, United States) C18 column (15 mm × 4.6 mm, 3.5 µm particle size) was used for chromatographic separation. The chromatographic data were processed using Shimadzu HPLC 1 LabSolutions (software processing system). The shaking incubator used for the incubation of the tubes was made by Eppendorf UK limited.

2.2.3 Cytochrome P450 Assay

2.2.3.1. Dexamethasone 6β-hydroxylation Assay for CYP3A2

Assay development and validation were carried out using a LC-2010A HT Module HPLC system (Shimadzu, Toyko, Japan). Target components (4-hydroxyoctanophenone used as

an internal standard, aspirin as inhibitor, dexamethasone as CYP3A2 substrate, and 6β-hydroxydexamethasone as CYP3A2 metabolite) were separated in a C18 column. A good separation of compounds of interest was achieved using the optimised acetonitrile/water (70%/30%, v/v) mobile phase. The retention time (t_R) of the four compounds is shown in Table 3. The chromatographic separation was performed at 25 °C and a flow rate of 0.6 mL/min. 10 µL solution volume was injected for HPLC analysis and all the components were detected at 243 nm wavelength. Table 3 gives information concerning efficiency (N) where $N = 5.54\times(t_R/W_{½})$ and $W_{½}$ = width at half peak height; plate height (H) where H(cm) = column length/N; asymmetry factor (AsF) where AsF = B/A and A is the distance from the leading edge of the peak to the midpoint of the peak measured at 10% of peak height and B is the distance from the midpoint of the peak to the trailing edge of the peak measured at 10% of peak height and resolution (R_s) where $Rs = \Delta t_R/0.5(W_1+W_2)$ and W is the width at peak base. As can be seen from Table 4, these chromatographic parameters show that the methodology has been suitably optimised with a total run time under 8 min.

Table 4. Column efficiency, plate height, asymmetry, and resolution of compounds of interest.

	Aspirin	**6β-hydroxydexamethasone**	**Dexamethasone**	**Internal standard**
Retention Time (t_R)	2.09	2.65	3.08	6.66
Efficiency (N)	1078	970	3363	6137
Plate Height (H)	1.39×10^{-2}	1.55×10^{-2}	4.46×10^{-3}	2.44×10^{-3}
Resolution (R_s)		0.79	0.67	5.51
Asymmetry Factor (AsF)	0.97	1.03	1.07	1.07

2.2.3.2 Microsomal Incubations Procedure

Microsomal protein (0.5 mg/mL) was incubated at 37 °C with a serial range of dexamethasone (10, 20, 30, 40 and 50 µM), magnesium chloride (3.0 mM), NADPH (1.0

mM), Glucose-6-Phosphate (5 mM), Glucose-6-Phosphate Dehydrogenase (1.7 units/mL), Ethylenediaminetetraacetic acid (1.0 mM EDTA) and 0.067 M potassium phosphate buffer (pH 7.4) in a final volume of 500 µL. A serial range of aspirin (0, 50, 100, and 200 µM, dissolved in the mobile phase) was added to the incubation mixture in triplicate. Incubations were for 40 min and initiated by the addition of $NADP^+$ (nicotinamide adenine dinucleotide phosphate) to the mixture after pre-incubation of all components for 5 min in a water bath (T = 37 °C).

Ice-cold grade acetonitrile containing 15 µM of 4-hydroxyoctanophenone (as an internal standard) was added to terminate the reaction. Dexamethasone and metabolite were extracted with ethyl acetate (3 ml) and then with diethyl ether (3 ml). The polar extracts were evaporated to dryness and residues were dissolved in the mobile phase (70% acetonitrile and 30% water, v/v) and made up to 1000 µL volume. 10 µL of each sample was injected into the HPLC instrument for analysis.

2.2.4 Preparation of Standard Substrate and Metabolite Solutions

For the cytochrome P3A2 enzyme assay, 4-hydroxyoctanophenone was used as an internal standard. 0.0010 g of the powder was dissolved in acetonitrile in a 10 mL volumetric flask. The final stock (15 µM) was prepared by adding 165 µl from stock in a volumetric flask containing 49.835 mL of mobile phase (70% methanol + 30% water, v/v).

Aspirin (0.0018 g) (C = 1000 µM) was weighed accurately and dissolved in a 10 mL volumetric flask in methanol. Serial dilutions of aspirin (200, 100, and 50 µM) were performed. 0.0039 g of dexamethasone (C = 1000 µM) was weighed and added to a 10 mL volumetric flask containing methanol. Different concentrations of dexamethasone (50, 40, 30, 20, and 10 µM) from the stock solution were prepared in the mobile phase (70% methanol + 30% water, v/v). The metabolite (6β-hydroxydexamethasone) stock solution of 2 µM was prepared in the mobile phase (70% methanol + 30% water, v/v) and serial dilutions (0.2, 0.4, 0.6, 0.8 and 1 µM) were prepared from the stock.

2.2.5 Optimisation of Incubation Time *in vitro*

The concentration of dexamethasone (substrate) and protein was fixed in the incubation system and samples were incubated for 10, 20, 30, 40, 50, 60, 70, and 100 minutes, respectively. The samples were prepared and incubated as described in section 2.2.3. The concentrations of produced metabolite 6β-hydroxydexamethasone were calculated from the standard calibration curve. The optimal incubation time was determined by the linear relationship between the time and metabolite concentration.

2.2.6 Data Analysis

Data were analysed using Microsoft Excel 2010 software for validation and kinetic parameters. All results are shown as mean ± S.D. The least-square regression analysis was performed to calculate the concentration of the produced metabolite by CYP reaction. Secondary Lineweaver-Burk plots and Michaelis-Menten plots were plotted to find kinetic parameters such as K_i, V_{max}, K_m, $Cl_{int,}$ and α'. Inhibition was assumed as competitive based on the obtained data and visual inspection of the Lineweaver-Burk plot. The concentration of inhibitor causing a 50% reduction in enzyme activity (IC_{50}) was calculated by plotting the percentage of remaining control enzyme activity versus the concentration of inhibitor. K_m values were used to calculate the percentage inhibition.

2.3 Results and Discussion

2.3.1 HPLC Method Development

The analytical method for the enzymatic assay was optimised and evaluated using the following chromatographic conditions: mobile phase consisting of acetonitrile and water (70% acetonitrile and 30% H_2O, v/v) with an injection volume of 10 µl, a flow rate of 0.6 mL/min, column temperature set at 25 °C and a run time of 8 min. The chosen wavelength (λ) was 243 nm [94]. The selected internal standard was 4-hydroxyoctanophenone.

2.3.2 HPLC Method Validation

2.3.2.1 Linearity and Range

According to ICH guidelines [143], the linearity was tested using different concentrations (0, 25, 50, 100, 150, and 200 µM) of working solutions of dexamethasone and 6β-hydroxydexamethasone (0, 0.2, 0.4, 0.6, 0.8, and 1 µM). Working solutions were prepared in the mobile phase (70% acetonitrile and 30% H_2O, v/v) and injected into the HPLC for the construction of the calibration curve. The mean peak area obtained from HPLC chromatograms was plotted against the concentrations of each analyte (dexamethasone and 6β-hydroxydexamethasone) to assess the calibration graph. All obtained data were corrected for the internal standard. Table 5 represents the results of the linearity study. The r^2 values were within the acceptable ICH criterion ($r^2 > 0.99$) and the relative standard deviation at each concentration (%RSD < 10%) met the criteria of ICH guidelines.

Table 5. Linearity data from the proposed analytical method.

Standards	Dexamethasone	6β-Hydroxydexamethasone
Regression equation	y = 0.2505x + 0.0945	y = 1.6775x + 0.0385
r^2	0.999	0.998
Linear range	25-200 µM	0.2-1 µM

2.3.2.2 Specificity and Selectivity

Specificity/selectivity was evaluated by running the diluent blank (70% acetonitrile and 30% H_2O, v/v) and internal standard solution (15 µM) in a 1 ml HPLC vial to check that the outcomes of the analytical method were not altered by the drugs' constituents (Figure 19). Figure 20 shows the separation of enzyme peak (NADPH (nicotinamide adenine dinucleotide phosphate hydrogen-regenerating system) from the inhibitor (aspirin 200 µM), metabolite (6β-hydroxydexamethasone), dexamethasone, and internal standard.

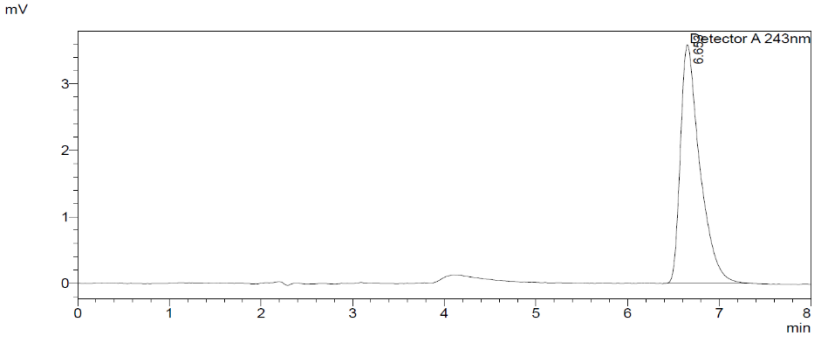

Figure 19. Negative control blank shows the specificity of the method.

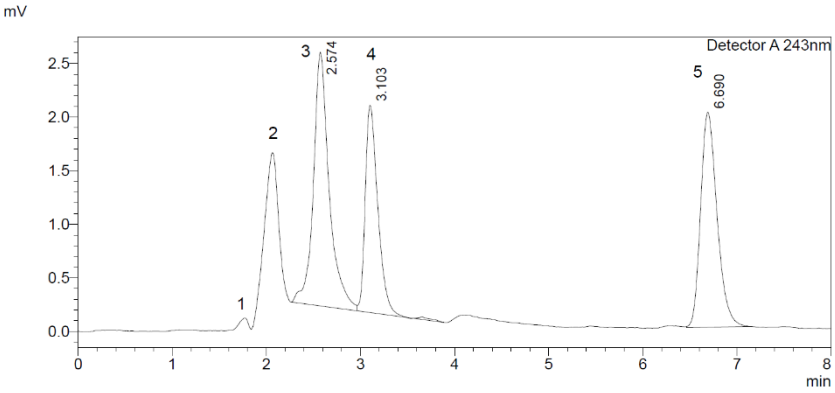

Figure 20. HPLC profile of CYP3A2 assay components. (1) NADPH (Nicotinamide AdenineDinucleotide Phosphate Hydrogen)-regenerating system, (2) aspirin, (3) 6β-hydroxydexamethasone, (4) dexamethasone and (5) 4-hydroxyoctanophenone (IS).

2.3.2.3 Limit of Detection (LOD) and Limit of Quantification (LOQ)

The sensitivity of the analytical method is achieved by the evaluation of its LOD and LOQ. The lowest detectable concentration of the analyte is LOD. The minimum measurable concentration by the analytical method and can be determined quantitatively with suitable

precision is LOQ. The standard deviation (σ) method was used to determine LOD and LOQ by using the following formulae:

$$LOD = (3.3 \times \sigma/S)$$

$$LOQ = (10 \times \sigma/S)$$

Where S is the slope of the calibration curve.

The values of LOD and LOQ for dexamethasone and 6β-hydroxydexamethasone are presented in Table 6.

Table 6. LOD and LOQ for dexamethasone and 6β-hydroxydexamethasone.

Standards	Dexamethasone	6β-Hydroxydexamethasone
LOD	5.60 µM	0.06 µM
LOQ	16.98 µM	0.19 µM

2.3.2.4 Precision

Intraday Precision of Dexamethasone

The intraday method precision was determined by analysing standard samples in triplicate at three different concentrations levels, i.e., low (40 µM), medium (110 µM), and high (185 µM) of dexamethasone. The results are summarised in Table 7. The percentage relative standard deviation (%RSD) was < 5% for dexamethasone and recovery values were found to be within the range of the ICH acceptance criterion (80-120%). The outcomes revealed that there is no large variation in the concentration of dexamethasone in intraday analysis. The obtained values were considered satisfactory for the planned use of the method.

Table 7. Intraday precision and recovery for dexamethasone (n=3).

Dexamethasone Standards	Mean (µM)	Recovery [a] (%)	RSD (%)
Low concentration (40 µM)	39.28±0.90	98.21	2.30
Medium concentration (110 µM)	99.06±3.06	90.05	3.09

High concentration (185 µM)	151.11±0.76	81.68	0.50

Note: Recovery is the ratio of the concentration of analyte recovered to the theoretical concentration. [a] % recovery = (concentration of dexamethasone at 5 hours/standard concentration of dexamethasone) x 100.

Interday Precision of Dexamethasone

The interday precision was determined by injecting standard samples solution for three consecutive days at three concentration levels (low (40 µM), medium (110 µM), and high (185 µM)). Each sample was run in triplicate. The results are summarised in Table 8 which shows that the recovery values are within the ICH guidelines range (80-120%) and the percentage relative standard deviation (%RSD) was < 5% for dexamethasone. The outcomes of the experiment revealed that there is no large variation in interday analysis.

Table 8. Interday precision and recovery for dexamethasone (n=3).

Dexamethasone Standards	Mean (µM)	Recovery [a] (%)	RSD (%)
Low concentration (40 µM)	45.01±2.09	112.52	4.65
Medium concentration (110 µM)	110.01±2.17	100.01	1.98
High concentration (185 µM)	178.92±3.13	96.72	1.75

Note: [a] % recovery = (concentration of dexamethasone at 5 hours/standard concentration of dexamethasone) x 100.

Intraday Precision of 6β-hydroxydexamethasone

Intraday precision of 6β-hydroxydexamethasone was assessed by measuring (low (0.3 µM), medium (0.5 µM), and high (0.85 µM) concentrations in triplicate in a batch experiment. The results are shown in Table 9 and illustrate that recovery values (80-120%) are within the ICH guidelines range and the percentage relative standard deviation values (% RSD) are < 10% for 6β-hydroxydexamethasone. The experiment outcomes revealed that there is no large variation present between the concentration of 6β-hydroxydexamethasone samples in the intraday precision analysis.

Table 9. Intraday precision and recovery for 6β-hydroxydexamethasone (n=3).

6β-hydroxydexamethasone Standards	Mean (µM)	Recovery [a] (%)	RSD (%)
Low concentration (0.3 µM)	0.33±0.01	108.60	2.21
Medium concentration (0.5 µM)	0.50±0.02	100.01	3.64
High concentration (0.85 µM)	1.02±0.09	119.38	8.82

Note: [a] % recovery = (concentration of 6β-hydroxydexamethasone at 5 hours/standard concentration of 6β-hydroxydexamethasone) x 100.

Interday Precision of 6β-hydroxydexamethasone

Interday precision was evaluated by measuring 6β-hydroxydexamethasone standard solution at three concentrations levels (low (0.3 µM), medium (0.5 µM) and high (0.85 µM) for three consecutive days. The results of the experiment are shown in Table 10. The %RSD (relative standard deviation) is < 10% for 6β-hydroxydexamethasone and recovery values are within the ICH guidelines range (80-120%). The experimental data revealed that no large variations are present in terms of inter-assay precision.

Table 10. Interday precision and recovery for 6β-hydroxydexamethasone (n=3).

6β-hydroxydexamethasone Standards	Mean (µM)	Recovery [a] (%)	RSD (%)
Low concentration (0.3 µM)	0.32±0.02	107.61	4.67
Medium concentration (0.5 µM)	0.50±0.03	99.28	5.90
High concentration (0.85 µM)	0.79±0.03	93.13	4.13

Note: [a] % recovery = (concentration of 6β-hydroxydexamethasone at 5 hours/standard concentration of 6β-hydroxydexamethasone) x 100.

2.3.2.5 Stability Study

Solution Stability of Substrate (Dexamethasone)

For stability testing, dexamethasone calibration curves were run for intraday and interday measurements at three concentration levels (40, 110, and 185 µM) at ambient temperature. Stability samples were analysed in triplicate. The results of the stability tests are shown in Table 11.

Table 11. Dexamethasone solutions stability at ambient temperature.

Analytical Parameters	**Actual Concentration (µM)**			
	Intraday	**40**	**110**	**185**
Calculated Concentration (µM)	0 hours	35.40	88.64	176.98
	5 hours	32.20	92.43	202.56
	10 hours	32.32	92.87	203.56
% Recovery	0 hours	88.51	80.58	95.66
	5 hours	80.50	84.03	109.49
	10 hours	80.80	84.43	110.03
% Accuracy [a]	0 hours	111.49	119.42	104.34
	5 hours	119.51	115.97	90.51
	10 hours	119.20	115.57	89.97
Calculated Concentration (µM)	**Interday**	**40**	**110**	**185**
	Interday 1	32.02	94.39	181.79
	Interday 2	34.99	100.43	193.84
	Interday 3	34.12	90.60	187.22
% Recovery	Interday 1	80.04	85.81	98.26
	Interday 2	87.31	91.30	104.78
	Interday 3	85.29	82.36	101.20
% Accuracy [a]	Interday 1	119.96	114.19	101.74
	Interday 2	112.70	108.70	95.22
	Interday 3	114.71	117.64	98.80

Note: [a]Accuracy = 100 – (calculated concentration – actual concentration)/actual concentration x 100

The outcomes of the interday and intraday stability checks indicate that there was no variation in the concentration of dexamethasone. In intraday stability analysis, the concentration of dexamethasone after 10 hours was the same as compared to the initial concentration at 0 hours whereas, in interday analysis, the chromatographic behaviour of dexamethasone remained the same on days 1, 2, and 3, compared to the initial concentrations. The r^2 value obtained from the calibration curves of intermediate (intraday) analysis was 0.9984 (in accordance with ICH guidelines). The calibration curve for repeatability analysis was averaged and the curve equation for dexamethasone was y = 0.277x + 0.6419, where the least regression square values (r^2) were within ICH guidelines (0.9981). Linear equations were further used to calculate dexamethasone concentrations (low, medium, and high) and their % recovery. The results reveal that the % recovery and accuracy values remained within the ICH guidelines range (80-120%). Furthermore, no substantial degradation within the day (intraday) and between days (interday) were observed (Table 11), thus showing that dexamethasone was stable for up to three days at ambient temperature, which is in accordance with the stability study performed by Heda *et al.* [144].

Solution Stability of 6β-hydroxydexamethasone (Metabolite)

Evaluation of the stability of the working standard solutions of 6β-hydroxydexamethasone was performed at ambient temperature by intraday and interday analysis at three concentration levels low (0.3 µM), medium (0.5 µM), and high (0.85 µM). Experiments were performed in triplicate and the results are summarised in Table 12, below.

Table 12. 6β-hydroxydexamethasone solutions stability at ambient temperature.

Analytical Parameters	**Actual Concentration (µM)**			
	Intraday	**0.3**	**0.5**	**0.85**
Calculated Concentration (µM)	0 hours	0.30	0.47	0.84
	5 hours	0.29	0.44	0.77
	10 hours	0.27	0.44	0.79
% Recovery	0 hours	98.18	94.82	99.34
	5 hours	97.22	87.58	90.45
	10 hours	88.89	87.75	92.98

% Accuracy [a]	0 hours	101.82	105.18	100.66
	5 hours	102.79	112.42	109.55
	10 hours	111.11	112.25	107.02
Calculated Concentration (µM)	**Interday**	**0.3**	**0.5**	**0.85**
	Interday 1	0.27	0.46	0.72
	Interday 2	0.32	0.47	0.69
	Interday 3	0.32	0.46	0.68
% Recovery	Interday 1	89.49	92.64	84.06
	Interday 2	105.46	94.15	81.57
	Interday 3	106.90	92.10	80.51
% Accuracy [a]	Interday 1	110.51	107.36	115.94
	Interday 2	94.54	105.85	118.43
	Interday 3	93.10	107.90	119.49

Note: [a]Accuracy = 100 – (calculated concentration – actual concentration)/actual concentration x 100

The results of the stability test of 6β-hydroxydexamethasone showed that there were no obvious changes perceived in the chromatographic behavior and elution profile of the metabolite. In intraday stability analysis, the chromatographic behaviour of 6β-hydroxydexamethasone after 10 hours remained the same as compared to the initial concentration at 0 hours whereas, in interday analysis, the concentration of 6β-hydroxy dexamethasone stayed the same at day 1, 2, and 3, compared to the initial concentrations. The calibration curve was plotted for intermediate analysis and the straight-line equation was y = 2.4559x + 0.0767. The averaged calibration curve of metabolites was constructed from three days' calibration data and the averaged straight-line equation was (y = 2.0023x + 0.0364). All the %recovery and % accuracy values were in the range specified by ICH guidelines (80-120%), demonstrating the fact that the metabolite solution was stable. Therefore, the results indicate that 6β-hydroxydexamethasone solution was stable at ambient temperature during intraday and interday analysis, which is in accordance with the literature [132]. It is evident that metabolite sample solutions need to be kept and run on HPLC for longer than overnight for the incubation process to see the inhibition.

2.3.2.6. Robustness of the Method

The robustness of the method (50 µM aspirin, 0.2 µM 6β-hydroxydexamethasone, 25 µM dexamethasone and 15 µM internal standard) was tested by changing the following

parameters: increasing wavelength by 5 nm, increasing temperature by 5 °C, and increasing flowrate. Therefore, replicate injections (n = 3) of standard multianalyte solution were performed. The observations were made based on peak areas and changes in retention time. Table 13 summarises the effect of wavelength, temperature and flow rate variation on the peak area and retention time of the compounds.

Table 13. Evaluation of robustness parameters (A) Change in temperature (B) Change in wavelength (C) Change in flow rate.

Analytes of Interest	Average t_R	Average peak area	Resolution
	Normal conditions (0.6 ml/min, 243 nm and 25 °C)		
Aspirin	2.04	16162.67	All compounds were well separated, and a good resolution was achieved.
6β-hydroxydexamethasone	2.64	127567.67	
Dexamethasone	3.08	58676.00	
4-hydroxyoctanophenone	6.67	31991.33	
	A: Temperature (30 °C)		
Aspirin	2.04	12351.00	All compounds were separated well, with a faster elution pattern as the temperature increased.
6β-hydroxydexamethasone	2.64	120462.67	
Dexamethasone	3.07	55890.67	
4-hydroxyoctanophenone	6.51	29137.67	
	B: Wavelength (248 nm)		
Aspirin	2.08	10039.33	All four compounds were separated but there was a decrease in intensity of metabolite peak.
6β-hydroxydexamethasone	2.67	75995.00	
Dexamethasone	3.08	49674.00	
4-hydroxyoctanophenone	6.61	53310.00	
	C: Flow rate (0.8 mL/min)		
Aspirin	1.42	6458.00	Peaks were separated with a 0.8 mL/min flow rate. All compounds showed a faster and narrow elution pattern.
6β-hydroxydexamethasone	1.99	97253.00	
Dexamethasone	2.33	38095.00	
4-hydroxyoctanophenone	5.02	22253.33	

The outcomes of the robustness test show that the developed method could optimally perform when small changes are made to parameters such as wavelength, temperature, and flow rate. Good separation of dexamethasone, 6β-hydroxydexamethasone, and internal standard were achieved for temperature, wavelength, and flow rate variations.

2.3.3 Optimisation of Incubation Time for Incubation System *in vitro*

The incubation time was optimised (Figure 21). The 6β-hydroxydexamethasone formation rate from dexamethasone (50 µM) by cytochrome P3A2 was linear and took place over 40 min. Thus, the optimal incubation time for CYP3A2 was 40 min.

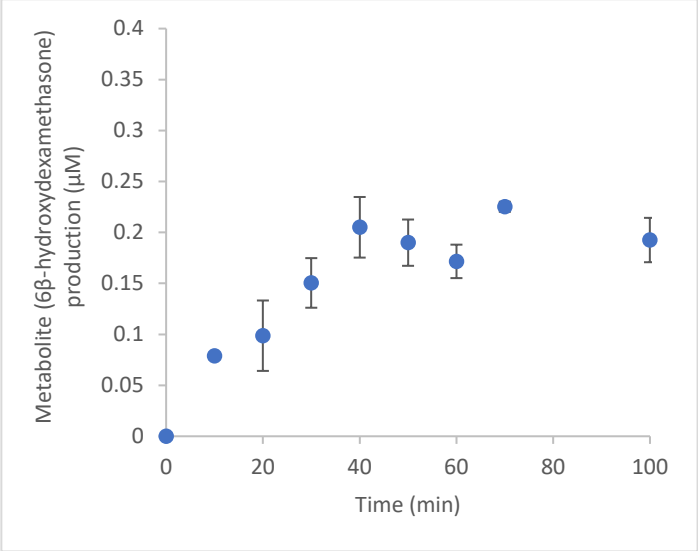

Figure 21. Effects of incubation time on 6β-hydroxydexamethasone production.

2.3.4 Inhibitory Effects of Aspirin on CYP3A2 Activity in Rat Liver Microsomes

To see the effects of aspirin on rat CYP activities, different concentrations of dexamethasone (10, 20, 30, 40, and 50 µM) in presence of 0, 50, 100, and 200 µM aspirin were investigated. Microsomal proteins (0.5 mg/mL) were incubated for 40 min at 37 °C with dexamethasone, 3.0 mM magnesium chloride ($MgCl_2$), 1.0 mM ethylenediaminetetraacetic acid (EDTA), 1.0 mM nicotinamide adenine dinucleotide phosphate hydrogen (NADPH) and 0.067 M phosphate buffer (pH 7.4). Aspirin competitively inhibited the production of 6β-hydroxydexamethasone as presented in Figure 22 and Table 14, whereas the effect of aspirin on 6β-hydroxydexamethasone production using 10-50 µM substrate is shown in Figure 23. Aspirin (0-200 µM), even at

lower than therapeutic relevant concentrations (150-300 µg/mL), causes 50% inhibition of CYP3A2 enzyme activity (IC_{50}), as presented in Table 13.

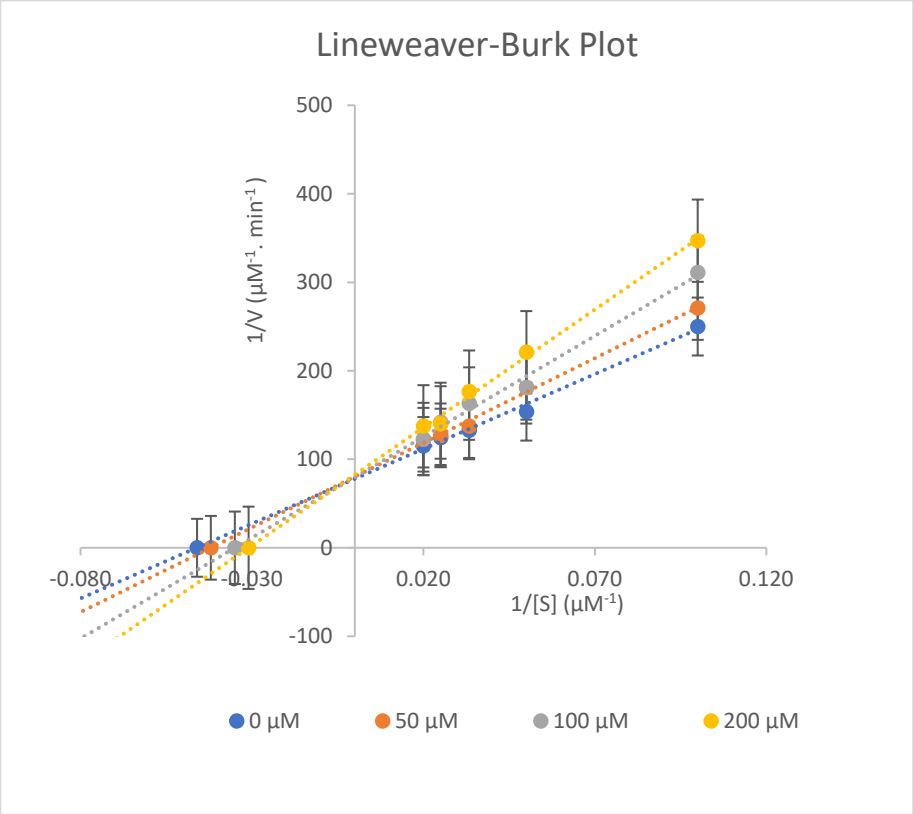

Figure 22. Representative Lineweaver-Burk plot for the inhibition of CYP3A2 enzyme on dexamethasone metabolism into 6β-hydroxydexamethasone with 0, 50, 100, and 200 µM aspirin in rat liver microsomes. Average data are taken from triplicate measurements.

Table 14. Pharmacokinetic parameters of inhibitory effects of aspirin on enzyme metabolism. The mean result is taken ± SD (n=3). Note: $p < 0.001$.

Aspirin Concentration	(Inhibition Parameters)				
	K_m (µM)	V_{max} ($\mu M^{-1} \cdot min^{-1}$)	Cl_{int} ($\mu M^{-2} \cdot min^{-1}$)	á	%Inhibition
0 µM Aspirin	21.23 ± 0.51	0.0127 ± 1.53 × 10^{-4}	0.0006 ± 1.10 × 10^{-5}	-	-
50 µM Aspirin	23.83 ± 0.31	0.0123 ± 1.15 × 10^{-4}	0.0005 ± 4.00 × 10^{-6}	1.03 ± 0.01	12.44 ± 1.20
100 µM Aspirin	26.13 ± 0.70	0.0127 ± 7.94 × 10^{-4}	0.0005 ± 5.00 × 10^{-5}	1.02 ± 0.06	23.29 ± 3.30
200 µM Aspirin	32.57 ± 0.35	0.0123 ± 1.73 × 10^{-4}	0.0004 ± 1.00 × 10^{-5}	1.04 ± 0.01	53.64 ± 1.76

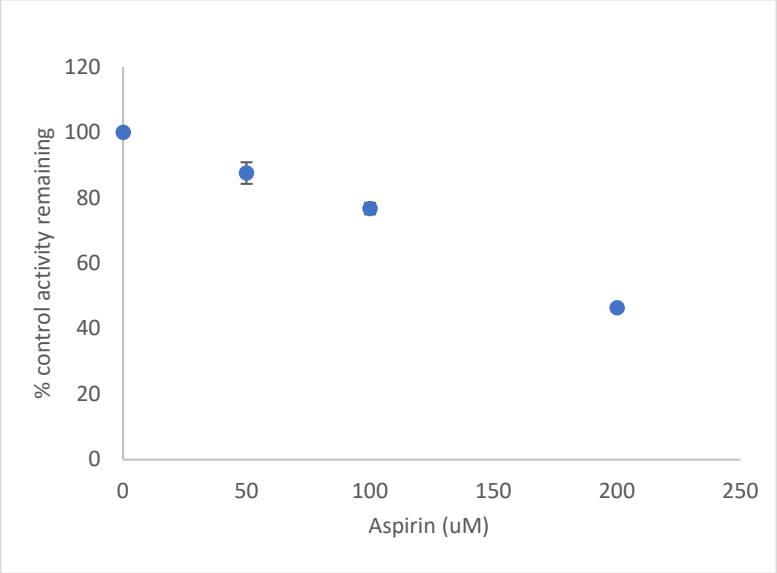

Figure 23. Effect of aspirin on CYP3A2 activity in rat liver microsomes. Control activity was taken as 100%. Average data are taken from triplicate measurements.

The inhibition of hepatic cytochrome P450 activities is one of the most significant mechanisms of drug interaction. Severe adverse events have been associated with drug interactions caused during coadministration [145]. Thus, regulatory authorities need interaction studies both *in vitro* and *in vivo* in drug development.

Aspirin and dexamethasone have been used for the treatment of COVID-19 during the pandemic (2020) and the associated use of aspirin and dexamethasone causes a reduction in COVID-19 mortality. This research is the first to investigate the effects of aspirin on the metabolism of dexamethasone (CYP3A2 enzyme activity).

This study has demonstrated that dexamethasone is metabolised in rat liver microsomes to 6β-hydroxydexamethasone. The *in vitro* findings indicated that aspirin at doses between 0-200 µM acts as a competitive inhibitor and may weakly inhibit cytochrome P4503A2 enzyme activity. The V_{max} (V_{max} is the maximum rate of a reaction catalysed by an enzyme) for the inhibition experiments at three concentration levels of aspirin (50, 100, and 200 µM) remained the same as it did for negative control (without Inhibitor). Whereas a higher K_m (the concentration of substrate requiring the half-maximal activity of enzyme) values were obtained in the presence of the inhibitor, as shown in Table 14. Alpha prime (α') indicates the effect of an inhibitor on the enzyme's affinity for its substrate, and similarly the effect of the substrate on the enzyme's affinity for the inhibitor. As indicated in Table

14, the α' values of aspirin are greater than 1.0 (competitive inhibitor) [146]. Being a weak inhibitor of CYP3A2 activity (as IC_{50} is nearly 200 µM), it has alpha prime (α') values very close to 1 (still greater than 1) and reflects the very weak binding modality while in case of strong competitive inhibitors theses values can be up to or more than 10 (reflecting very strong binding). CL_{int} (the intrinsic ability of hepatic CYP450 enzymes to metabolise the drug) of drugs is often predicted based on *in vitro* data obtained from kinetic analysis (Michaelis-Menten). It was calculated as a ratio of *in vitro* kinetic constants V_{max} and K_m [147], as presented in Table 14.

The results show that aspirin is a competitive inhibitor that binds to the active site of CYP3A2 enzyme and decreases the activity of the CYP3A2 isoform, which is responsible for 6β-hydroxylation of dexamethasone in male rats, with the K_i (the binding affinity between the enzyme and inhibitor) = 95.46 ± 4.25 µM and IC_{50} (inhibitor concentration required to inhibit 50% of the enzyme activity) = 190.92 ± 8.50 µM. A compound with an IC_{50} value below 1 µM is considered a strong inhibitor and it is considered a weak inhibitor if the IC_{50} value is more than 50 µM [148]. Therefore, aspirin has a weak inhibitory effect on CYP3A2 isoform activity.

These *in vitro* findings would be useful for future *in vivo* studies in the healthcare sector. The simple metabolic profile of dexamethasone shows that this steroid could be useful as an *in vivo* probe for CYP3A4 [135]. Further *in vitro* and *in vivo* clinical studies on potential risks associated with the interactions of dexamethasone and aspirin in humans are required.

The present study is further concerned about the validation of extraction efficiency as the accuracy of the entire extraction procedure was not validated for 6β-hydroxydexamethasone concentrations (produced metabolite) involved in the assay. It remained unknown how much metabolite was available after the enzymatic reaction and how much was actually extracted. This highlights the need for method validation to determine the quantity and reproducibility of produced metabolites before carrying out further research in *in vivo* settings.

2.4 Conclusion

In conclusion, an HPLC method was developed and analytical parameters including linearity, precision, %recovery, linear regression, LOD, and LOQ were derived for dexamethasone and 6β-hydroxydexamethasone. All the analytical parameters were validated in accordance with the ICH guidelines. *In vitro*, incubation assays using rat liver microsomes were adopted to determine the effects of aspirin on the dexamethasone metabolism (CYP3A2 activity), as aspirin and dexamethasone have been used together in COVID-19 treatment. Our findings revealed that aspirin acts as a competitive inhibitor and has a weak inhibitory effect on dexamethasone metabolism in rat liver microsomes. The outcomes of the study further suggest the safe use of aspirin and dexamethasone in clinical practice. Nevertheless, further *in vivo* inhibition studies are required to consider this interaction and its implications more completely for patient care.

CHAPTER 3

POTENTIAL EFFECTS OF IBUPROFEN, REMDESIVIR AND OMEPRAZOLE ON DEXAMETHASONE METABOLISM IN CONTROL SPRAGUE DAWLEY MALE RAT LIVER MICROSOMES (DRUGS OFTEN USED TOGETHER ALONGSIDE COVID-19 TREATMENT)

Publication

A. Hussain, D.P. Naughton, and J. Barker. “Potential Effects of Ibuprofen, Remdesivir and Omeprazole on Dexamethasone Metabolism in Control Sprague Dawley Male Rat Liver Microsomes (Drugs Often Used Together Alongside COVID-19 Treatment),”. *Molecules*, 2022; vol. 27, no. 7, pp. 2238, March 2022.

3.1 Introduction

The drug-metabolising enzyme system also known as the CYP450s superfamily is responsible for the biotransformation of a large number of endogenous (fatty acids, hormones, bile acids, steroids, prostaglandins) and exogenous compounds (toxic chemicals, carcinogens, drugs, organic solvents, environmental pollutants) [149]. The use of a combination of medicine can result in potential drug-drug interactions, which in turn, can change the drug metabolism in both Phase I and Phase II [150]. Many drug-drug interactions change the pharmacokinetic behaviour of the drugs in addition to the drug's bioavailability (absorption, distribution, and elimination) [150]. In the majority of cases, the detoxification of the substrate occurs due to the action of CYP450, either as a direct effect or through the phase II enzyme actions. To date, biotransformation of most of the drugs is catalysed by CYP1, CYP2, and CYP3 families in the clinic [151]. The CYP3A isoenzymes metabolise almost 50% of clinical therapeutic drugs [152].

CYP3A4 is primarily accountable for 6β-hydroxylation of testosterone, cortisol, progesterone, and androstenedione [94]. CYP3A2 isoform in male rats is the major contributor to testosterone 6β-hydroxylation [153]. Shayeganpou *et al.* validated the role of rat CYP3A2 isoform in the metabolism of amiodarone while CYP3A4 metabolises amiodarone in the human liver [154]. In another *in vitro* study, the effects of plumbagin on CYP3A2/4 activities both in rat and human liver microsomes were investigated [155]. Previous studies have shown that CYP3A4 is accountable for dexamethasone metabolism and that the dexamethasone CYP3A4 substrate can competitively inhibit other drugs which are strong substrates for CYP3A4 [156]. CYP3A2 is abundantly expressed in the rat liver microsomes and metabolises several drugs of clinical importance [157]. The CYP3A2 isoform in male-specific rat liver microsomes (RLMs) is accountable for 6-hydroxylation of dexamethasone (corticosteroid) and is close to the human metabolite profile [136]. Li *et al.* have reported that dexamethasone is a significant inducer of both rat CYP3A1/2 and human CYP3A4 [158].

COVID-19 is a mainly self-limited disease and up to 20% of the cases will develop severe symptoms such as hypercoagulation, acute respiratory distress syndrome, pneumonia, and multiorgan system dysfunction [159]. Various drugs against SARS-CoV-2 have been

investigated and have been used to reduce the mortality caused by COVID-19, such as remdesivir, famotidine, and omeprazole (Figure 24) [160]. In a clinical study, dexamethasone appeared to reduce the death rate by 35% in ventilated intensive care unit (ICU) patients and 20% in nonventilated patients with supplemental oxygen [161].

Remdesivir is an antiviral drug that was originally used to treat hepatitis C, while omeprazole is a proton pump inhibitor and is used to treat excessive gastric acid production in the body. A reduction in recovery time in ICU patients has been associated with remdesivir therapy [161]. Aguila and Cua indicated in their study that remdesivir with omeprazole may represent therapeutic candidates for the treatment of COVID-19 [160]. Ibuprofen is a nonsteroidal anti-inflammatory drug and is used to treat inflammation, fever, and pain. It has been reported in a study that ibuprofen-related mortality rates were lower as compared to laxative-related mortality [159]. It was found in a randomised trial in the UK that ibuprofen helps to decrease the infection severity of acute respiratory tract infection in patients [162].

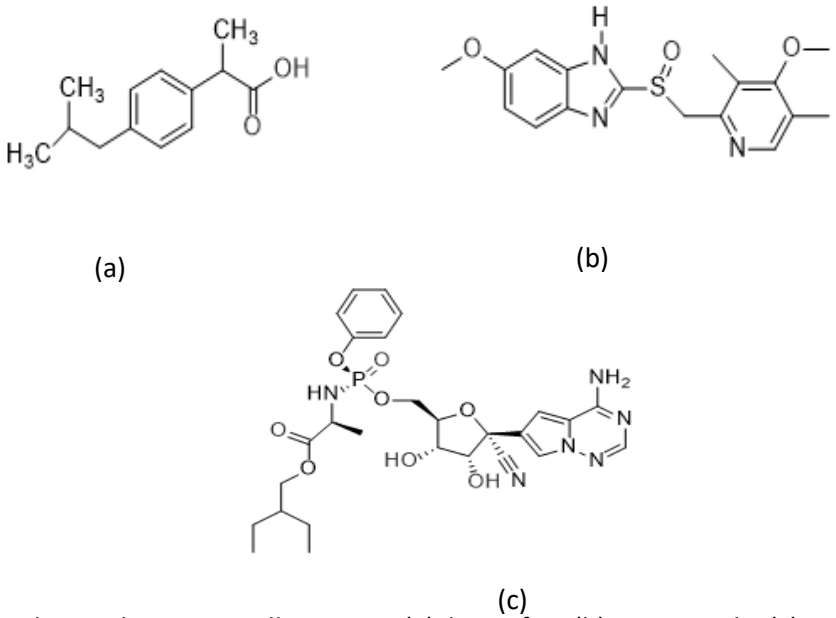

(a) (b)

(c)

Figure 24. Chemical structures illustrating: (a) ibuprofen, (b) omeprazole, (c) remdesivir.

There are no data relating to the effects of ibuprofen, remdesivir, and omeprazole on dexamethasone metabolism (CYP3A2 activity). Our previous study showed that aspirin exhibits a weak competitive inhibition of CYP3A2 isoenzyme activity and has a low potential to cause drug-drug toxicity [163].

Thus, in this report, we aimed to study the potential inhibitory impacts of these three compounds on the activity of CYP3A2 isoenzymes in rat liver microsomes using dexamethasone as a probe substrate in the presence of different concentrations of inhibitor drugs. These findings could provide significant information for the safe co-administration of these drugs in clinical settings.

3.2 Materials and Methods

3.2.1 Chemicals

Remdesivir was procured from Tocris Bioscience, UK, and was stored at -20 °C. Omeprazole was obtained from Carbosynth Ltd (UK). HPLC grade acetonitrile was purchased from Merck, Co. (UK). Ibuprofen was purchased from Sigma-Aldrich, Co. (USA). Glucose-6-phosphate, phosphoric acid (85% w/w), ethylenediaminetetraacetic acid, potassium phosphate monobasic, potassium phosphate dibasic, glucose-6-phosphate dehydrogenase, nicotinamide adenine dinucleotide phosphate, and magnesium chloride was purchased from the suppliers as stated in Chapter 2 (refer to section 2.2.1). Ethyl acetate, diethyl ether, dexamethasone, 4- hydroxyoctanophenone, and 6β-hydroxydexamethasone were purchased from the suppliers as mentioned in Chapter 2 (refer to section2.2.1).

3.2.2 Rat Liver Microsomes

The pooled liver microsomes from male rats (Sprague-Dawley) were purchased and stored as specified in Chapter 2 (refer to section 2.2.1).

3.2.3 Instruments

The shaking incubator, high-performance liquid chromatographic system and C18 column were used for the analysis, as stated in Chapter 2 (section 2.2.2).

Assay components (NADPH enzyme, 6β-hydroxydexamethasone, dexamethasone, inhibitors (remdesivir, omeprazole, and Ibuprofen) and 4'-hydroxyoctanophenone were separated using an isocratic elution mode. The mobile phase composition was (70% acetonitrile and 30% water, v/v). The HPLC instrument was controlled at 0.6 mL/min of flow rate, 10 µL of injection volume, the column was set at 25 °C and the detection wavelength was chosen at 243 nm [163]. The results are presented as the standard deviation of triplicate measurements.

3.2.4 Potential Effects of Inhibitors on CYP3A2 Activity *in Vitro*

To determine the potential effects of ibuprofen, remdesivir and omeprazole on CYP3A2 activity, 6β-hydroxydexamethasone formation after different time intervals was quantified on the HPLC instrument. In microcentrifuge tubes, a final volume of 500 µL contained microsomal protein (0.5 mg/mL), a range of dexamethasone (10, 20, 30, 40 and 50 µM), NADPH (1.0 mM), Glucose-6-Phosphate (5 mM), magnesium chloride (3.0 mM), (Glucose-6-Phosphate Dehydrogenase (1.7 units/mL), 0.067 M potassium phosphate buffer (pH 7.4) and ethylenediaminetetraacetic acid (1.0 mM EDTA). Microcentrifuge tubes containing assay components were incubated at 37 °C for 40 min in the presence of ibuprofen (0, 50, 100 and 200 µM), remdesivir (0, 30, 50 and 100 µM), and omeprazole (0, 30, 50 and 100 µM), respectively. The percentage of organic solvent in the assay was not more than 1% v/v.

15 µM of 4-hydroxyoctanophenone (internal standard) dissolved in ice-cold acetonitrile was added to the reaction tubes to quench the reaction. The quenched reaction masses were transferred to the new vials and substrate and metabolite were double extracted with ethyl acetate (3 ml) and diethyl ether (3 ml), respectively. The organic extracts were evaporated to dryness. The mobile phase (70% acetonitrile and 30% water, v/v) was used to dissolve the residues. 10 µL of the solution was injected for HPLC analysis.

3.2.5 Analytes Stock and Standard Solutions Preparation

For the cytochrome P3A2 enzyme assay, a stock solution of dexamethasone yielding a 1000 µM concentration was prepared. Serial dilutions of dexamethasone (50, 40, 30, 20, and 10 µM) were prepared from the stock solution in the mobile phase (70% methanol + 30% water, v/v). The stock solution of 6β-hydroxydexamethasone (2 µM) was prepared in the mobile phase (70% methanol + 30% water, v/v) and standard solutions (0.2, 0.4, 0.6, 0.8 and 1 µM) were prepared from the stock by serial dilutions. 4-hydroxyoctanophenone powder (0.0010 mg) was dissolved in 10 mL of acetonitrile. The final stock of 15 µM concentration was prepared by combining 165 µl of 4-hydroxyoctanophenone from stock and 49.835 mL of mobile phase in a volumetric flask.

Remdesivir stock (2 mg/ml) was prepared in a 5 mL volumetric flask in methanol. Serial dilutions of remdesivir (100, 50, and 30 µM) were performed. A stock solution of ibuprofen of 1000 µM was prepared by weighing 1000 mg of ibuprofen and dissolving in 5 mL of methanol. Standard solutions of ibuprofen (50, 100, and 200 µM) were prepared by serial dilution. Omeprazole of 1000 µM was prepared in methanol as a stock solution. Standard solutions of omeprazole (30, 50, and 100 µM) were prepared by serial dilution in the mobile phase (70% methanol + 30% water, v/v).

3.2.6 Optimisation of Substrate Concentration *in Vitro*

In order to determine the optimal concentrations of dexamethasone (as a probe substrate), a series of dexamethasone concentrations (0, 25, 50, 100, 150 and 200 µM) was added to the incubation system *in vitro*. The formation of 6β-hydroxydexamethasone (metabolite) was calculated from the standard calibration curve. The optimal concentrations were determined by the linear relationship between the substrate concentrations and metabolite formation.

3.2.7 Statistical Analysis

Statistical analyses were completed using Microsoft Excel 2010 software for kinetic parameters. The concentration of dexamethasone metabolite produced at different time intervals in the presence and absence of different inhibitors (ibuprofen, remdesivir, and omeprazole) were determined from 6β-hydroxydexamethasone calibration curve for CYP3A2 inhibition studies. Analysis of variance (ANOVA) test was also performed (at a 0.05 significance level).

In the case of ibuprofen, inhibition data demonstrated non-competitive inhibition. Schwarz criterion (SC) and Akaike information criterion (AIC) were acquired from nonlinear regression analysis. IC_{50} values were calculated by nonlinear regression analysis and GraphPad Prism software was used for this purpose. The following equation was used to calculate the percentage of inhibition, % inhibition = $V_{max(inh)} = V_{max}/(1+I/K_i)$, in which $V_{max(inh)}$ is the inhibited velocity, Vmax is the maximal rate of reaction, I is inhibitor concentration, and K_i is an inhibitory constant.

The type of CYP3A2 inhibition for remdesivir inhibitor was believed to be a mixed type of inhibition based on Lineweaver–Burk plots shape, AIC, SC, and standard error. The IC_{50} value was calculated by using the formula: $V = [V_0/(1+(I/IC_{50})^S)]$, in which V is the observed velocity, V_0 is uninhibited velocity, I is the concentration of inhibitor and ^{S} is the slope factor.

For omeprazole, inhibition was considered as uncompetitive inhibition. The Lineweaver-Burk plot was used to assess the inhibition parameters such as K_m, V_{max}, and Cl_{int}. The following equation was used to calculate these parameters: $V = V_{max} \times [S]/[S] + K_m (1 + [I]/K_i)$, in which V_{max} is the maximal rate of the reaction, V is the observed velocity, S is the substrate concentration, K_i is an inhibitory constant, K_m is Michaelis-Menten constant, and I is the inhibitor concentration.

3.3 Results and Discussion

3.3.1 HPLC Method Development and Validation

The HPLC method was developed and validated according to the ICH guidelines in terms of specificity, linearity, accuracy, and precision. Separation of dexamethasone, 6β-hydroxydexamethasone, inhibitors (Ibuprofen, remdesivir, and omeprazole), and internal standard were attained using conditions presented in Table 15. The method showed specificity with metabolite (6β-hydroxydexamethasone) separated from other compounds with sufficient resolution. A representative chromatogram is shown in Figure 25.

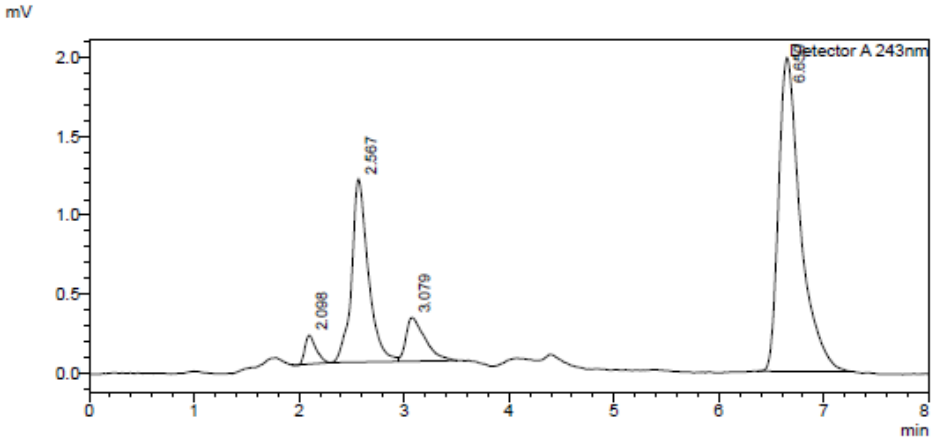

Figure 25. HPLC chromatogram displaying CYP3A2 assay components: ibuprofen (tR: 2.098), 6β-hydroxydexamethasone (tR: 2.567), dexamethasone (tR: 3.079) and 4-hydroxyoctanophenone (IS) (tR: 6.650) separation.

Table 15. Displaying HPLC investigated parameters.

Investigated Parameters	Characteristic
Mobile phase	70% acetonitrile and 30% H_2O, v/v
Column temperature	25 °C
Wavelength	243 nm
Flow rate	0.6 mL/min
Internal standard	4-hydroxyoctanophenone
Injection volume	10 µl
Run time	8 min
Column	Waters C18 column, 15 mm × 4.6 mm, 3.5 µm

The obtained calibration curves for dexamethasone and 6β-hydroxydexamethasone (Figure 26) showed good linearity over the concentration range of 25-200 µM and 0.2-1 µM, respectively. The representative linear equation for dexamethasone was y = 0.2505x + 0.0945 and for 6β-hydroxydexamethasone was y = 1.6775x + 0.0385 with correlation coefficient (r^2) of 0.99. For dexamethasone, good intra-sample and inter-sample precision were achieved with %RSD (% relative standard deviation) < 5%.

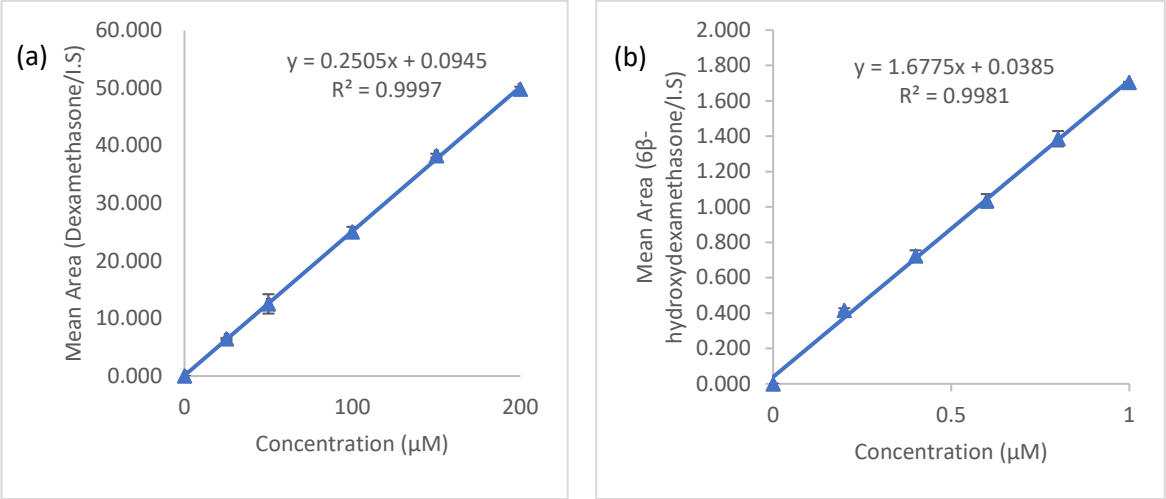

Figure 26. Calibration curves displaying linearity over the selected range: (a) dexamethasone, (b) 6β- hydroxydexamethasone.

Good intra-day and inter-day precision was also obtained with %RSD < 10% for 6β-hydroxydexamethasone. The standard deviation ranged between 0.01 and 3.13. The percentage recovery values for dexamethasone were between 81.68% and 112.52% and for 6β-hydroxydexamethasone between 93.13% and 119.38% (ICH acceptance criteria: %Recovery: 80–120%), representing good accuracy.

The developed method could be optimally performed with slight variations in peak areas, retention time, and peak heights. The calculated LOD and LOQ for dexamethasone were 5.60 µM and 16.98 µM, respectively. LOD and LOQ for 6β-hydroxydexamethasone were calculated to be 0.06 µM and 0.19 µM, respectively.

3.3.2 Optimisation of Substrate Concentration for Incubation System *In Vitro*

The optimised incubation time was 40 min [17]. For optimisation of substrate concentration, a series of dexamethasone concentrations (10-200 µM) was added to the incubation system *in vitro.* The formation rate of the metabolite (6β-

hydroxydexamethasone) from the substrate (dexamethasone) was increased up to 50 µM and then it became linear (Figure 27). Thus, the optimal substrate concentration range for the CYP3A2 inhibition study was 10-50 µM.

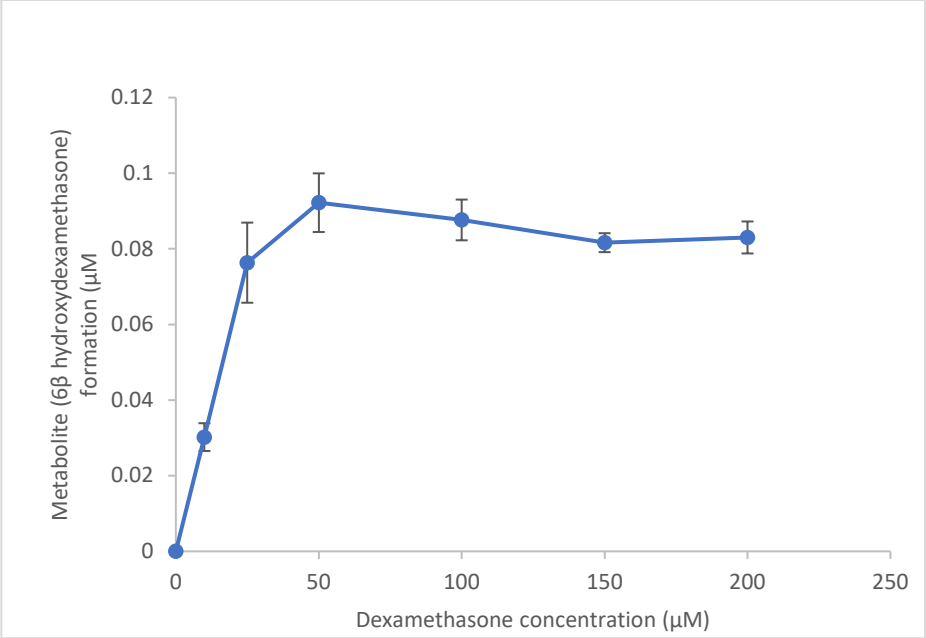

Figure 27. Effects of substrate concentration on 6β-hydroxydexamethasone formation.

3.3.3 Inhibitory Effects of Ibuprofen on CYP3A2 Enzyme Activity in Rat Liver Microsomes (RLMs)

Rat liver microsomes (0.5 mg/mL) were incubated with various concentrations of dexamethasone (10-50 µM) and Ibuprofen (0-100 µM) in the presence of a NADPH regenerating system for 40 minutes at 37 °C. The metabolite was extracted using ethyl acetate and diethyl ether. The rates of 6β-hydroxydexamethasone formation were determined using High-Performance Liquid Chromatography (HPLC) technique. Figure 28, Figure 29, and Table 16 show the inhibition of CYP3A2 activity by ibuprofen with apparent K_m, V_{max}, % inhibition, and Cl_{int} values (±SD).

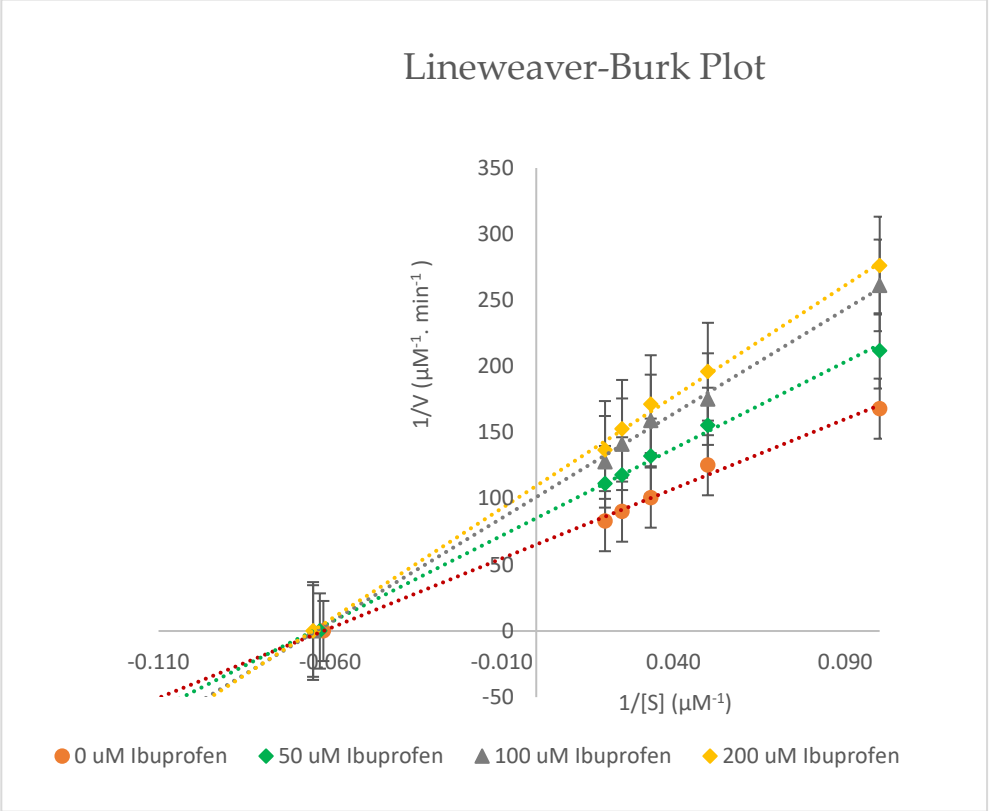

Figure 28. Lineweaver–Burk plot for the inhibition of CYP3A2-mediated dexamethasone metabolism by various concentrations of ibuprofen (0–200 µM) in rat liver microsomes. Values are expressed as the average of triplicate measurements.

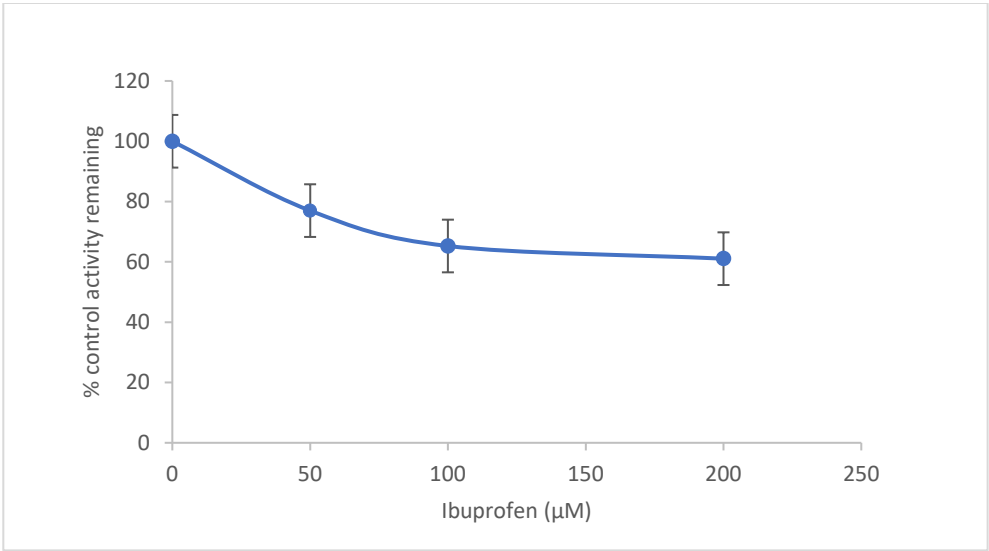

Figure 29. Inhibition of CYP3A2 enzyme activity by ibuprofen (0–200 µM) in rat liver microsomes. Values are expressed as the average of triplicate measurements. Control activity was taken as 100%.

Table 16. Pharmacokinetic parameters for inhibition patterns of CYP3A2 isoenzyme in the presence of dexamethasone substrates and Ibuprofen (inhibitor). The mean of three experiments is taken ± SD (n=3). Note: $p < 4.653x10^{-07}$.

Ibuprofen Concentration	Pharmacokinetic Parameters for 6β-hydroxylase			
	K_m (μM)	V_{max} ($\mu M^{-1} \cdot min^{-1}$)	Cl_{int} ($\mu M^{-2} \cdot min^{-1}$)	%Inhibition
0 μM Ibuprofen	15.967 ± 1.582	0.0151 ± 0.058×10^{-3}	0.0009 ± 0.093×10^{-3}	-
50 μM Ibuprofen	15.873 ± 1.680	0.0116 ± 0.608×10^{-3}	0.0007 ± 0.054×10^{-3}	22.998 ± 4.341
100 μM Ibuprofen	15.443 ± 1.034	0.0099 ± 0.040×10^{-3}	0.0006 ± 0.043×10^{-3}	34.734 ± 0.336
200 μM Ibuprofen	15.153 ± 0.446	0.0092 ± 0.100×10^{-3}	0.0006 ± 0.024×10^{-3}	38.939 ± 0.476

V_{max}: Maximal reaction rate. K_m: Michaelis-Menten constant. Cl_{int}: Hepatic Intrinsic Clearance.

3.3.4 Inhibitory Effects of Remdesivir on CYP3A2 Enzyme Activity in RLMs

Incubation of probe substrate dexamethasone (10-50 μM) with multiple remdesivir concentrations (0-100 μM) in RLMs showed that remdesivir inhibits CYP3A2 activity as a mixed inhibitor (Figure 30 and Figure 31). These primary data were then utilised to construct Lineweaver-Burk and Michaelis-Menten plots for the inhibition of dexamethasone metabolism (CYP3A2 activity) by remdedisivir in RLMs. The obtained experimental data were analysed in triplicate and applied to estimate the resultant K_i (inhibition constant) and IC_{50} (half-maximum inhibitory concentration) values. Table 17 summarises the mean K_m, V_{max}, Cl_{int}, IC_{50}, and K_i values (±SD).

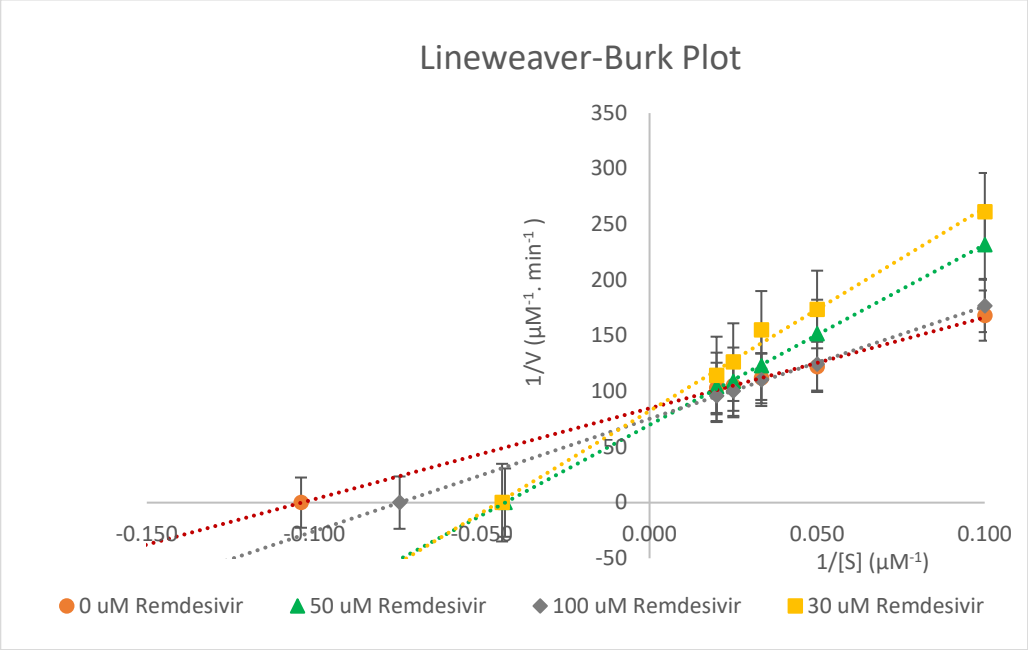

Figure 30. Lineweaver–Burk plot for the inhibition of CYP3A2-mediated dexamethasone metabolism by various concentrations of remdesivir (0–100 µM) in rat liver microsomes. Values are expressed as the average of triplicate measurements.

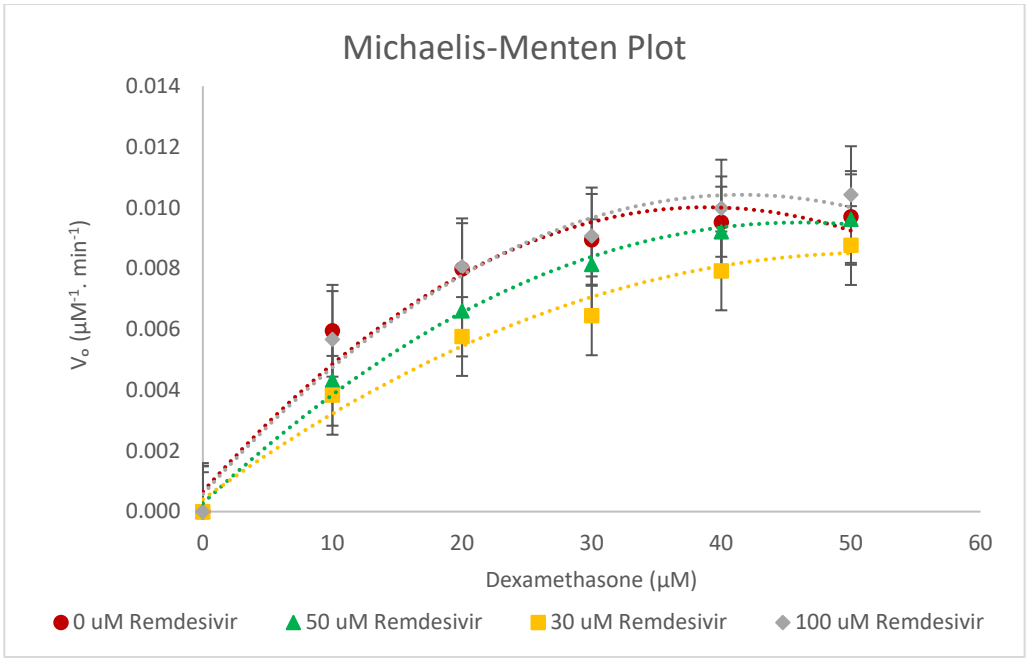

Figure 31. Michaelis–Menten plot for the inhibition of CYP3A2-catalysed dexamethasone 6-hydroxylation by remdesivir (0-100 µM). The polynomial function of order 2 was used to fit the curves. Values are expressed as the average of triplicate measurements.

Table 17. V_{max}, K_m and Cl_{int} values and inhibition patterns of CYP3A2 isoenzyme in the presence of dexamethasone substrates and remdesivir (inhibitor). The mean of three experiments is taken ± SD (n=3). Note: $p < 0.002$.

Remdesivir Concentration	Pharmacokinetic Parameters for 6β-hydroxylase				
	K_m (μM)	V_{max} ($\mu M^{-1} \cdot min^{-1}$)	Cl_{int} ($\mu M^{-2} \cdot min^{-1}$)	IC_{50} (μM)	K_i (μM)
0 μM Remdesivir	9.637 ±0.550	0.0119 ±0.700×10^{-3}	0.0001 ±0.010×10^{-3}	45.007 ± 0.016	22.504 ±0.008
30 μM Remdesivir	22.097 ± 0.922	0.0122 ± 0.306×10^{-3}	0.0006 ± 0.011×10^{-3}	-	-
50 μM Remdesivir	23.167 ± 1.002	0.0146 ± 0.586×10^{-3}	0.0006 ± 0.018×10^{-3}	-	-
100 μM Remdesivir	13.300 ± 0.436	0.0132 ± 0.153×10^{-3}	0.0010 ± 0.025×10^{-3}	-	-

V_{max}: Maximal reaction rate. K_m: Michaelis-Menten constant. Cl_{int}: Hepatic Intrinsic Clearance

3.3.5 Inhibitory Effects of Omeprazole on CYP3A2 Enzyme Activity in RLMs

An enzyme study was carried out to determine the CYP inhibition by omeprazole in RLMs with different concentrations of probe substrate (10-50 μM) in the absence and presence of omeprazole (inhibitor). The data was taken as a mean of triplicate. The Lineweaver-Burk plot and Michaelis-Menten plot (Figure 32 and Figure 33) show the type of inhibition for the selected enzyme activity. The K_m, V_{max}, C_{lint}, IC_{50}, and K_i values (±SD) were determined and summarised in Table 18.

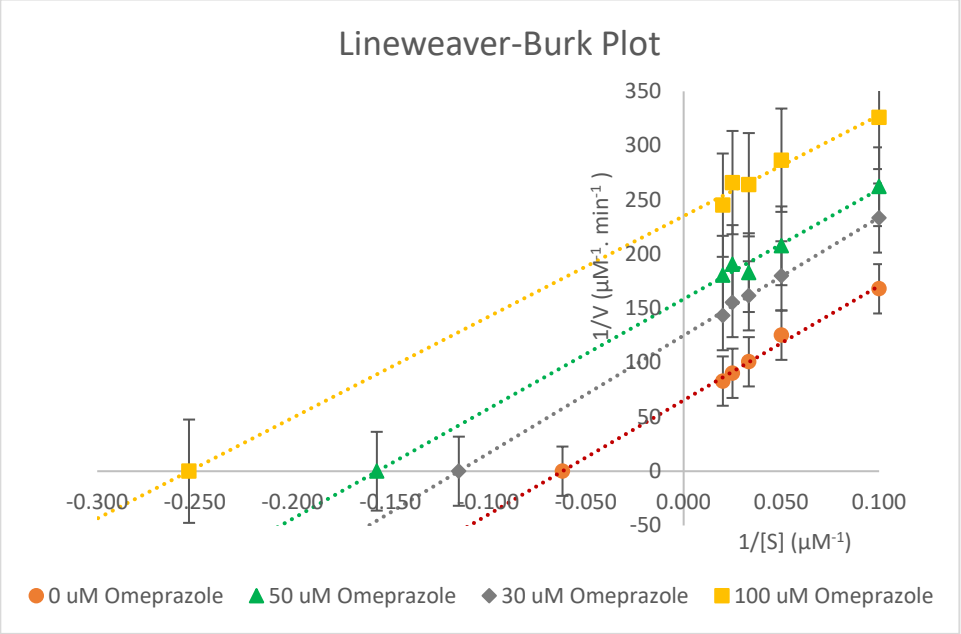

Figure 32. Lineweaver–Burk plot for the inhibition of CYP3A2-mediated dexamethasone metabolism by various concentrations of omeprazole (0–100 µM) in rat liver microsomes. Values are expressed as the average of triplicate measurements.

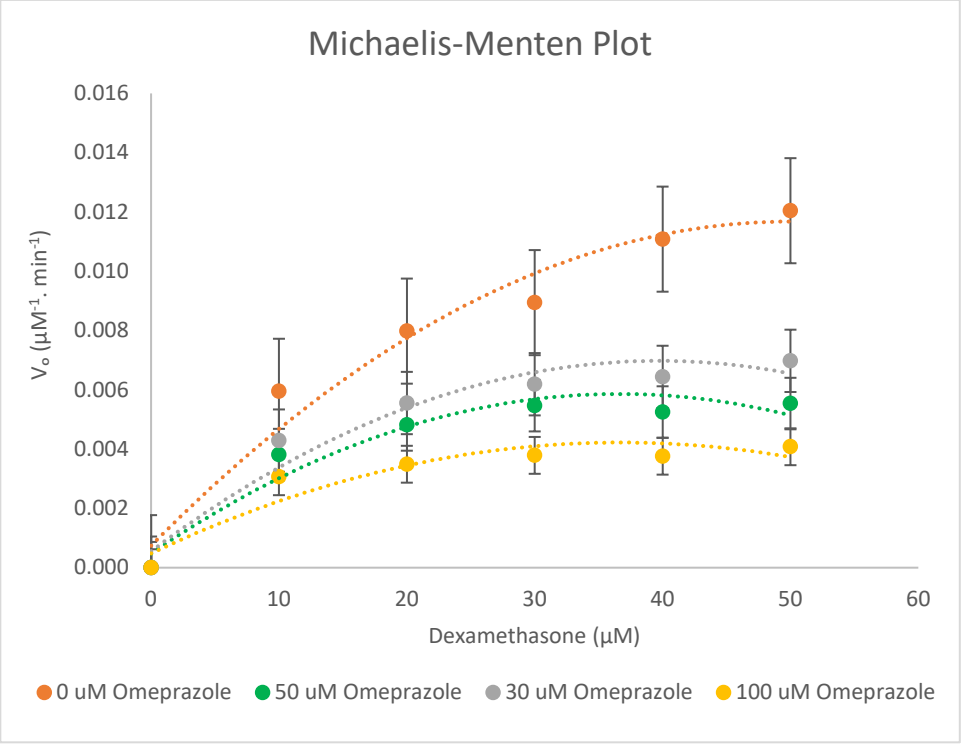

Figure 33. Michaelis–Menten plot for the inhibition of CYP3A2-catalysed dexamethasone 6-hydroxylation by omeprazole (0-100 µM). The polynomial function of order 2 was used to fit the curves. Values are expressed as the average of triplicate measurements.

Table 18. K_m, V_{max}, and Cl_{int} values for 6β-hydroxylase formation. The mean of three experiments is taken ± SD (n=3). Note: $p < 1.389x10^{-14}$.

Omeprazole Concentration	Pharmacokinetic Parameters for 6β-hydroxylase				
	K_m (μM)	V_{max} ($\mu M^{-1} \cdot min^{-1}$)	Cl_{int} ($\mu M^{-2} \cdot min^{-1}$)	IC_{50} (μM)	K_i (μM)
0 μM Omeprazole	16.033 ± 1.498	$0.0152 \pm 0.208 \times 10^{-3}$	$0.0010 \pm 0.093 \times 10^{-3}$	78.351 ± 0.460	39.175 ± 0.230
30 μM Omeprazole	8.800 ± 1.307	$0.0080 \pm 0.346 \times 10^{-3}$	$0.0009 \pm 0.091 \times 10^{-3}$		
50 μM Omeprazole	6.423 ± 1.050	$0.0062 \pm 0.473 \times 10^{-3}$	$0.0010 \pm 0.093 \times 10^{-3}$		
100 μM Omeprazole	3.867 ± 0.230	$0.0042 \pm 0.058 \times 10^{-3}$	$0.0011 \pm 0.066 \times 10^{-3}$		

V_{max}: Maximal reaction rate. K_m: Michaelis-Menten constant. Cl_{int}: Hepatic Intrinsic Clearance

The inhibition of CYP450 enzymes by a number of drugs causes potential clinical consequences [164]. The use of combination drugs cannot be avoided in the treatment for COVID-19. The combination of remdesivir (antiviral drug) and dexamethasone (anti-inflammatory drug) is currently in use to treat viral infection as well as reduce the inflammation caused by COVID-19 infection. Evidence from the literature indicates apotential role for the use of corticosteroids and nonsteroidal anti-inflammatory drugs NSAIDs (ibuprofen) in the treatment of COVID-19 patients [165]. Recent literature also confirmed that ibuprofen is not associated with worse clinical outcomes in COVID-19 patients [166]. Interestingly, it is reported in a recent study that at therapeutic concentrations, omeprazole improved the anti-SARS-CoV-2 effects of remdesivir [160].

This study provided the first complete *in vitro* data that enable us to see the interactions of drugs used in COVID-19 treatment and investigated the inhibitory effects of ibuprofen, remdesivir, and omeprazole on CYP3A2 activity using a High-Performance Liquid Chromatography.

Dexamethasone is metabolised through the CYP3A2 enzyme in rat liver microsomes to 6β-hydroxydexamethasone. The *in vitro* findings have revealed that CYP3A2 enzyme activity was inhibited non-competitively by ibuprofen in rat liver microsomes at doses between 0-200 μM. Based on Table 16, the maximal rate of reaction (V_{max}) decreased compared to the V_{max} of uninhibited reaction (negative control assay) while Michaelis constant (K_m) stayed

the same as the inhibitor is not competing with the substrate for the active site. The ibuprofen concentrations used (50-200 µM) are similar to the amounts found in plasma (49-242 µM), and cause 50% inhibition of CYP3A2 enzyme activity (IC_{50}) [167]. As a result, ibuprofen is a weak inhibitor of CYP3A2 isoenzyme activity with half-maximum inhibitory concentration (IC_{50}) = 230.552 ± 2.020 µM and inhibitory constant (K_i) = 224.981 ± 1.845 µM.

Previous *in vitro* studies report that the anti-inflammatory agent ibuprofen (COX non-selective inhibitor) has no inhibitory effect on the cytokine expression [168]. With IC_{50} of 270 µM, ibuprofen very weakly inhibits the hydrolysis of arachidonoylethanolamide by the enzyme fatty acid amide hydrolase [169]. This result is consistent with our findings. *In vivo*, peak plasma concentrations (Cmax) of ibuprofen are in the range of 110–150 µM after two single doses of 200 mg from two different ibuprofen preparations [170]. Another *in vitro* study showed that the short-term administration of ibuprofen in rats did not affect trimethadione metabolism [171]. In our study, ibuprofen showed higher K_i and IC_{50} values against dexamethasone, so drug-drug interaction should be unlikely.

It is evident from this *in vitro* study (Figure 30 and Figure 31), that remdesivir exhibits mixed inhibition (competitive and non-competitive) properties based on graphical inspection of Lineweaver-Burk plot and remdesivir's K_i value = 22.504 ± 0.008 µM and IC_{50} value 45.007 ± 0.016 µM. The chosen concentration of remdesivir used (30-100 µM) was well above the plasma concentration range of remdesivir (0.1-7.3 µM), after a single dose of 3-225 mg of remdesivir [172]. No inhibition was found at concentrations lower than 30 µM. Table 17 shows that V_{max} and K_m are different for each remdesivir concentration which further confirms the mixed type of inhibition. In a mixed type of inhibition, remdesivir (inhibitor) can bind to the CYP3A2 enzyme at the same time as dexamethasone (substrate)[153].

Thus, remdesivir binding may influence the CYP3A2 substrate (dexamethasone) binding. It is also possible that remdesivir binds to a different active site of the CYP3A2 enzyme (allosteric effect). Change in the confirmation of CYP3A2 may occur due to the binding of remdesivir to this allosteric site and this has resulted in reducing the substrate affinity for the active site. Furthermore, 50 µM remdesivir concentration can be assumed as saturated

concentration because of high K_m values as compared to other remdesivir concentrations (30 and 100 µM).

However, a detailed metabolism study (*in vitro or in vivo*) of remdesivir has not been conducted [172]. Yang reported that remdesivir is a weak inhibitor of CYP3A4, which is consistent with our findings [173]. He also reported that even though remdesivir is a substrate of several CYP isoforms, drug interactions of remdesivir with CYP3A4 inducers or inhibitors were unlikely [173]. Remdesivir's hepatic clearance is not mediated by metabolic enzymes but is driven by hepatic blood flow.

A compound with an IC_{50} value below 1 µM is considered to be a strong inhibitor, and it is considered to be a weak inhibitor if the IC_{50} value is more than 50 µM [163]. Thus, the high values of IC_{50} of remdesivir in rat liver microsomes would have a low potential for drug interaction and in causing toxicity involving CYP enzymes.

Our *in vitro* study with omeprazole has shown that it inhibits the CYP3A2 enzyme activity uncompetitively in rat liver microsomes with a K_i of 39.175 ± 0.230 µM. The IC_{50} value was twice the value of K_i, i.e., 78.351 ± 0.460 µM. According to the Lineweaver-Burk plot of enzyme kinetics, a decrease in V_{max} and K_m from 0 to 100 µM omeprazole has been observed in the presence of an uncompetitive inhibitor, as presented in Table 18. Interestingly, the omeprazole showed uncompetitive inhibition of CYP3A2 activity. Uncompetitive inhibition is a rare phenomenon for most enzymes. In this case, omeprazole may bind to the enzyme-substrate complex and change (inhibit) the activity of CYP3A2 and, thus, have a very specific effect. Because of the nonproductive nature of the ES-inhibitor (ESI) complex, a high concentration of inhibitors can decrease the reaction velocity.

Omeprazole was studied at higher concentrations (30-100 µM) than its therapeutic plasma concentration (1.1-2.0 µM). No inhibition was found at concentrations lower than 30 µM. Keeling *et al.* reported that *in vitro* administration of omeprazole for up to 60 minutes at pH 6.1 or pH 7.4 showed no substantial inhibition of the ATPase activity [174]. This is consistent with our study, as no inhibition of dexamethasone substrate was found. The results from an *in vivo* study demonstrated that several daily oral doses of omeprazole

(40 mg, C_{max} was 1207 ng/mL) had no substantial effect on the pharmacokinetics of roxadustat [175].

Another *in vitro* study confirmed that omeprazole was a poor inhibitor of bufuralol 1'-hydroxylation with IC_{50} > 200 μM [176]. The high values of IC_{50} and K_i of omeprazole in rat liver microsomes would have a low possibility for drug interactions.

This research showing the effects of ibuprofen, remdesivir and omeprazole on dexamethasone metabolism will be useful for further *in vivo* study of dexamethasone metabolism (CYP3A activity). Additionally, our findings also provide a rationale for the safe and effective administration of these inhibitor drugs with other drugs. However, an interaction potential of dexamethasone with ibuprofen, remdesivir, and omeprazole has to be considered *in vivo* before a conclusion can be made.

3.4 Conclusion

In summary, an *in vitro* study using rat liver microsomes emphasizes the inhibition of CYP3A2 enzyme activity by ibuprofen, remdesivir, and omeprazole as these drugs have been used in COVID-19 treatment. Our data demonstrated that ibuprofen, remdesivir, and omeprazole possibly inhibit CYP3A2 enzyme activity as a non-competitive, mixed, and uncompetitive inhibition mode, respectively. The outcomes of this research guide the safe use of dexamethasone and other COVID-19 drugs (ibuprofen, remdesivir, and omeprazole) in healthcare screening. More *in vivo* trials should be performed to assess the safe administration of taking ibuprofen, remdesivir, and omeprazole drugs with dexamethasone for patient care.

CHAPTER 4

DEVELOPMENT AND VALIDATION OF A HIGH-PERFORMANCE LIQUID CHROMATOGRAPHY METHOD FOR THE QUANTITATIVE DETERMINATION OF VITAMIN D METABOLITES TO SEE THE INHIBITORY EFFECT OF TESTOSTERONE ON CYP2C11 ACTIVITY *IN VITRO*

4.1 Introduction

The CYPs are drug-metabolizing enzymes and mainly catalyse the hydroxylation reaction in the presence of molecular oxygen within the electron transport system. This Phase I enzyme reactions also prepare the drug for elimination and are thus responsible for maintaining the therapeutic drug levels in the human body [18].

Vitamin D is not a single compound, but a group of fat-soluble secosteroids and is obtained from cholesterol. Vitamin D is also colloquially named “sunshine vitamin”, as it can be made in the skin in the presence of adequate sunlight [177]. 7-dehydrocholesterol is activated by UV radiation and converts to Vitamin D_3 in the skin [178]. As it is produced from cholesterol and then moved through the body through the bloodstream, it is better to classify Vitamin D as a steroid hormone [177]. The metabolism of Vitamin D in humans comprises three main steps: 25-hydroxylation, 1α-hydroxylation, and 24-hydroxylation, with all hydroxylation reactions being performed by cytochrome P450 mixed-function oxidases [179].

In male rats, CYP2C11 facilitates some endogenous steroids’ hydroxylation e.g., testosterone and androstenedione, Vitamin D hydroxylation, and epoxygenation of arachidonic acid [180]. CYP2C11 shows a 77% amino acid sequence homology, a functional analogy, and some substrate predilection with human CYP2C9, which is responsible for catalysing the metabolism of some clinically significant drugs such as S-warfarin, ibuprofen, phenytoin, diclofenac, antidepressant drugs, tolbutamide, arachidonic acid and steroids [180].

Vitamin D_2 (ergocalciferol) is produced by plants but Vitamin D_3 (cholecalciferol) is produced in the skin. $25(OH)D_3$ is very abundant and present at 20-50 ng/mL in blood circulation under normal conditions [181]. Vitamin D deficiency is a common cause of bone diseases such as osteoporosis, rickets, and osteomalacia [181]. Excessive amounts of Vitamin D can have harmful effects and are affected by drug interactions which can result in cardiovascular diseases and cancer [182].

Various drug classes are known which Vitamin D can interact with, such as bile acid sequestrants which decrease the absorption of Vitamin D and anticonvulsants interaction which reduces the vitamin D activity in the body. A study published in 2012 by Grober *et al.* examined the Vitamin D drug interaction through the Pregnane X receptor (PXR) [183]. Testosterone is a steroid (male sex hormone) that is made in the testes [184]. Levels of testosterone hormone play an important role in normal sexual function and development. The use of testosterone in androgen replacement therapy is common to treat male hypogonadism [184]. Athletes have also used testosterone for years for its muscle-building properties.

The aim of this study was the development and validation of a novel HPLC method that can precisely identify and quantify 25OHD$_3$ and 25OHD$_2$ to see the inhibitory effects of testosterone on CYP2C11 activity using rat liver microsomes.

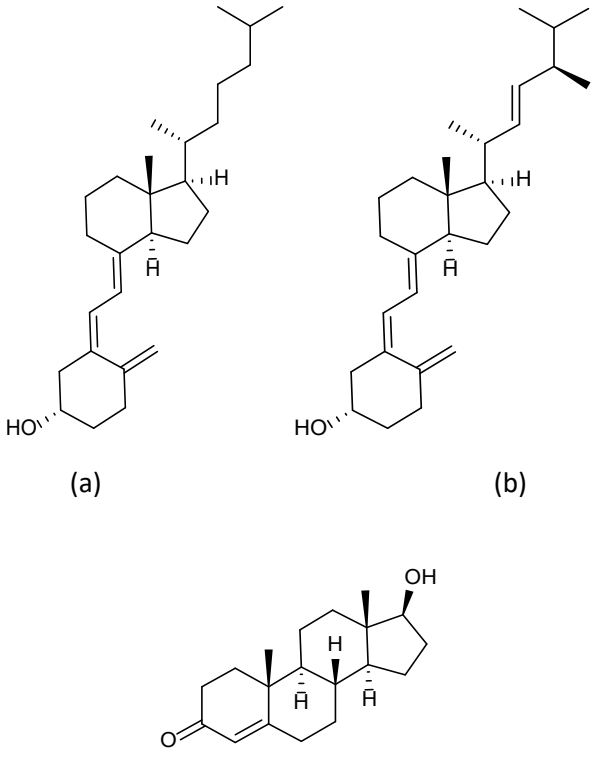

Figure 34. (a) Vitamin D$_3$, (b) Vitamin D$_2$, (c) Testosterone.

4.2 Materials and Methods

4.2.1 Chemicals

4-hydroxyoctanophenone (4-HP) with purity greater than 99% was obtained from the supplier as mentioned in Chapter 2 (refer to section 2.2.1). 25-hydroxyvitamin D_2 was obtained from Cayman Chemical (USA). Vitamin D_3, Vitamin D_2, 25(OH)D_3, and inhibitor Testosterone were obtained from Sigma-Aldrich UK. Metabolites (25(OH)D_3 and 25$(OH)_2$) were dissolved in methanol (MeOH) and stored at -20 °C. Acetonitrile and H_2O were procured from Sigma-Aldrich UK. All reagents and solvents used were of HPLC or analytical grade.

Phosphoric acid (85% w/w), Potassium phosphate monobasic, EDTA (Ethylenediaminetetraacetic acid), Glucose-6-phosphate (G-6-P), potassium phosphate dibasic, glucose-6-phosphate dehydrogenase (G-6-PDH), magnesium chloride ($MgCl_2$), testosterone, and nicotinamide adenine dinucleotide phosphate ($NADP^+$), was purchased as stated in Chapter 2 (refer to section 2.2.1).

The pooled human liver microsomes (human male) were purchased from Merck (UK). CypExpress 3A4 Cytochrome P450 human was purchased from Sigma-Aldrich UK and stored at -70 °C.

4.2.2 Instrumentation and Chromatographic Conditions

To choose the best wavelength for HPLC analysis, a standard multianalyte solution (0.02 mg/mL) was passed through a Carry 100 Bio (Varian) UV spectrophotometer from Agilent Technologies LDA (UK) to record their absorption. The HPLC system was used for analysis as mentioned in Chapter 2 (section 2.2.2). Various solvent systems such as methanol: Buffer (MeOH: Buffer), methanol: water (MeOH: H_2O), acetonitrile: methanol: water (ACN: MeOH: H_2O), and acetonitrile: water (ACN: H_2O), with isocratic and gradient elution were tried out, but the optimum separation was achieved with acetonitrile and water. The analyses were carried out using an isocratic mode of separation (90% acetonitrile: 10% water, v/v) at a flow rate of 1 mL/min. The column oven temperature was set at 35°C, and

the UV detector at 265 nm. Each analysis was set to inject 10 µL of sample solution. The analysis run time was 23 minutes for the Vitamin D assay. Data were processed using the software as mentioned in Chapter 2 (section 2.2.2). LCMS sample analysis was performed on the Agilent 6430-Triple Quad LC/MS instrument (Agilent Technologies, US). The LC-MS instrument was controlled at 0.5 mL/min of flow rate, and 10 µL of injection volume and the column temperature was set at 35 °C.

4.2.3 Preparation of Solutions

4.2.3.1 Standard Solution of Internal Standard

HPLC grade 4-Hydroxyoctanophenone (98%) was used as an internal standard. 1 mg/mL stock solution was prepared by dissolving 0.005 g of 4-HP in a 5 mL mobile phase in a volumetric flask. 500 ng/mL standard solution was prepared from the stock.

4.2.3.2 Standard Solutions of Vitamin D_3 and Vitamin D_2

For analysis, Vitamin D_3 and Vitamin D_2 were prepared in a 1 mg/mL solution fresh every day, and working solutions were prepared from stock solution by diluting in the mobile phase (90% acetonitrile: 10% water, v/v). Stock and standard solutions were covered with aluminium foil.

4.2.3.3 Standard Solutions of 25-hydroxyvitamin D_3 and 25-hydroxyvitamin D_2

A stock of 25-hydroxyvitamin D_3 (0.2 mg/mL) was prepared by dissolving 1 mg of 25-hydroxyvitamin D_3 in 5 mL methanol. A stock of 25-hydroxyvitamin D_2 (0.3 mg/mL) was prepared by dissolving 1 mg of 25-hydroxyvitamin D_2 in 3.3 mL methanol. The stock solutions were covered with foil and stored at -20 °C. Working solutions of metabolites of Vitamin D were prepared from their stock solution before use.

4.2.4 UV-Vis Spectroscopy

The standard solution of each analyte (Vitamin D_3, Vitamin D_2, 25(OH)D_2, 25(OH)D_3, Testosterone, 4-Hydroxyoctanophenone (I.S) was passed through a UV-Vis spectrophotometer to select the suitable wavelength for the analysis.

4.2.5 Method Validation of CYP2C11 Assay (Vitamin D)

The reverse phase-high performance liquid chromatography (RP-HPLC) method validation was performed according to ICH guidelines for linearity and range, precision, accuracy, the limit of detection, the limit of quantification, robustness, specificity/selectivity, and stability.

4.2.5.1 Linearity

According to ICH guidelines, the linearity of an analytical method demonstrates its ability to attain a response directly proportional to the analyte concentration in a certain range. Different concentrations (0-500 ng/mL) of working solutions from Vitamin D_3 and Vitamin D_2 stock solutions (1 mg/mL) were prepared in the mobile phase (ACN 90%: H_2O10%, v/v) for the construction of the calibration curves. Working solutions of 25(OH)D_3, and 25(OH)D_2 covering the range 0-100 ng/mL were also prepared from their stocks (0.2 mg/mL and 0.3 mg/mL, respectively) to construct their calibration curves. Batches were performed for the prepared dilutions and data were processed as described in Chapter 2 (section 2.3.2.1).

4.2.5.2 Limit of Detection (LOD) and Limit of Quantification (LOQ)

The LOD and LOQ of the method were determined as explained in Chapter 2 (section 2.3.2.3).

4.2.5.3 Precision

Precision was evaluated by injecting triplicate of standard samples of Vitamin D_3 and Vitamin D_2 at low (80 ng/mL), medium, (190 ng/mL), and high (350 ng/mL) within the calibration range. The metabolites' precision was determined using triplicates of their

standard samples at low (17 ng/mL), medium (40 ng/mL), and high (65 ng/mL). The estimation of interday and intraday precision was achieved by the mean of the measured concentration for all the prepared samples.

Relative standard deviation (RSD %), recovery (%) as well as standard error (SE %) were calculated for each concentration of different analytes.

4.2.5.4 Robustness

The evaluation of variations of the method parameters (chromatographic conditions) that can be tolerated by the method is called robustness. Robustness was determined by altering the column temperature (±5 °C), flow rate (±0.2 mL/min) as well as changing wavelength (± 5 nm).

4.2.5.5 Specificity/Selectivity

Specificity was attained by selecting the optimised mobile phase composition, the appropriate column, detector wavelength, and column temperature. Specificity/selectivity was evaluated as stated in Chapter 2 (section 2.3.2.2).

4.2.5.6 Solution Stability

The stability of the vitamin D_3, Vitamin D_2, and their metabolites (25 (OH)D_3 and 25(OH)D_2) were tested in analytical solutions by replicate inter-day (n = 3) and intraday analysis (n = 3) measurements at ambient temperature. Three control samples of Vitamin D_3 and Vitamin D_2 were tested at concentrations 80 ng/mL (low), 190 ng/mL (medium) and 350 ng/mL (high), and the metabolites at concentrations 17 ng/mL (low), 40 ng/mL (medium) and 65 ng/mL (high). For intraday stability analysis, the analytical solutions were examined at 0 hrs, 4 hrs, and 8 hrs against freshly pre-pared solutions while for interday stability analysis, the analytical solutions were examined for three consecutive days against freshly prepared calibrant solutions. The results of all stability experiments were compared with the Vitamin D_3, Vitamin D_2, 25 (OH)D_3, and 25(OH)D_2 initial standard concentrations.

4.2.6 Microsomal Incubations Procedure - Method 1

The oxidative metabolism of Vitamin D_3 and Vitamin D_2 was evaluated by incubating microsomal protein (0.5 mg/mL) with a serial range of Vitamin D_3 and Vitamin D_2 (0-10,000 ng/mL) concentrations, NADPH (1.0 mM), magnesium chloride (3.0 mM), Glucose-6-Phosphate Dehydrogenase (1.7 units/mL), 0.067 M potassium phosphate buffer (pH 7.4), Glucose-6-Phosphate (5 mM) and ethylenediaminetetraacetic acid (1.0 mM EDTA) in a final volume of 500 µL at 37 °C for 60 min. The reaction was initiated by the addition of nicotinamide adenine dinucleotide phosphate (NADP+) to the mixture after pre-incubation of all components for 5 min in a water bath (T = 37 °C). The final concentration of organic solvent in the reaction mixture did not exceed 1% v/v.

Ice-cold grade acetonitrile containing internal standard (125 ng/mL) was added to the incubation mixture to stop the reaction. Reaction tubes were centrifuged for 12 min in a microcentrifuge (13,000× *rpm*) to precipitate the liver protein. Next, the supernatant was collected and dissolved in a mobile phase (90% acetonitrile and 10% water, v/v) and the volume was made up to 1 mL. A 10 µL sample was injected into the HPLC system for analysis.

4.2.7 Microsomal Incubations Procedure - Method 2

The assay mixture was incubated as reported previously with minor changes [185]. The typical assay mixture (0.98 mL) contained 0.5 mg/mL rat liver microsomes, 1 µM EDTA, 100 µM Tris-HCl buffer (pH 7.4), 50 mM NADPH regenerating system, and 100 µM Vitamin D_3 and Vitamin D_2 dissolved in 10 µL of methanol. The assay mixture was pre-incubated for 5 minutes at 37 °C and the reaction was initiated by adding 60 µL of NADPH regenerating system. The assay mixture was incubated for 10 min in a microcentrifuge at 37 °C at 150 rpm. The termination of the reaction was achieved by adding 1 ml of ice-cold methanol. The extraction of reaction products was accomplished by adding 4 mL of benzene, toluene, and petroleum ether. 3 mL of the organic phase was evaporated to dryness and the collected residue was dissolved in the mobile phase containing Internal Standard (125 ng/mL). The 10 µL of each sample was injected into HPLC for analysis.

4.2.8 Rat S9 Fractions Incubation Procedure

Rat S9 fractions were incubated with Vitamin D_3 and Vitamin D_2 under the same reaction conditions as described in section 4.2.7. The reaction products were extracted with benzene and 10 µL of the sample was injected for analysis into the HPLC system.

4.2.9 Extraction of Metabolites with Dichloromethane (DCM)

The microsomal incubation with Vitamin D_3 to measure the 25 hydroxylations was based on an enzymatic assay developed by Tuckey *et al.* [186] with minor modifications. Rat liver microsomes (0.5 mg/ml) were incubated in 50 mM Tris-HCl buffer (pH 7.0), 50 mM sucrose, and 5 mM $MgSO_4$ with 500 µM Vitamin D_3 and D_2 (added from a methanol stock). 1.0 ml of typical assay mixture was preincubated for 5 min in an incubator at 37 °C. The reaction was started by the addition of a 50 mM NADPH regenerating system. The reaction was stopped by 2.5 ml of ice-cold dichloromethane after 30 min of incubation at 37 °C. Samples were vortexed and centrifuged at 670×*g* for 10 min. The extraction of the top aqueous layer was repeated two times more with 2.5 ml of dichloromethane and extracts were combined and dried out under nitrogen gas at ambient temperature, then dissolved in a mobile phase containing internal standard for HPLC analysis.

4.2.10 Derivatisation of Reaction Products using Benzoyl Chloride (BzCl)

500 µL of the sample solution (reaction products extracted with benzene and dissolved in the mobile phase (90% acetonitrile and 10% water, v/v) was derivatised by the addition of 250 µL of BzCl (2% (v/v) in acetonitrile) and 250 µL of 100 mM sodium carbonate. The sample vial was vortexed for 10 minutes [187] and an aliquot was run on HPLC for analysis.

4.2.11 Derivatisation of Reaction Products using 4-phenyl-1,2,4-triazoline-3,5-dione (PTAD)

For the Vitamin D analysis, several Cookson-type reagents have been suggested, though the most common one is 4-phenyl-1,2,4-triazoline-3,5-dione (PTAD). For this purpose, 10 ug/ml of Vitamin D_3, Vitamin D_2, 25(OH)D_3, and 25(OH)D_2 and sample solution (products of incubation reaction) were allowed to react with 0.75 mg/ml PTAD at room temperature for

1 hour respectively. Aliquots were quenched with an equal volume of methanol and run on HPLC.

4.2.12 CYP2R1 Enzyme Assay for Vitamin D 25-hydroxylation using Human Liver Microsomes

The incubation process was performed, as reported previously, with minor changes [188]. Vitamin D_3 and Vitamin D_2 were dissolved in methanol. The reaction mixture comprises each substrates (100 µM) and human liver microsomes (0.5 mg/mL) in 50 mM potassium phosphate buffer (pH 7.4). The reaction was started by adding 0.5 mM NADPH at 37 °C. The reaction was stopped at 20 min with 1 mL ice-cold methanol and was extracted with a chloroform/methanol mixture (3:1, v/v). The organic phase was pipetted out and then dried under nitrogen. The collected residue was solubilized in the mobile phase and analyzed using HPLC.

Concurrently, the same set of conditions as described in section (4.2.7) was used for the incubation of the reaction mixture, and samples were extracted with benzene and dried up under nitrogen. Residues were dissolved in the mobile phase containing IS and analyzed by HPLC in triplicate.

4.2.13 Vitamin D Metabolism by Pure CYP3A4Express Enzyme

The assay was performed with the provided protocol by the supplier. The typical assay mixture (1 ml) contains 100 mM of potassium phosphate buffer (pH 7.4), 5 mM glucose-6-phosphate, 2.0 mM NADP, and 500 µM Vitamin D_2 (Substrate). Cyp3A4Express powder (100 mg) was added to initiate the reaction. The assay mixture was incubated for two hours at 30 °C at 150 rpm. The reaction was quenched with 1 ml methanol, separated into two centrifuge tubes and centrifuged at 6000 x rpm for 10 min at room temperature. The supernatant was removed and analysed by HPLC in triplicate while the supernatant was removed from other centrifuging tubes and extracted with benzene.

4.2.14 Characterisation of Peaks by quantitative Nuclear Magnetic Resonance Analysis (qNMR)

4.2.14.1 Sample preparation

NMR sample (Vitamin D_2 after incubation with CY3A4Express enzyme and extraction with benzene) was spiked with sodium d_4-dimethylsilylpropionate (TSP). TSP concentration was 1 mmol/ml in the spiked sample and was consistent with the Vitamin D_2 concentration. All standards (Vitamin D_2 and 25(OH)D_2, NADP, and incubation mixture) samples were prepared and run in DMSO-d_6 solutions (1 mg/ml) at 300 K by Bruker Advance III 600 MHz FT-NMR [189].

4.2.15 Peaks Identification by Liquid Chromatography-Mass Spectrometry (LCMS)

The HPLC developed method was modified to suit LCMS. Sample (Vitamin D_2 after incubation with CY3A4Express enzyme, extracted with benzene and derivatised with PTAD) was analysed using LCMS at 0.5 µL flow rate and suitable mobile phase (90% acetonitrile: 10% water (0.1% formic acid), v/v), (70% acetonitrile: 30% water (0.1% formic acid), v/v), (50% acetonitrile: 50% water (0.1% formic acid), v/v).

4.3 Results and Discussion

4.3.1 Selection of Analytical Wavelength: Ultraviolet-Visible (UV-VIS) Scans of Working Standards

The working multianalyte solution (0.02 mg/ml) of each component such as Vitamin D_3 and Vitamin D_2 (substrate), 25(OH)D_3 and 25(OH)D_2 (metabolites), 4-Hydroxyoctanophenone (I.S), testosterone (inhibitor) was passed through UV-VIS spectrophotometer to find the best suitable wavelength (Figure 35). From CYP2C11 assay components spectra, it is indicated that the maximum absorption band for all Vitamin D assay components is 265 nm [178].

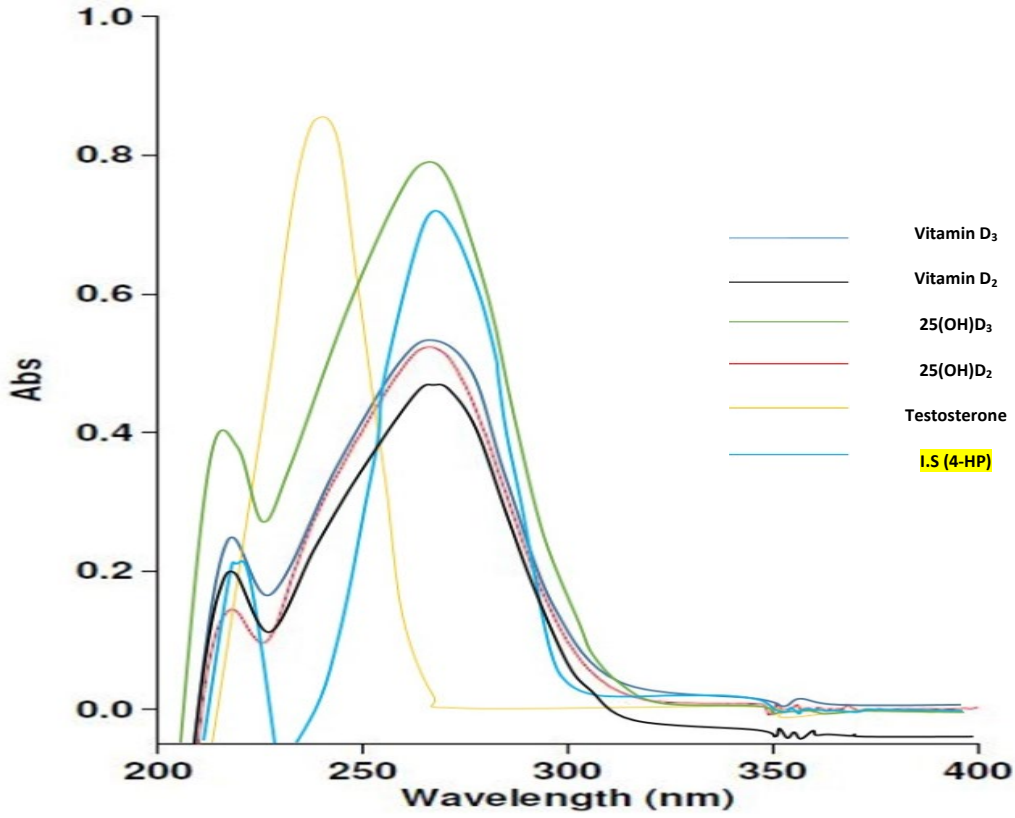

Figure 35. UV spectra of Vitamin D assay components (Vitamin D3, Vitamin D_2, 25(OH)D_3, 25(OH)D2, 4-Hydroxyoctanophenone (internal standard), Testosterone (inhibitor).

4.3.2 Optimisation of the Mobile Phase and Columns for the Development of CYP2C11 Assay (Testosterone as Inhibitor)

A multianalyte solution (1000 ng/mL) was passed through the HPLC system using different C18 columns. Table 19 explains the varieties of mobile phases and columns which were

used to select the one with good separation and reasonable retention times. The column which worked best was XBridge C18 (150 x 4.6 mm, I.D., 3.5 µm, particle size). A new method was developed with isocratic elution using 90% acetonitrile and 10% water as mobile phase at 35 °C and 1 mL/min flow rate. Figure 36 represents a good separation of all Vitamin D assay components. Thus, the optimised assay time was 23 minutes with an isocratic mode of separation which is quite reasonable for an inhibition study while the literature shows long analysis times along with gradient elution for Vitamin D_3 and Vitamin D_2 and their metabolites [190].

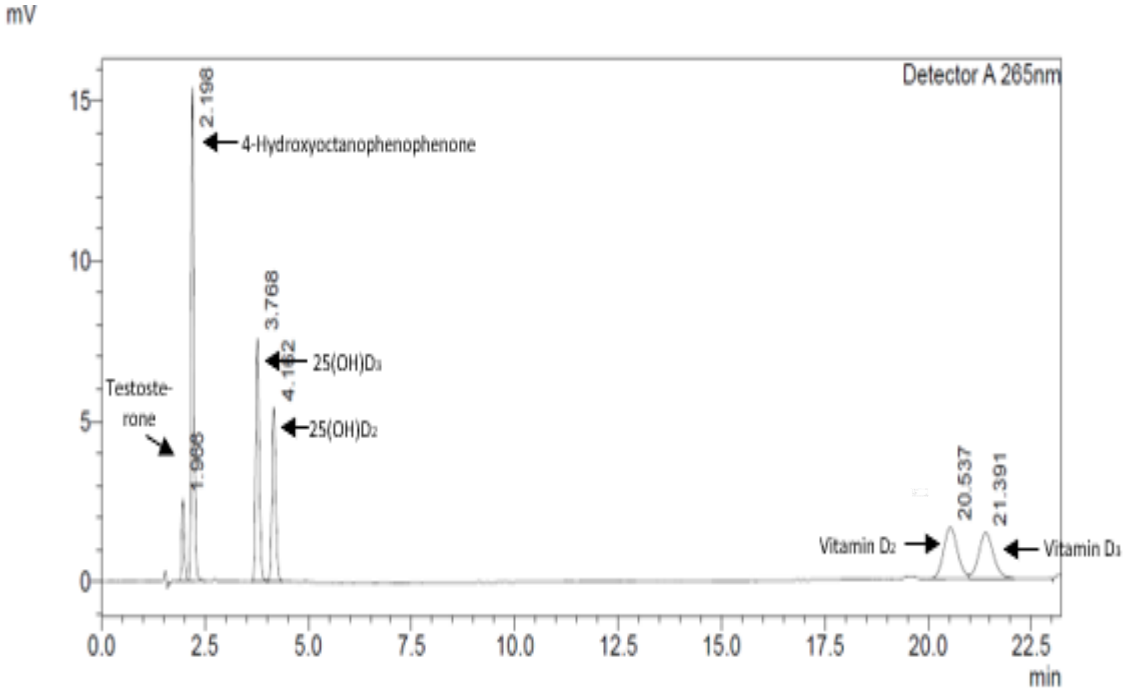

Figure 36. Chromatogram of a standard multianalyte (Vitamin D_3, Vitamin D_2, 25(OH)D_3, 25(OH)D_2, 4-hydroxyoctanophenone (I.S) solution using isocratic elution ACN : H_2O (90%:10%, v/v).

Table 19. The HPLC columns and mobile phases investigated (Vitamin D_3, Vitamin D_2, 25(OH)D_3, 25(OH)D_2, internal standard (phenacetin, paracetamol, 4-hydroxyoctanophenone) and testosterone (inhibitor) at 265 nm at column temperature 25°C and flow rate of 1 mL/min.

Stationary phase	Mobile phase	Note
C18 (250 x 4.6 mm, I.D., 5 µm, particle size)	Isocratic elution: ($MeOH+H_2O$ and $ACN+H_2O$, 50%+50%, 70%+30%, 80%+20%, 40%+60%, 30%+70%, v/v)	-No peak observed

Hypersil C18 BDS (150 x 4.6 mm, I.D., 5 µm, particle size)	Isocratic elution: (MeOH+Phosphate buffer 0.02 M, pH 2.6, 50%+50%, 15%+85%, 80%+20%, 70%+30%, 60%+40%, v/v)	-Four peaks (Phenacetin, testosterone, 25(OH)D_3, 25(OH)$D_{2)}$ observed -No peak observed for Vitamin D_3 and Vitamin D_2
Luna C18 BDS (150 x 4.6 mm, I.D., 5 µm, particle size)	Isocratic elution: (MeOH+Phosphate buffer 0.02 M, pH 2.6, 50%+50%, 15%+85%, 80%+20%, 70%+30%, 60%+40%, v/v)	-Four peaks (Phenacetin, testosterone, 25(OH)D_3, 25(OH)$D_{2)}$ observed -No peak observed for Vitamin D_3 and Vitamin D_2
XTerra RP18 (150 x 4.6 mm, I.D., 3.5 µm, particle size)	Isocratic elution: (MeOH + H_2O, 95%+5%, 90%+10%, v/v)	-Six peaks observed -Good separation of internal standard (phenacetin) and inhibitor (testosterone) -Coelution of metabolites peaks -Poor separation of Vitamin D_3 and Vitamin D_2 -Short analysis time < 5min
XTerra RP18 (150 x 4.6 mm, I.D., 3.5 µm, particle size)	Isocratic elution: (MeOH + H_2O, 85%+15%, v/v)	-Poor separation of metabolites and Vitamin D_3 and Vitamin D_2 -Long analysis time > 25min
XTerra RP18 (150 x 4.6 mm, I.D., 3.5 µm, particle size)	Isocratic elution: (MeOH + H_2O, 84%+16%, 80%+20%, v/v)	-Good separation of metabolites -Poor separation of Vitamin D_3 and Vitamin D_2 -Long analysis time ~48min
XTerra RP18 (150 x 4.6 mm, I.D., 3.5 µm, particle size)	Isocratic elution: (MeOH+ H_2O, 75%+25%, 50%+50%, v/v)	-Good separation of metabolites -Poor separation of Vitamin D_3 and Vitamin D_2 -Long analysis time ~90min
XTerra RP18 (150 x 4.6 mm, I.D., 3.5 µm, particle size)	Isocratic elution: (MeOH+ACN, 50%+50%, 65%+35%, 75%+25%, 80%+20%, 85%+15%, v/v)	-Good separation of internal standard (phenacetin) and inhibitor (testosterone) -Coelution of metabolites and Vitamin D_3 and Vitamin D_2 -Short analysis time < 10 min
XTerra RP18 (150 x 4.6 mm, I.D., 3.5 µm, particle size)	Isocratic elution: (MeOH + Phosphate buffer 0.02 M, pH 2.6, 95%+5%, v/v)	-Good separation of internal standard (1αOHD_3) and inhibitor (testosterone) -Coelution of metabolites, Vitamin D_3 and Vitamin D_2

		-Short analysis time < 5min
XTerra RP18 (150 x 4.6 mm, I.D., 3.5 µm, particle size)	Isocratic elution: (MeOH + Phosphate buffer 0.02 M, pH 2.6, 90%+10%, 85%+15%, v/v)	-Poor separation of internal standard ($1\alpha OHD_3$) and inhibitor -Coelution of metabolites, Vitamin D_3 and Vitamin D_2 -Short analysis time < 20min
XTerra RP18 (150 x 4.6 mm, I.D., 3.5 µm, particle size)	Isocratic elution: (MeOH + Phosphate buffer 0.02 M, pH 2.6, 80%+20%, v/v)	-Good separation of internal standard but tailing of inhibitor -Good separation of metabolites -Coelution of Vitamin D_3 and Vitamin D_2 -Reasonable analysis time ~20min
XTerra RP18 (150 x 4.6 mm, I.D., 3.5 µm, particle size)	Isocratic elution: (MeOH + Phosphate buffer 0.02 M, pH 2.6, 75%+25%, v/v)	-Good separation of internal standard and testosterone -Good separation of metabolites -Coelution of Vitamin D_3 and Vitamin D_2 -Reasonable analysis time ~25min
XTerra RP18 (150 x 4.6 mm, I.D., 3.5 µm, particle size)	Gradient elution: (MeOH + Phosphate buffer 0.02 M, pH 2.6, 50-100%+50-100%, v/v)	-Same separation as isocratic -Gradient didn't work with different compositions of mobile phases
XBridge C18 (150 x 4.6 mm, I.D., 3.5 µm, particle size)	Isocratic elution (ACN : MeOH, 99%+1%, v/v)	-Good separation of internal standard (Phenacetin) and inhibitor (testosterone) -Coelution of metabolites -Good separation of Vitamin D_3 and Vitamin D_2 -Short analysis time ~10 min
XBridge C18 (150 x 4.6 mm, I.D., 3.5 µm, particle size)	Gradient elution: ACN+H_2O+MeOH (91%+8%+1%, v/v) for 5 min. then ACN+H_2O+MeOH (7%+8%+85%, v/v) for 19 min, finally reconditioning ACN+H_2O+MeOH (91%+8%+1%, v/v) for 3 min. -Temperature 35 °C	-Good separation of internal standard (paracetamol) and inhibitor -Good separation of metabolites -Good separation of Vitamin D_3 and Vitamin D_2 -Reasonable analysis time ~22 min
XBridge C18 (150 x 4.6 mm, I.D., 3.5 µm, particle size)	Isocratic elution (ACN : H_2O, 90%+10%, v/v) -Temperature 35 °C	-Good separation of internal standard (4-Hydroxyoctanophenone) and inhibitor (testosterone)

		-Good separation of metabolites -Good separation of Vitamin D_3 and Vitamin D_2 -Reasonable analysis time ~23 min
XBridge C18 (150 x 4.6 mm, I.D., 3.5 µm, particle size)	Gradient elution with different compositions of mobile phase	-Didn't observe any difference between gradient and isocratic elution

4.3.3 Assay Validation (Testosterone as Inhibitor)

4.3.3.1 Calibration and Linearity

Different concentrations of Vitamin D and its metabolites were injected into the HPLC instrument for the construction of calibration curves. Each dilution was injected in triplicate. The construction of calibration curves for Vitamin D_3 and Vitamin D_2 and metabolites ($25(OH)D_3$ and $25(OH)D_2$) was performed by plotting concentration (ng/mL) versus the peak area ratio to the internal standard (4-hydroxyoctanophenone) using Excel software 2010 system. Table 20 shows the outcomes of the linearity study.

Table 20. Analytical performances of HPLC method.

Standards	**Vitamin D_3**	**Vitamin D_2**	**$25(OH)D_3$**	**$25(OH)D_2$**
Analytical range	75-500 ng/mL	75-500 ng/mL	15-100 ng/mL	15-100 ng/mL
r^2	0.999	0.999	0.999	0.998
Regression Equation	y=0.0094x-0.0689	y=0.0078x-0.0476	y=0.0066x-0.0087	y=0.0049x-0.0059

The results confirmed the good linearity values for Vitamin D_3, Vitamin D_2, $25(OH)D_3$, and $25(OH)D_2$. The obtained r^2 (linear regression coefficient) values were within the analytical ICH guidelines range ($R^2 > 0.99$). Demonstration of linear responses for the procedure is necessary to assist the quantitative analysis of Vitamin D in pharmacological measures [178].

4.3.3.2 Precision

Intraday Precision of Vitamin D and Metabolites

The method precision of Vitamin D_3 and Vitamin D_2 were determined by carrying out the measurements of three standard samples, i.e. low (80 ng/mL), medium, (190 ng/mL), high (350 ng/mL). Whereas metabolites precision was evaluated by injecting standard samples, i.e. low (17 ng/mL), medium, (40 ng/mL), high (65 ng/mL) into the HPLC system. The standard samples were analysed in triplicate. Relative standard deviation (RSD %), recovery (%) as well as standard error (SE) were calculated for each concentration of different analytes. Results of the intraday assay are summarised in Tables 21 and Table 22. Results show that the percentage error was less than 10 % for each Vitamin D and metabolites concentration level. % Recovery values were found to be within the range of ICH guidelines as the acceptance criterion for a method recovery is 80-120%. The % RSD values for the intraday assay are > 10%. The acceptable deviation criteria for accuracy are ±15% from the nominal values [191]. Thus, the outcomes revealed that there is no variation in the concentration of Vitamin D_3 and Vitamin D_2 and metabolites between intraday analysis. The obtained values were considered satisfactory for the planned use of the method.

Table 21. Intraday Precision of Vitamin D_3 and Vitamin D_2.

Intraday Precision	**Vitamin D_3 Concentration**			**Vitamin D_2 Concentration**		
	80 ng/mL	**190 ng/mL**	**350 ng/mL**	**80 ng/mL**	**190 ng/mL**	**350 ng/mL**
Mean (ng/mL)	78.77	185.02	353.28	79.36	188.63	349.49
% SE	± 2.99	± 4.23	± 2.75	± 1.36	± 6.20	± 8.99
% Recovery	98.47	97.38	100.94	99.20	99.28	99.85
% RSD	3.79	2.29	0.78	1.72	3.29	2.53

Table 22. Intraday Precision of 25(OH)D_3 and 25(OH)D_2.

Intraday Precision	25(OH)D_3 Concentration			25(OH)D_2Concentration		
	17 ng/mL	40 ng/mL	65 ng/mL	17 ng/mL	40 ng/mL	65 ng/mL
Mean (ng/mL)	16.79	39.36	66.30	18.30	38.47	62.37
% SE	± 0.60	± 0.84	± 3.61	± 0.89	± 0.89	± 1.07
% Recovery	98.74	98.41	101.99	107.67	96.18	95.96
% RSD	3.57	2.12	5.44	4.87	2.32	1.72

Interday Precision of Vitamin D and Metabolites

Inter-assay precision and accuracy were determined by measuring Vitamin D standards of three concentrations levels, i.e. low (80 ng/mL), medium, (190 ng/mL), high (350 ng/mL), and metabolites standards of three concentration levels, i.e. low (17 ng/mL), medium, (40 ng/mL), high (65 ng/mL) for three consecutive days. Tables 23 and 24 show the outcomes of the interday precision analysis. The %RSD (relative standard deviation) and standard error values were <15% for Vitamin D and metabolites. % Recovery values were within the ICH guidelines range (80-120%). The experiment results showed that there is no large variation in interday measurements.

Table 23. Interday Precision of Vitamin D_3 and Vitamin D_2.

Interday Precision	Vitamin D_3 Concentration			Vitamin D_2 Concentration		
	80 ng/mL	190 ng/mL	350 ng/mL	80 ng/mL	190 ng/mL	350 ng/mL
Mean (ng/mL)	77.31	176.59	339.09	78.18	198.02	351.66
% SE	± 8.16	± 11.50	± 5.28	± 2.26	± 14.02	± 9.26
% Recovery	96.64	92.94	96.88	97.72	104.22	100.47
% RSD	10.56	6.51	1.56	2.89	7.08	2.63

Table 24. Interday Precision of 25(OH)D_3 and 25(OH)D_2.

Interday Precision	25(OH)D_3 Concentration			25(OH)D_2Concentration		
	17 ng/mL	**40 ng/mL**	**65 ng/mL**	**17 ng/mL**	**40 ng/mL**	**65 ng/mL**
Mean (ng/mL)	18.27	40.69	66.45	16.48	41.61	65.09
% SE	± 1.55	± 1.59	± 1.09	± 0.75	± 2.09	± 2.45
% Recovery	107.44	101.73	102.23	96.96	104.02	100.13
% RSD	8.47	3.93	1.63	4.55	5.01	3.77

4.3.3.3 Limit of Detection (LOD) and Limit of Quantification (LOQ)

According to the ICH guidelines, the LOD and LOQ of the planned method were calculated mathematically by the relationship between the standard deviation of the response and the slope of the calibration curve. Table 25 displays the calculated LOD and LOQ values for Vitamin D and metabolites.

Table 25. LOD and LOQ for Vitamin D and metabolites.

Standards	Vitamin D_3 (ng/mL)	Vitamin D_2 (ng/mL)	25(OH)D_3 (ng/mL)	25(OH)D_2 (ng/mL)
LOD	24.10	15.27	3.86	2.04
LOQ	73.04	46.28	11.68	6.17

4.3.3.4 Specificity/Selectivity

To evaluate the specificity of the method or possible interferences with the analyte's retention times, a diluent blank (90% ACN :10% H_2O%, v/v) was run with the internal standard solution under the optimised HPLC conditions. Only one peak was observed for the internal standard (2.2 min) which proves the absence of interferences in the retention time windows for other compounds and showed the specificity of the method as shown in Figure 37 (a).

The chromatogram in Figure 37 (b) showed good separation of Vitamin D_3, and Vitamin D_2, from their metabolites (25(OH)D_3, and 25(OH)D_2) and testosterone (inhibitor).

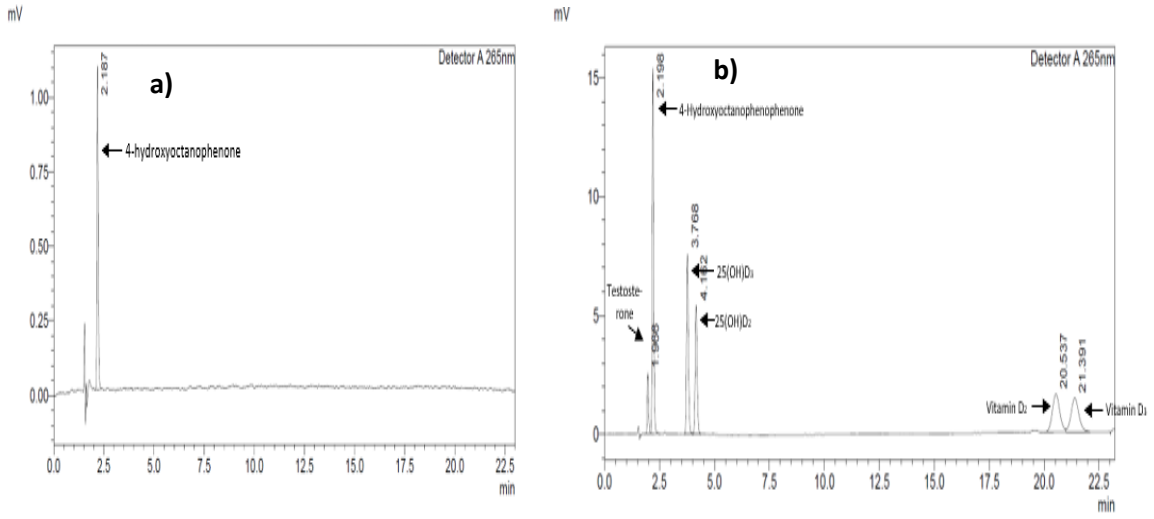

Figure 37. HPLC chromatograms show the specificity/selectivity of the method.

4.3.3.5 Robustness

The robustness of the method was evaluated by changing the column temperature (± 5 °C), wavelength (± 5 nm), and flow rate (± 0.2 mL/min) using HPLC. Tables 26, 27, 28, and 29 illustrate the change in flow rate, wavelength, and temperature on both retention time and peak area of each compound. No significant change was observed in the peak areas of analytes by changing these parameters. Low % RSD values (< 10%) for each parameter further confirm the robustness of the method. Thus, this indicates that the CYP2C11 assay method is robust, considering the change in flow rate, wavelength, and temperature.

Table 26. Robustness of the Vitamin D assay at normal conditions.

Normal Multianalyte run (Wavelength 265 nm, 35 °C, 1 mL/min)				
Analytes	**Average t_R (min)**	**Average ratio of Analyte/I.S**	**SD of Average Ratio**	**%RSD**
Testosterone	2.02	0.171	0.002	1.43
4-Hydroxyoctanophenone	2.24	1	0	0
25(OH)D_3	3.82	0.67	0.004	0.56
25(OH)D_2	4.20	0.53	0.005	0.95
Vitamin D_2	20.43	0.97	0.012	1.25
Vitamin D_3	21.31	0.61	0.006	0.98

Table 27. Robustness of the Vitamin D assay at 0.8 mL/min.

Multianalyte run (Wavelength 265 nm, 35 °C, 0.8 mL/min)				
Analytes	**Average t_R (min)**	**Average ratio of Analyte/I.S**	**SD of Average Ratio**	**%RSD**
Testosterone	2.53	0.17	0.009	5.32
4-Hydroxyoctanophenone	2.80	1	0	0
25(OH)D_3	4.79	0.67	0.008	1.15
25(OH)D_2	5.29	0.53	0.006	1.07
Vitamin D_2	25.95	0.98	0.008	0.82
Vitamin D_3	27.06	0.60	0.006	0.98

Table 28. Robustness of the Vitamin D assay at 260 nm.

Multianalyte run (Wavelength 260 nm, 35 °C, 1 mL/min)				
Analytes	**Average t_R (min)**	**Average ratio of Analyte/I.S**	**SD of Average Ratio**	**%RSD**
Testosterone	2.02	0.48	0.001	0.27
4-Hydroxyoctanophenone	2.24	1	0	0
25(OH)D_3	3.82	0.76	0.001	0.10
25(OH)D_2	4.22	0.61	0.005	0.90
Vitamin D_2	20.51	1.10	0.005	0.49
Vitamin D_3	21.38	0.69	0.001	0.12

Table 29. Robustness of the Vitamin D assay at 40 °C.

Multianalyte run (Wavelength 265 nm, 40 °C, 1 mL/min)				
Analytes	**Average t_R (min)**	**Average ratio of Analyte/I.S**	**SD of Average Ratio**	**%RSD**
Testosterone	1.99	0.16	0.001	0.83
4-Hydroxyoctanophenone	2.20	1	0	0
25(OH)D_3	3.65	0.66	0.001	0.17
25(OH)D_2	4.01	0.52	0.004	0.68
Vitamin D_2	17.84	0.97	0.002	0.23
Vitamin D_3	18.55	0.60	0.004	0.74

4.3.3.6 Stability Indicating Study of CYP2C11 Assay (Testosterone)

The stability study aimed to ensure that sample solutions do not degrade during their preparation and analysis time using HPLC. Evaluation of the stability of the working standard solutions (Vitamin D and metabolites) was performed at ambient temperature by intraday and interday analysis.

Stability of Substrates (Vitamin D_3 and Vitamin D_2)

Intraday and interday stability of Vitamin D_3 and Vitamin D_2 was studied at three different concentrations levels (low (80 ng/mL), medium (190 ng/mL), and high (350 ng/mL)). 4-hydroxyoctanophenone (as an internal standard of 125 ng/mL) was added to each batch. Each stability sample was analysed in triplicate (n = 3) measurement. The stability test results are presented in Table 30 and Table 31.

Table 30. Vitamin D_3 solutions stability at ambient temperature.

Stability Test Parameters	**Actual Concentration (ng/mL)**			
	Intraday	**80**	**190**	**350**
Calculated Concentration (ng/mL)	0 hours	68.91	191.26	394.11
	4 hours	71.44	179.10	391.02
	8 hours	72.24	197.60	376.44
% Recovery [a]	0 hours	86.14	100.66	112.60
	4 hours	89.29	94.26	111.72
	8 hours	90.29	104.00	107.55
% Accuracy [b]	0 hours	113.86	99.34	87.40
	4 hours	110.71	105.74	88.28
	8 hours	109.71	95.99	92.45
Calculated Concentration (ng/mL)	**Interday**	**80**	**190**	**350**
	Interday 1	74.60	185.37	374.88
	Interday 2	69.29	186.92	360.99
	Interday 3	70.70	186.08	371.15
% Recovery [a]	Interday 1	93.25	97.56	107.11
	Interday 2	86.61	98.38	103.14
	Interday 3	88.37	97.94	106.04

% Accuracy [b]	Interday 1	106.75	102.44	92.89
	Interday 2	113.39	101.62	96.86
	Interday 3	111.63	102.06	93.96

Note: [a] % recovery = (concentration of Vitamin D_3 at 8 hours/standard concentration of Vitamin D_3) x 100. [b] Accuracy = 100 – (calculated concentration – actual concentration)/actual concentration x 100.

Table 31. Vitamin D_2 solutions stability at ambient temperature.

Stability Test Parameters	**Actual Concentration (ng/mL)**			
	Intraday	**80**	**190**	**350**
Calculated Concentration (ng/mL)	0 hours	79.86	184.54	370.82
	4 hours	76.15	182.96	384.42
	8 hours	77.10	186.65	366.17
% Recovery [a]	0 hours	99.82	97.13	105.95
	4 hours	95.18	96.93	109.84
	8 hours	96.37	98.24	104.62
% Accuracy [b]	0 hours	100.18	102.87	94.05
	4 hours	104.82	103.70	90.17
	8 hours	103.63	101.76	95.38
Calculated Concentration (ng/mL)	**Interday**	**80**	**190**	**350**
	Interday 1	84.40	206.24	395.01
	Interday 2	77.27	181.98	401.17
	Interday 3	84.59	187.858	393.42
% Recovery [a]	Interday 1	105.50	108.55	112.86
	Interday 2	96.58	95.78	114.62
	Interday 3	105.73	98.87	112.41
% Accuracy [b]	Interday 1	94.50	91.45	87.14
	Interday 2	103.42	104.22	85.38
	Interday 3	94.27	101.13	87.60

Note: [a] % recovery = (concentration of Vitamin D_2 at 8 hours/standard concentration of Vitamin D_2) x 100. [b] Accuracy = 100 – (calculated concentration – actual concentration)/actual concentration x 100.

The outcomes of the interday and intraday stability check indicate that there was no variation in the concentration of Vitamin D_3 and Vitamin D_2. In the intraday stability study, the sample solutions were compared after every 4 hours. The concentration of Vitamin D after 8 hours was the same as compared to the initial concentration at 0 hours and showed acceptable recovery and accuracy (80-120%). Vitamin D_3 and Vitamin D_2 calibration curves

were plotted for intraday where r^2 met the criteria of ICH guidelines (0.9955 and 0.9996 respectively).

For interday analysis, the chromatographic behaviour of Vitamin D remained the same on days 1, 2, and 3, compared to the initial concentrations. All three calibration curves were averaged, and the average straight-line equation for Vitamin D_3 was: y= 0.0062x - 0.0371 (r^2 = 0.9994) and for Vitamin D_2 was: y = 0.0051x - 0.0658 (r^2 = 0.9959) where r^2 met ICH guidelines. Intraday % recovery and accuracy values were high and were within an acceptable range (80-120%) of ICH guidelines [192],[193].

Stability of Metabolites (25(OH)D_3 and 25(OH)D_2)

Solution stability studies of metabolites were carried out by intraday and interday (n=3) analysis for three low, medium, and high concentrations (17, 40, and 65 ng/mL) at ambient temperature. An internal standard (4-hydroxyoctanophenone, 125 ng/mL) was added to each metabolite concentration batch. Each batch was analysed in triplicate (n = 3) measurements. Table 32 and Table 33 show the stability test outcomes for metabolites.

Table 32. 25(OH)D_3 solutions stability at ambient temperature.

Stability Test Parameters	**Actual Concentration (ng/mL)**			
	Intraday	**17**	**40**	**65**
Calculated Concentration (ng/mL)	0 hours	18.84	45.17	65.67
	4 hours	18.94	46.07	70.10
	8 hours	19.02	43.68	65.27
% Recovery [a]	0 hours	110.82	112.92	101.04
	4 hours	111.40	115.18	107.85
	8 hours	111.89	109.20	100.41
% Accuracy [b]	0 hours	89.19	87.08	98.96
	4 hours	88.60	84.82	92.16
	8 hours	88.11	90.80	99.59
Calculated Concentration (ng/mL)	**Interday**	**17**	**40**	**65**
	Interday 1	15.44	37.97	54.49
	Interday 2	19.95	40.75	57.87
	Interday 3	20.01	38.77	54.14

% Recovery [a]	Interday 1	90.80	94.94	83.83
	Interday 2	117.35	101.88	89.04
	Interday 3	117.71	96.92	83.29
% Accuracy [b]	Interday 1	109.20	105.07	116.170
	Interday 2	82.65	98.12	110.97
	Interday 3	82.29	103.80	116.71

Note: [a] % recovery = (concentration of 25(OH)D_3 at 8 hours/standard concentration of 25(OH)D_3) x 100. [b] Accuracy = 100 – (calculated concentration – actual concentration)/actual concentration x 100.

Table 33. 25(OH)D_2 solutions stability at room temperature.

Stability Test Parameters	**Actual Concentration (ng/mL)**			
	Intraday	**17**	**40**	**65**
Calculated Concentration (ng/mL)	0 hours	18.75	38.00	62.40
	4 hours	19.45	41.90	61.99
	8 hours	20.07	47.15	60.11
% Recovery [a]	0 hours	110.27	95.01	96.00
	4 hours	114.44	104.75	95.37
	8 hours	118.05	117.87	92.48
% Accuracy [b]	0 hours	89.73	104.99	104.00
	4 hours	85.56	95.25	104.64
	8 hours	81.95	82.13	107.52
Calculated Concentration (ng/mL)	**Interday**	**17**	**40**	**65**
	Interday 1	16.589	38.05	54.40
	Interday 2	19.74	39.23	62.94
	Interday 3	20.30	38.36	54.43
% Recovery [a]	Interday 1	97.56	95.11	85.23
	Interday 2	116.12	98.08	96.84
	Interday 3	119.40	95.89	82.19
% Accuracy [b]	Interday 1	102.44	104.89	114.77
	Interday 2	83.88	101.92	103.16
	Interday 3	80.60	104.11	117.81

Note: [a] % recovery = (concentration of 25(OH)D_2 at 8 hours/standard concentration of 25(OH)D_2) x 100. [b] Accuracy = 100 – (calculated concentration – actual concentration)/actual concentration x 100.

The outcomes of the intraday stability test show that the concentration of 25(OH)D_3 and 25(OH)D_2 and the peak areas were consistent after 8 hours when compared with 0 hours. However, in interday analysis, the chromatographic behaviour of Vitamin D_3 and Vitamin

D_2 metabolites remained the same on days 1, 2, and 3, compared to the initial concentrations. 25(OH)D_3 and 25(OH)D_2 calibration curves were constructed for intraday analysis and the obtained r^2 was 0.9998 for 25(OH)D_3 and r^2 = 0.9969 for 25(OH)D_2, which shows a good relationship with ICH guidelines. All calibration curves were averaged for interday analysis (n=3) and thus, the average calibration curve equation for 25(OH)D_3 was: y = 0.0059x + 0.001 (r^2 = 0.9995) and the average calibration curve equation for 25(OH)D_2 was: y = 0.0044x + 0.003 (r^2 = 0.9975). % Recovery and % accuracy values of metabolites at their low (17 ng/mL), medium (40 ng/mL), and high (65 ng/mL) concentrations complied with the range given in ICH guidelines which are 80-120%.

The results revealed that Vitamin D metabolites were stable during the day (intraday) and for consecutive three days (interday) at ambient temperature.

4.3.4 CYP2C11 Enzyme Assay

4.3.4.1 Vitamin D 25-hydroxylation Assay for CYP2C11 Enzyme Activity - Method 1

In vitro, CYP2C11 incubation system contained rat liver microsomes (0.5 mg/mL), different concentrations of Vitamin D_3 and Vitamin D_2 (substrate), magnesium chloride (3 mM), 5.0 mM glucose-6-phosphate (G6P), 1.7 units/mL glucose-6-phosphate dehydrogenase (G6PDH), 1.0 mM nicotinamide adenine dinucleotide phosphate hydrogen (NADPH), 1 mM of ethylenediaminetetraacetic acid (EDTA). The reaction was stopped after 60 minutes. The control reaction results are shown in Figure 38.

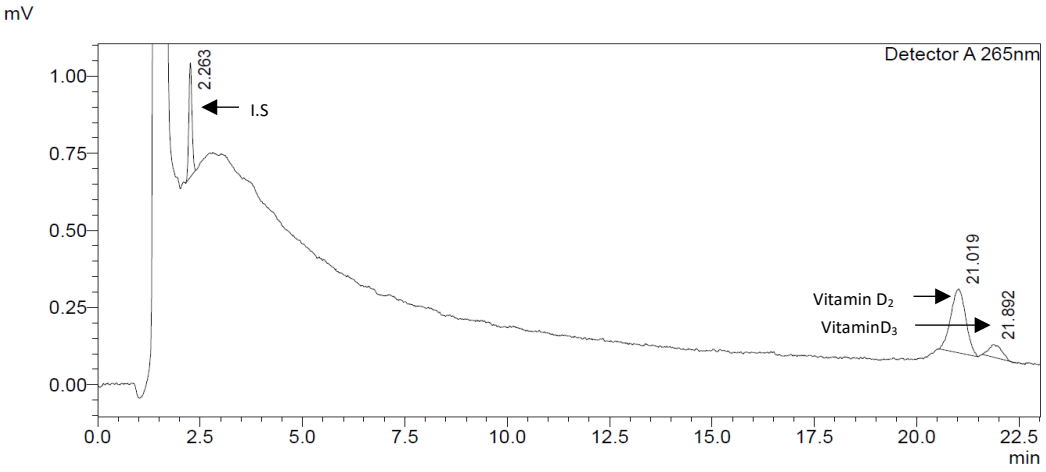

Figure 38. HPLC Chromatogram of control incubation reaction with rat liver microsomes.

4.3.4.2 Optimisation of Enzyme and Substrate Concentration for Incubation System *in Vitro*

For the purpose of optimisation of substrate concentration, a range of Vitamin D_3 and Vitamin D_2 (substrates) from 1000 ng/mL to 100,000 ng/mL were analysed under the same incubation system conditions (4.3.4.1) except a five-fold dilution of the enzyme (0.2 mM) was used to initiate the reaction. The outcomes of the optimisation experiment are presented in Figure 39.

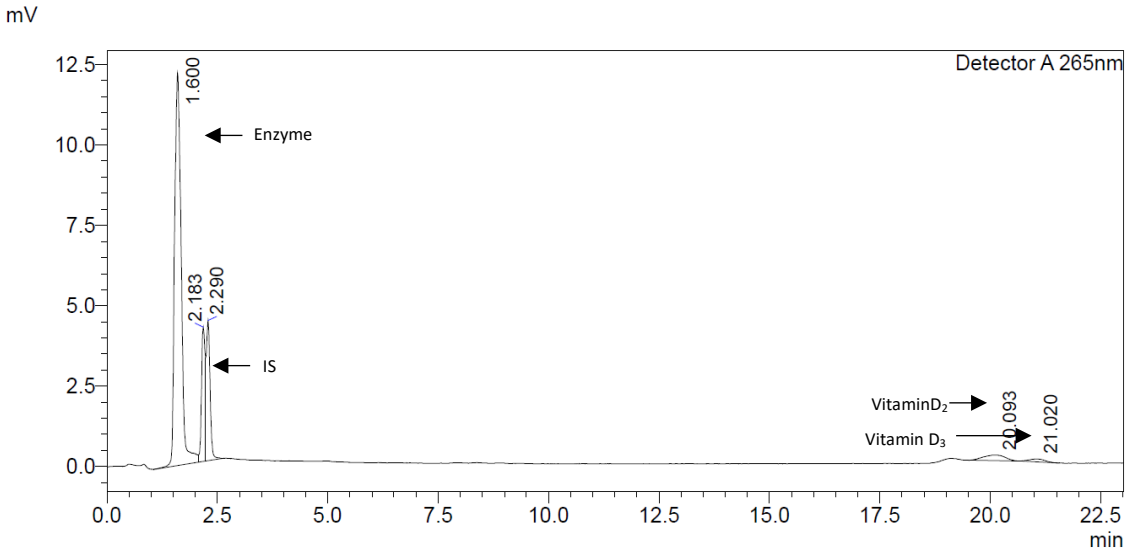

Figure 39. HPLC chromatogram of optimisation of conditions for control experiment.

4.3.4.3 CYP2C11 Enzyme Assay for Vitamin D 25-hydroxylation using Rat Liver Microsomes - Method 2

Rat liver microsomes were incubated with Vitamin D_3 and Vitamin D_2 in the presence of EDTA (1 µM), Tris-HCl buffer (100 µM, pH 7.4), NADPH regenerating system (50 mM), and the reaction was terminated at 10 min. The HPLC chromatogram of extracted reaction products with benzene is shown in Figure 40 below.

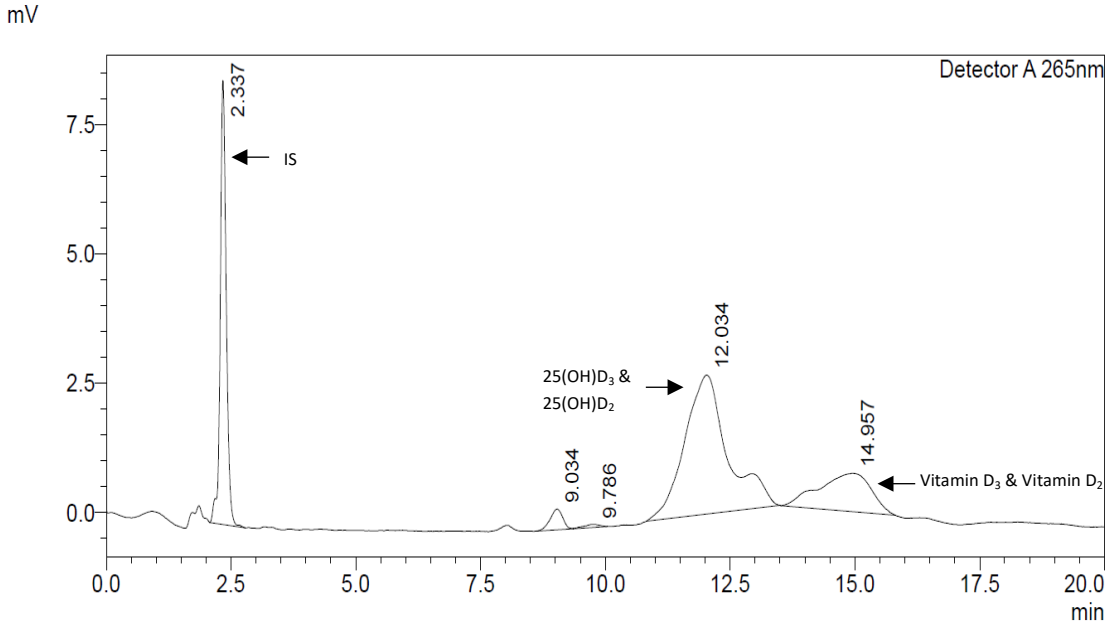

Figure 40. HPLC chromatogram of extracted reaction products with benzene.

4.3.4.4 CYP2C11 Enzyme Assay for Vitamin D 25-hydroxylation using Rat S9 Fractions

Rat S9 fractions were incubated with Vitamin D_3 and Vitamin D_2 under the same reaction conditions (Chapter 4, section 4.2.7). The HPLC chromatogram of extracted reaction products is shown in Figure 41 below.

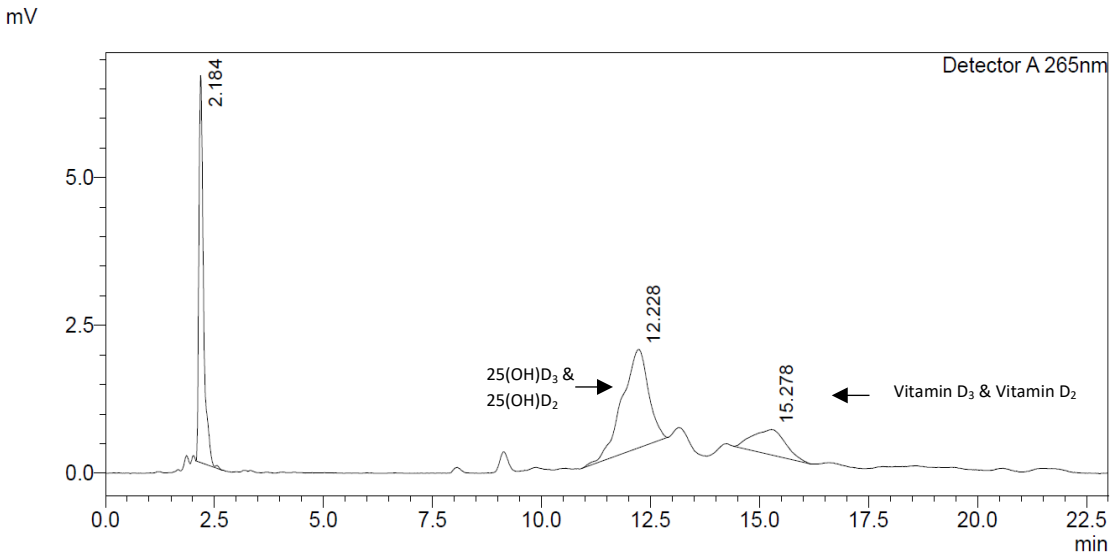

Figure 41. HPLC chromatogram of extracted reaction products (S9 fractions) with benzene.

4.3.4.5 Extraction of Reaction Products with Toluene and Petroleum Ether

The CYP2C11 enzyme assay was performed under the same incubation conditions as mentioned above in section 4.3.4.3. The reaction was terminated after 10 minutes. The reaction products extracted with 4 mL toluene were analysed by HPLC. Figure 42 shows the Vitamin D and metabolite extraction with toluene and petroleum ether.

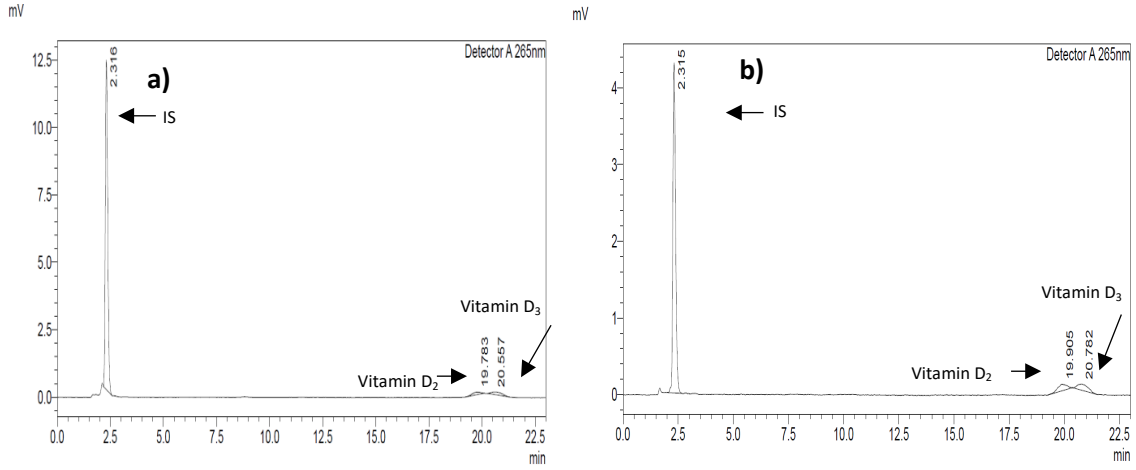

Figure 42. HPLC chromatogram of extraction of reaction products with (a) toluene, (b) petroleum ether.

4.3.4.6 Extraction of Metabolites with Dichloromethane (DCM)

To extract the products with dichloromethane, the assay incubation was based on Tuckey *et al.* with minor modifications [194]. Rat liver microsomes were incubated with Vitamin D_3 and Vitamin D_2 for 30 minutes. The reaction products were extracted with dichloromethane. Figure 43 shows the Vitamin D and metabolite extraction with DCM.

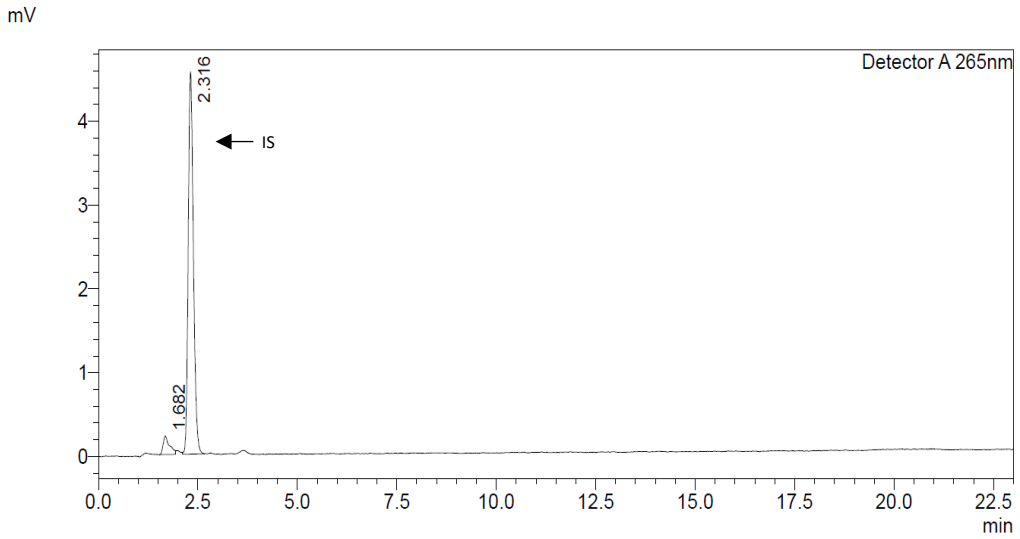

Figure 43. HPLC chromatogram of extraction of reaction products with dichloromethane.

4.3.4.7 Extraction of Metabolites with Naphthalene

Vitamin D_3 and Vitamin D_2 were incubated with rat liver microsomes as mentioned in section 3.4.3. Samples were extracted with 10% naphthalene solution in diethyl ether as well as 0.01 % naphthalene solution in petroleum ether. Figure 44 illustrates the extraction of Vitamin D products with naphthalene.

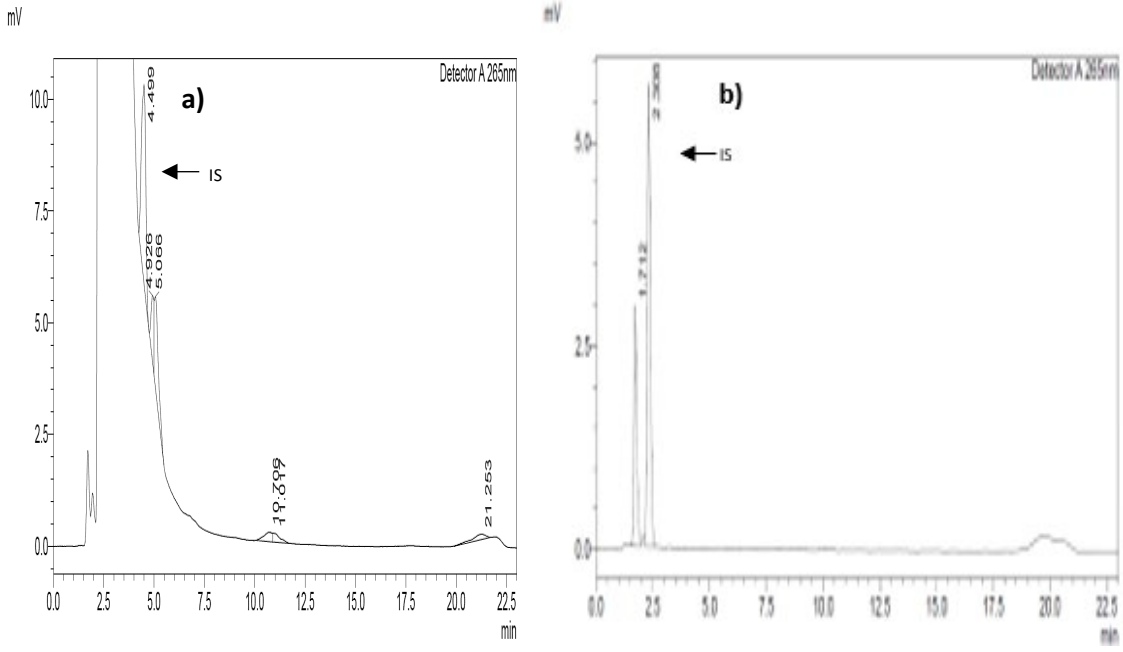

Figure 44. HPLC chromatogram of extraction of reaction products (a) with 10% solution of naphthalene in diethyl ether, (b) with 0.01 % solution of naphthalene in petroleum ether.

4.3.4.8 CYP2R1 Enzyme Assay for Vitamin D 25-hydroxylation using Human Liver Microsomes

The Vitamin D_3 and Vitamin D_2 were incubated with human liver microsomes, and the reaction products were extracted with a chloroform/methanol mixture (3:1, v/v) and simultaneously with benzene. Figure 45 shows the products of the metabolic reaction with human liver microsomes.

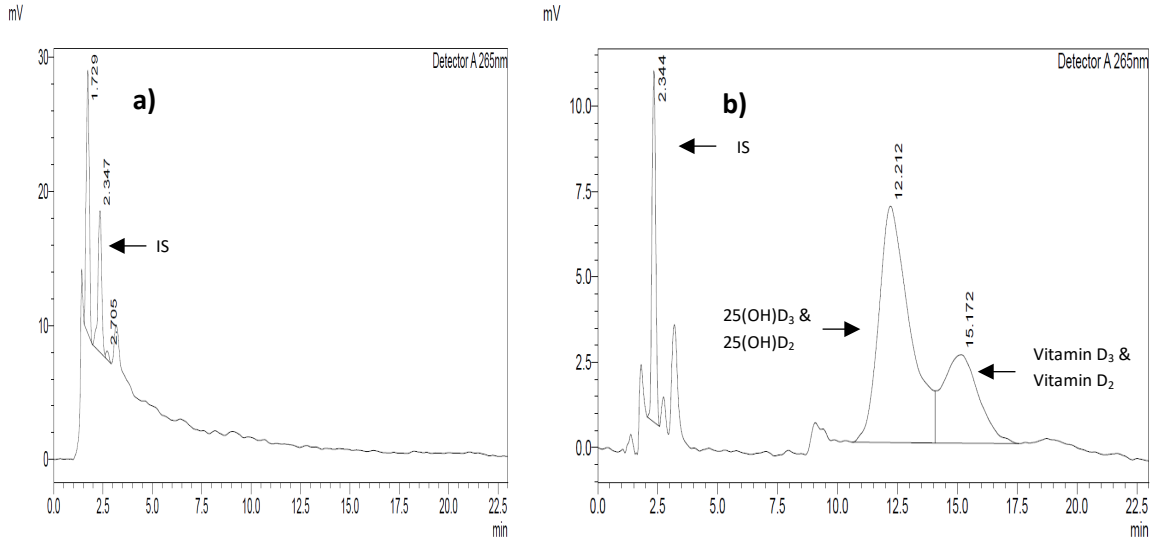

Figure 45. HPLC chromatogram of extraction reaction products with (a) chloroform/methanol mixture (3:1, v/v), (b) benzene.

4.3.4.9 Vitamin D Metabolism by Pure CYP3A4Express Enzyme

The Vitamin D_2 (Substrate) was incubated with 100 mM of potassium phosphate buffer (pH 7.4), 5 mM glucose-6-phosphate, 2.0 mM NADP, and 100 mg of Cyp3A4Express powder. The reaction was quenched after two hours. The reaction products were obtained after centrifuging and extraction with benzene, as shown in Figure 46.

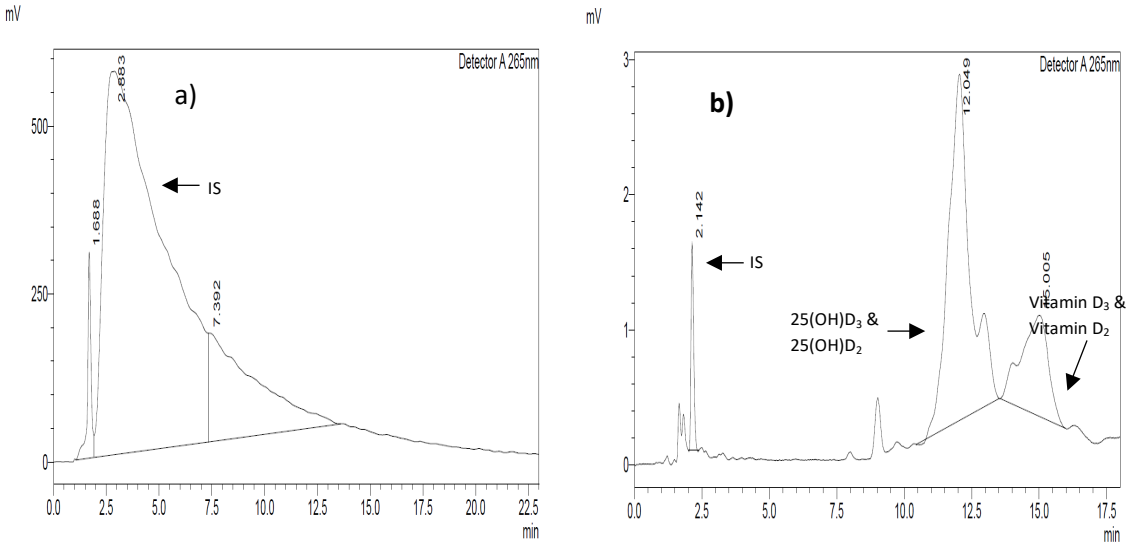

Figure 46. Chromatogram showing reaction products (a) after centrifuging, (b) extraction with benzene.

A very popular tool for the vitamin's extraction is liquid–liquid extraction and a large range of mixed or pure solvents are in use for this purpose with distinct solubility and selectivity ranges [195]. Furthermore, the apparatus needed to perform this separation stage is simple as well as, in many cases/situations, the phases are compatible with the mobile phases used in the subsequent chromatographic stage. Commonly, vitamin D extraction requires a large number of organic solvents, for example acetonitrile, diethyl ether, $CHCl_3$–light petroleum mixture, methanol–toluene mixture [195]. However, the traditional method for the extraction of vitamin D is with benzene. The metabolic reaction products of Vitamin D were extracted with benzene [185]. Benzene is classified as carcinogenic to humans, and it causes acute myeloid leukemia (AML). To avoid this, the reaction products were extracted with toluene (a mono-substituted benzene derivative but little carcinogenic potential), petroleum ether (Hayashi, S-C, 1986), and dichloromethane [186]. However, it appeared chromatographically that metabolic reaction products were only soluble in benzene (Figure 40). The produced metabolites (Vitamin D) were expected to appear at 3.8 and 4.2 minutes on the HPLC chromatogram (Figure 36), but due to the formation of other metabolic products (by-products, isobars, epimers, etc), the peaks moved to 10-15 min on the HPLC chromatogram (Figure 40). *In vitro*, Vitamin D studies have also been performed with human liver microsomes and CYP3A4 Express enzyme (metabolise Vitamin D_2). The only possibility to extract reaction products was with benzene (Figure 46 (b)) as discussed earlier.

4.3.4.10 Separation of Reaction Products Peaks using Benzoyl Chloride as Derivatising Agent

Vitamin D_3 and Vitamin D_2 were incubated in separate vials with rat liver microsomes and the extracted samples (with benzene) were dissolved in the mobile phase and derivatised with Benzoyl Chloride (2% (v/v) in acetonitrile). Figure 47 indicates the outcomes of the derivitisation reaction.

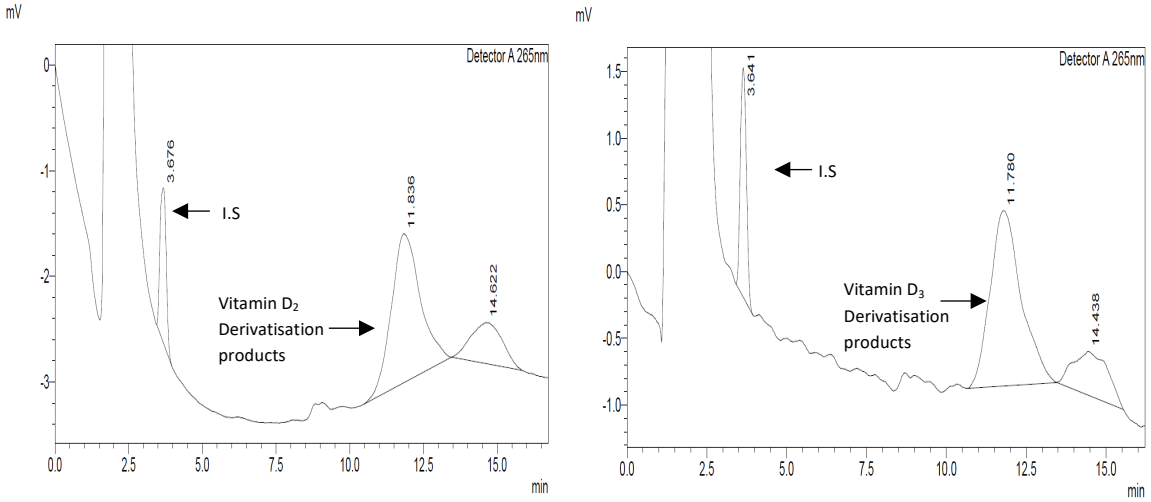

Figure 47. HPLC chromatogram of derivatised compounds with benzoyl chloride.

For separation of metabolic reaction peaks using HPLC, Benzoyl Chloride (BzCl) was chosen for the derivatisation of reaction products (R-OH group present on the metabolite), since it is less susceptible to photo-degradation and derivatisation reaction works on a wider pH range. As shown in Figure 47, the reaction of derivitisation of Vitamin D metabolites was not successful. This might be because of the reason that the reaction products were extracted, dried, and dissolved in the organic mobile phase (90% acetonitrile: 10 % water), although other studies added benzoyl chloride to aqueous samples without using an organic solvent [196].

4.3.4.11 Separation of Reaction Products Peaks using 4-phenyl-1,2,4-triazoline-3,5-dione (PTAD) as Derivatising Agent

Vitamin D_3 and Vitamin D_2 were incubated in separate vials with rat liver microsomes and the extracted samples (with benzene) were dissolved in the mobile phase and derivatised

with PTAD. The derivatisation reaction was quenched with methanol. The outcomes of PTAD derivatised products are shown in Figure 48.

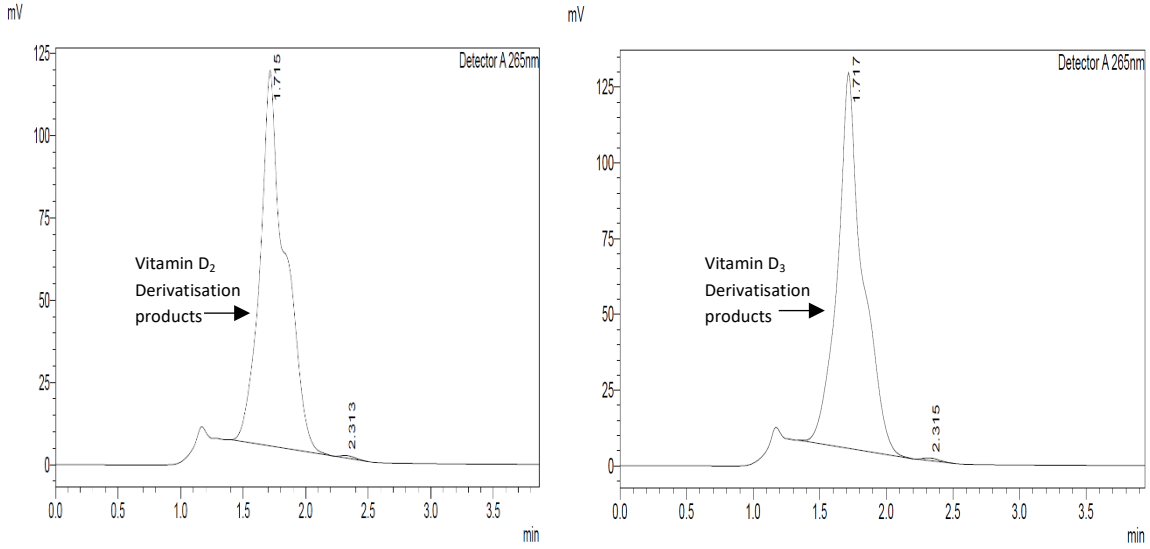

Figure 48. HPLC chromatogram of derivatised compounds with PTAD.

To improve the sensitivity of the HPLC-UV method for Vitamin D and metabolites, a Diels–Alder derivatisation with PTAD was performed. Vitamin D and metabolites appeared as one peak (Figure 48) on the HPLC chromatogram. This might be because of the formation of interfering epimers and isobars (1α-hydroxyvitamin-D_3 (1αOHD_3) and 7α-hydroxy-4-cholestene-3-one (7αC4)) as a result of *in vitro* incubation reaction with rat liver microsomes. Isomers and isobars can overlap with Vitamin D metabolites in chromatographical determinations [197] and they all have very similar molecular masses.

4.3.5 Characterisation of Peaks by qNMR

4.3.5.1 Initial Reference Acquisition and Pure Shift Acquisition for Resolution Improvement

For easier assignment of peaks in the reaction mixture to Vitamin D_2, the expected product Vitamin D_2 (25-OH), 1D 1H acquisitions were conducted.

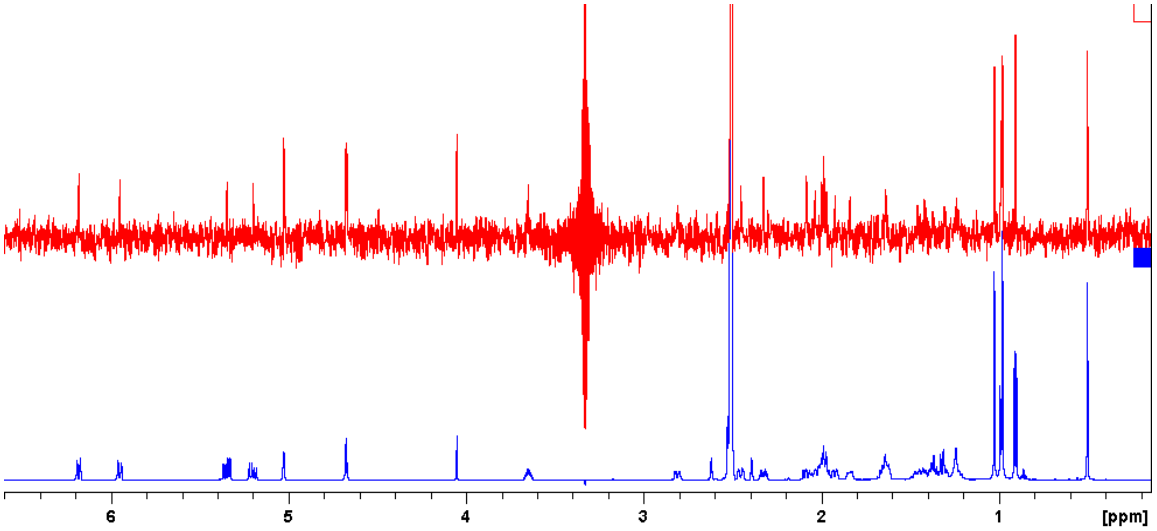

Figure 49. Top: Pure shift 1D1H of Vitamin D_2(25-OH), Bottom: Standard acquired 1D1H Vitamin D_2(25-OH) with coupling included.

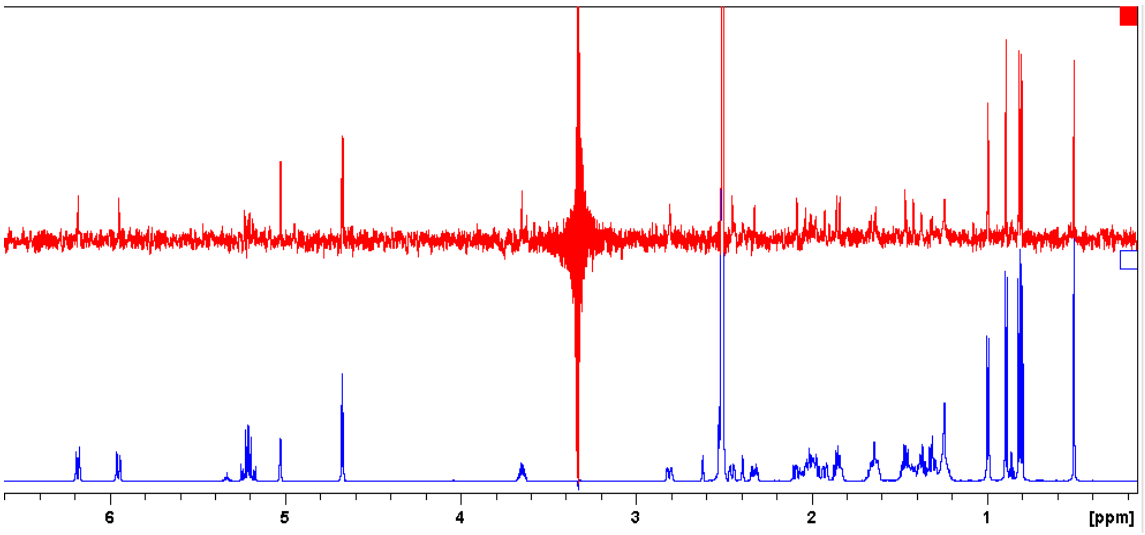

Figure 50. Top: Pure shift 1D1H of Vitamin D_2, Bottom: Standard acquired 1D1H of Vitamin D_2 with coupling included.

4.3.5.2 Comparison of Vitamin D_2 and Expected Derivative Spectra's

Acquisitions of both starting material and expected product were conducted to compare peaks of both to see which peaks can be targeted for quantitation for each analyte. This would allow us to simultaneously quantify both products from one acquisition if quantitative conditions are met.

From observation of the pure shift peaks of each component, it is easy to distinguish between the Vitamin D_2 and metabolite (D_2(25-OH) by observing unique peaks for Vitamin D_2 in the aliphatic region at 0.8 ppm as identified by a star (Figure 51). In the D_2(25-OH),

two new peaks at 4.1 ppm and 5.3 ppm were observed that distinguish it from the Vitamin D_2 (Figure 52). These are most likely caused by hydrogens on the carbon adjacent to the added OH groups.

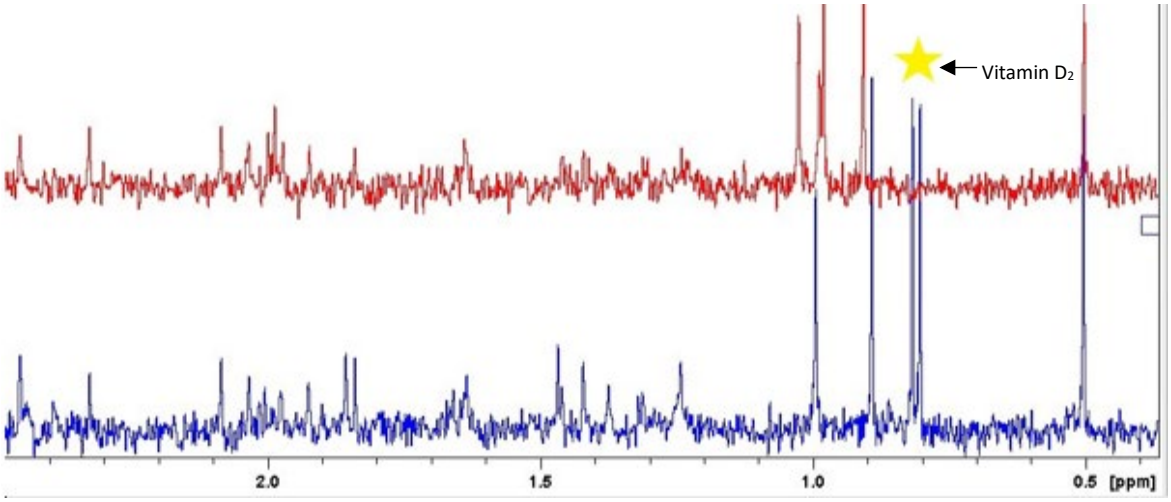

Figure 51. Pure Shift spectra of aliphatic regions for D_2(25-OH) (Top) and Vitamin D_2 (Bottom).

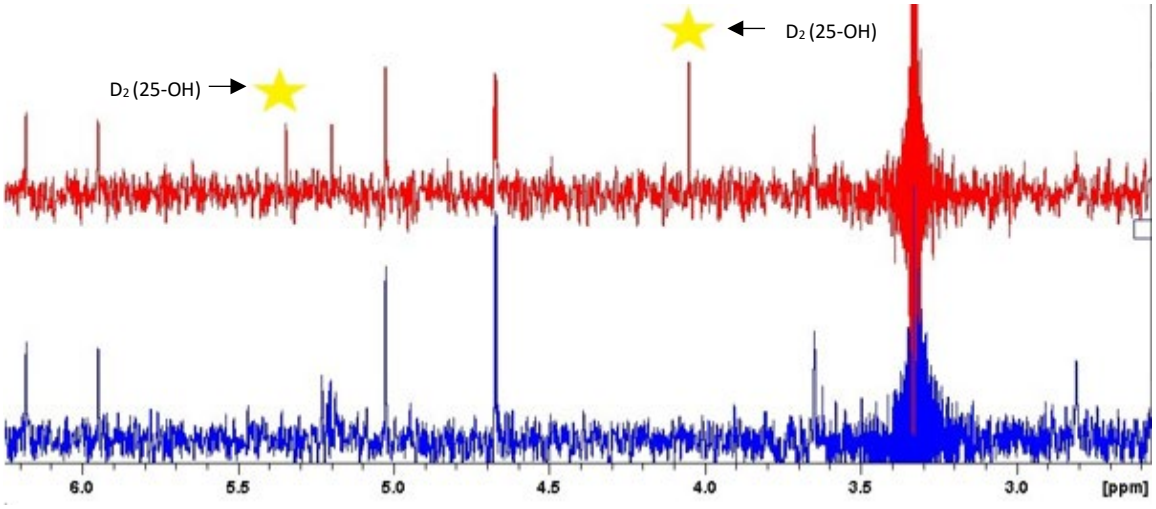

Figure 52. Pure Shift spectra of allylic regions for D_2(25-OH) (Top) and Vitamin D_2 (Bottom).

4.3.5.3 Assignment of Possible Peaks of Vitamin D_2 and Derivatives (metabolite) in the Reaction Mixture as Targets for Quantitation

The spectra acquired for the individual components (Vitamin D_2, D_2(25-OH), and NADPH) were used as noted in Figure 53. Several highlighted peaks could be selected for quantitation in the reaction mixture spectra which have been spiked with the internal reference TSP.

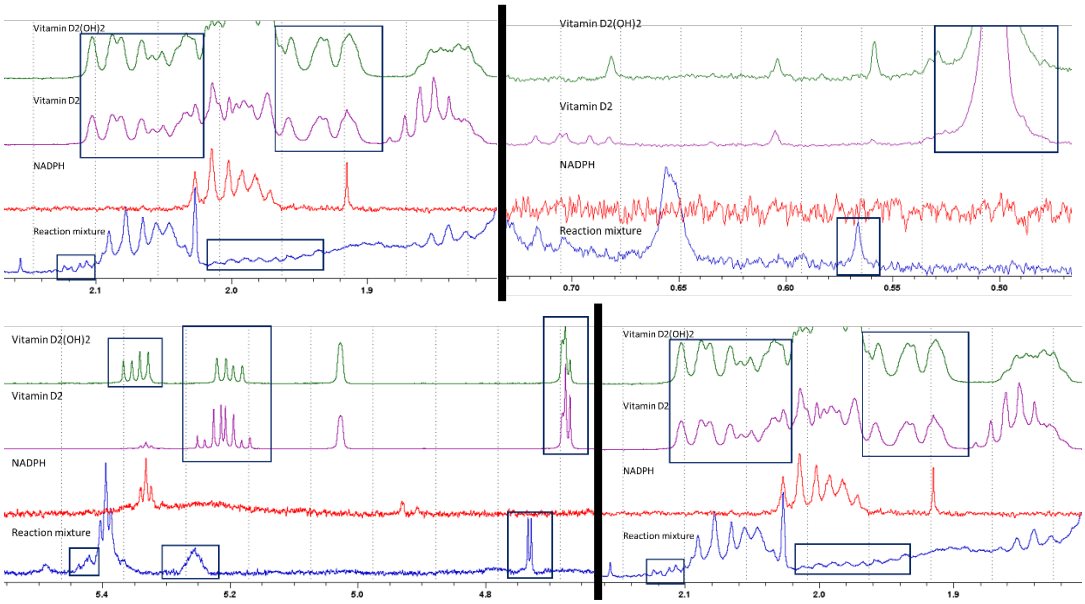

Figure 53. Annotated multiple display spectra highlighting peaks of interest for Vitamin D_2 and D_2 metabolite quantitation.

Looking at the peaks that are proposed to belong to either Vitamin D_2 or D_2(25-OH), the peak at 0.5 ppm or 4.67 ppm for quantitation were selected for S/N and resolution consideration. Further, by knowing the number of protons that produce each peak, a direct integral ratio quantitation can be done. Then either NMR db or a database of the peaks for Vitamin D could give some information to fully characterise and assign structure. This would allow the comparative analysis of different derivatives.

There are 3 protons at 0.5 ppm peak and at 4.67 ppm there are 2 protons rather than in the reference spectra where there would be one. This is because the peaks produced at 4.6 and 5.1 in the reference signal are for two protons on an allylic carbon which splits them into slightly different environments. The explanation for this could be the breaking of the alkene bond and addition of an OH, or the environments of the two H's locking close together by other compounds in the mixture. However, looking at the J HH coupling value of 3 Hz, this suggests the alkene bond is still present from the geminal coupling or an aldehyde group has been added. However, this would leave one proton not two which is seen from the concentration calculations, meaning aldehyde generation is unlikely to happen.

Table 34. Showing concentration calculations (*Averaged from values at 4.74 ppm and 0.65 ppm).

Concentration calculator for NMR		
Peak Integral value	23.27	
No. of protons in peak	3	
MW of the target compound	396.6	
TSP integral	10000	
The concentration of Compound in µM	0.698*	(Integral of peak/TSP Integral) *(9/No. of Protons))*0.1

It is obvious from Table 34 that quantitation of the two peaks at 0.5 ppm and 4.75 ppm give quite different results, however, quantitation of the peak at 0.65 ppm gives the same concentration determined. This shows that the peak at 0.65 ppm and 4.74 ppm is most likely on the same molecule.

qNMR results reveal that quantitation of the compound is possible, but because of the low concentration compared to other compounds in the mixture (Figure 53), it is very hard to characterize which compound this is. It can be assumed as Vitamin D_2 or a metabolite as peaks that are common to the reference and the reaction mixture are visible, however further purification and longer higher resolution experiments with selectivity are required.

4.3.6 Identification of Peaks by LCMS

Vitamin D_2 was incubated with CY3A4Express enzyme, as mentioned in section 3.4.9. Samples were extracted with benzene and derivatised with PTAD and analysed using LCMS at 0.5 µL flow rate and suitable mobile phase (90% acetonitrile: 10% water (0.1% formic acid), v/v), (70% acetonitrile: 30% water (0.1% formic acid), v/v), (50% acetonitrile: 50% water (0.1% formic acid), v/v). The HPLC developed method was modified to suit LCMS. The LCMS chromatograms of extracted and derivatised reaction products are shown in Figures 54, 55, 56, and 57 below.

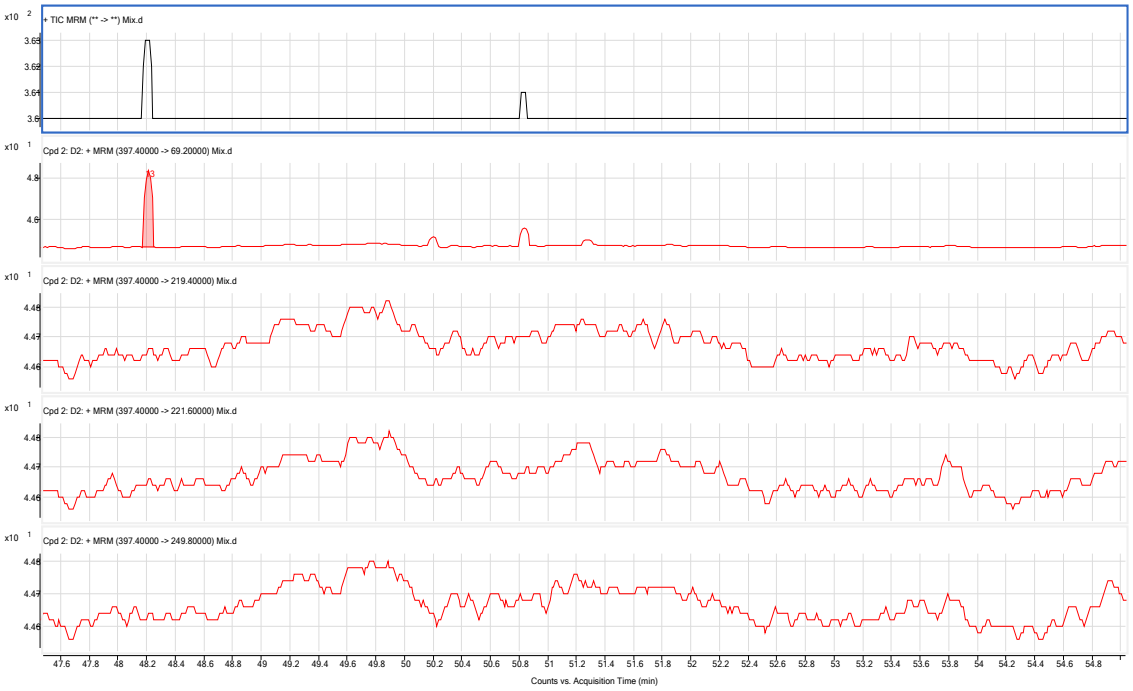

Figure 54. LCMS chromatogram display of Vitamin D_2 extracted after CYP3A4Express reaction.

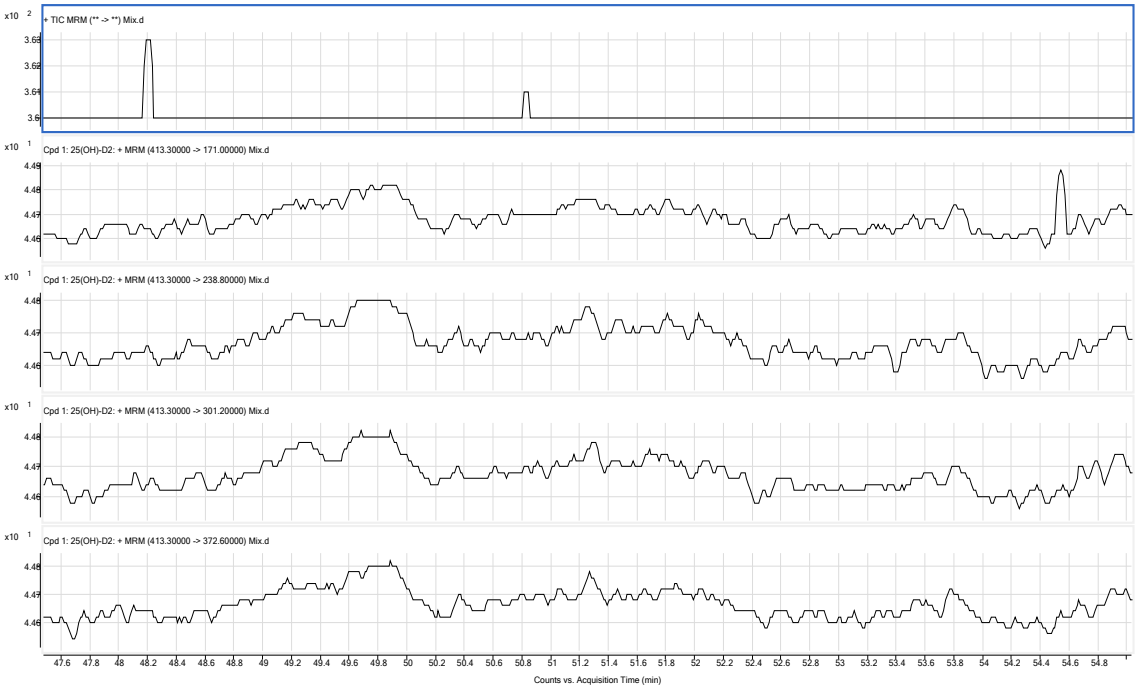

Figure 55. LCMS chromatogram display of 25(OH)D_2 extracted after CYP3A4Express reaction.

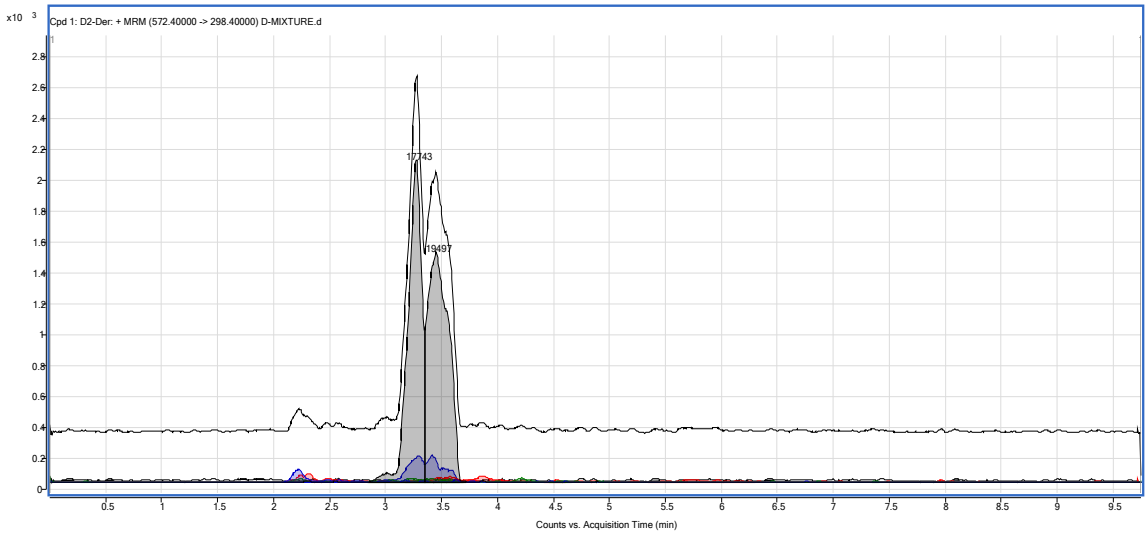

Figure 56. LCMS chromatogram display of Vitamin D_2 and 25(OH)D_2 extracted and derivatized with PTAD after CYP3A4Express reaction.

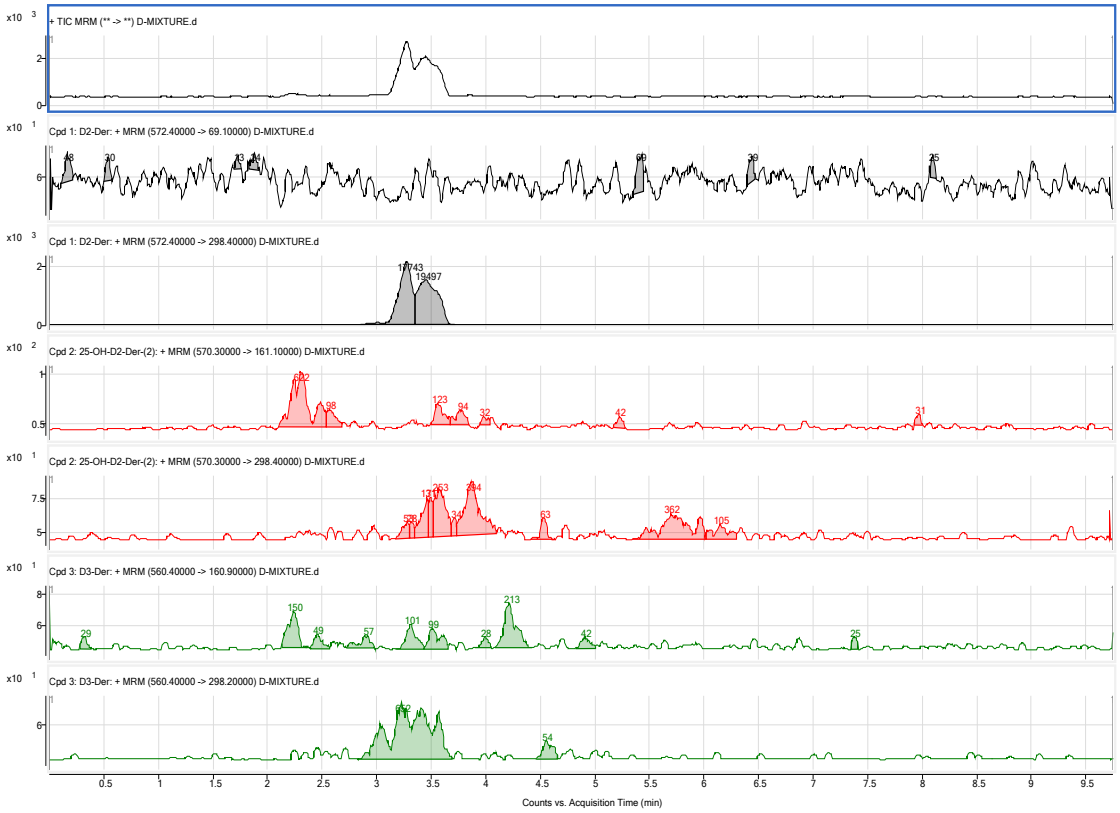

Figure 57. LCMS chromatogram displaying fragments.

LCMS results show that Vitamin D and metabolite were not detected due to the low sensitivity of the LCMS instrument for these compounds (Figures 54, 55, 56, and 57). Zelzer *et al.* stated that Vitamin D metabolites' detection with low concentrations range ESI (electron spray ionisation) does not attain a satisfactory LOD [198]. The LOD for 25(OH)D_3 and 25(OH)D_2 are 2–5 times higher with ESI than with APCI (atmospheric-pressure chemical ionization). Furthermore, the presence of interfering compounds

(supernatant after protein precipitation still has multiple interfering compounds), also reduces the sensitivity of the method. The sensitivity of the instrument depends on the derivatised sample volume. The PTAD method of derivatisation requires a larger sample volume to obtain reliable sensitivity [199].

4.4 Conclusion

In conclusion, a novel HPLC method was developed, and analytical parameters including linearity, precision, accuracy, LOD, LOQ, %recovery, and linear regression were validated for Vitamin D and metabolites. All the analytical parameters for CYP2C11 substrate (Vitamin D) and its metabolites (25(OH)D) were validated as per the ICH guidelines The solution stability experimental data proved that sample solutions of Vitamin D, and metabolites were stable in intraday and interday analysis. *In vitro*, incubation assays using rat liver microsomes and human liver microsomes were adopted to assess the inhibition of the CYP2C11 enzyme activity by testosterone. Our findings show that due to the extremely low concentration of Vitamin D and metabolites (*in vitro* incubation mixture), interferences (formation of other products (by-products, epimers, isobars)), and sensitivity issues, the measurement of Vitamin D in samples was difficult using NMR, HPLC, and LCMS, respectively. The outcomes of the study further suggest that a more sensitive analytical instrument (LCMS with APCI) and sample pre-analytical treatment is required.

CHAPTER 5

CONCLUSION

5 Conclusion

With the discovery of new drugs testing drug-drug interactions in clinical trials before they are released in the market has become a necessity. This thesis has addressed the *in vitro* inhibitory effects of aspirin, ibuprofen, remdesivir, and omeprazole on CYP3A2 isoenzyme activity and the effect of testosterone on CYP2C11 isoenzyme activity. The main findings of this research indicate the type of inhibition of the drugs (often used within COVID-19 treatments) on selected isoenzyme activities and to create awareness among the health sector about the adverse effects of selected inhibitors on the other drugs which are the substrate for CYP3A2 and CYP2C11. Thus, it is important to look at the screening pathway of the *in vitro* inhibitory effect of aspirin, ibuprofen, remdesivir, and omeprazole on CYP450 activities to avoid any further drug-drug interactions.

There are various methods to analyse drug-drug interactions such as measurement of changes in protein levels via Western Blot analyses, alteration in gene expression levels, fluorescence, UV etc. Western Blot analyses are useful to determine obvious changes in protein levels, but, in general, they are less quantitative, and it doesn't detect changes in CYP2E1 isoenzyme levels in which protein stabilisation plays a main role in the inductive response [200]. Ng and Yuen have described methods for the rapid measurement of steroids/testosterone using radioimmunoassay (RIA) but the RIA methods specificity could be compromised because of cross-reactivity with other steroids. Another limitation is that the obtained concentration values may differ significantly dependent on the antibodies utilised [184]. Ultraviolet detection is simple, reliable, and robust but shows poor sensitivity when a chromophore is not present. HPLC coupled with UV provides highly accurate analytes separation along with high resolution.

As reported in the literature*, in vitro* drug-drug interaction studies can be performed using radiolabeled substrates and non-radiolabeled substrates. Standard bioanalytical methods such as HPLC, LCMS, etc. are in use to quantify the substrate or metabolite in *in vitro* experiments with non-radiolabeled compounds. Standard assay procedures include a defined range of standard curves, a blank standard to check assay interferences by endogenous components present in the assay matrix, as well as quality control standards to confirm or validate the assay's accuracy and precision [201]. Special assurance is required that the substrate or inhibitor does not affect the analysis of the substrate metabolite. Long-term storage stability is not as essential for designed analytical methods

to measure *in vitro* samples (it is not common to store *in vitro* study samples for long periods). Analyte stability through the length of analysis time and *in vitro* sample storage conditions needs to be determined [201]. In *in vitro* studies, a quantitative HPLC radiometric method can be used, if a radiolabeled investigational compound is available instead of authentic standards. In this method, recovery of the radiolabeled compound from the incubation is assessed using HPLC. Quantitation is achieved by the percentages that each metabolite peak contains the total radioactivity in the chromatogram. While to quantify non-radiolabeled compounds by HPLC standard curves for metabolite quantitation are used [201].

Thus, due to its sufficient precision and remarkable selectivity, HPLC is the most utilised LC method for drugs analyses as compared to previously reported techniques; RP-HPLC is the most common method in pharmaceutical drug development for instance analysis of drug substances present in biological samples [200].

To expand the extent of current knowledge on the drugs utilised for COVID-19 treatment, the inhibitory effects of different drugs on dexamethasone metabolism were studied in the laboratory. To study these in vitro drug-drug interactions, analysis techniques, HPLC was developed and validated in compliance with ICH guidelines. Quantitative analysis of dexamethasone metabolite was conducted to determine the effects of other drugs on dexamethasone metabolism.

Mainly, this research focused on the two different HPLC methods development and validation for CYP3A2 and CYP2C11 assays and then *in vitro* inhibitions studies on these selected enzyme activities. Thus, for this purpose, HPLC methods were developed using optimal conditions, and all the analytical parameters including linearity and range, precision and accuracy, LOD and LOQ, recovery, and stability were validated in accordance with ICH guidelines for each substrate and metabolite. Before the inhibition study, substrate concentration and reaction time was optimised. The inhibition study was performed and produced metabolites (6β-hydroxydexamethasone and 25(OH)D_3 and 25(OH)D_2) were quantified from obtained HPLC chromatograms of each assay. Quantification of metabolite was performed by running the calibration curve of each metabolite solution on the day of the incubation experiment. Linear equations were obtained with HPLC-based methods with LOD and LOQ values. Thus, the present research showed that the developed quantitative HPLC method which is used for the quantification of metabolites was simple, precise, and accurate and can be applied in *in vivo* settings.

The *in vitro* studies significantly showed the type of inhibition such as aspirin act as a competitive inhibitor, ibuprofen as non-competitive, remdesivir as mixed, and omeprazole showing uncompetitive inhibition of CYP3A2 enzyme activity using rat liver microsomes. Inhibition studies were not performed due to the extremely low concentration and interferences present in the Vitamin D sample. Thus, this research suggests the safe use of dexamethasone and other COVID-19 drugs (aspirin, ibuprofen, remdesivir, and omeprazole) in healthcare screening. These findings have certain limitations like low sensitivity issues were present at the time of Vitamin D samples analysis which could be resolved using a more sensitive (LCMS with APCI) and sample pre-analytical treatment instrument in the future.

5.1 Future work

The conclusions accumulated from this research provide a foundation for future studies. Few recommendations are listed below:

-Studying the inhibition effect of aspirin, ibuprofen, remdesivir, and omeprazole on dexamethasone metabolism using human liver microsomes. Since this research concluded that tested drugs could have negligible effects on the drugs which are the substrate for CYP3A2, but still the relationship between obtained data and human CYP450s is unknown. Thus, this would be useful for the safe co-administration of tested drugs and with the other drugs.

-Studying the induction effect of aspirin, ibuprofen, remdesivir, and omeprazole on dexamethasone metabolism using rat/human liver microsomes. CYP3A4 is known to be a highly inducible enzyme isoform. Thus, this research would provide useful knowledge to determine the effect of tested drugs (aspirin, ibuprofen, remdesivir, omeprazole, and dexamethasone) co-administration in humans to evaluate the efficacy of treatment.

-Moreover, it would be interesting to develop and validate the HPLC assay and see the inhibitory effects of tested drugs on dexamethasone metabolism using CYP3A2 isoenzyme versus CYP3A1, CYP2C11, CYP2B1, CYP2B2, and CYP2D6 isoforms. In this way, comparison would provide us with a broad spectrum to know the type of inhibition.

6 References

[1] R. Kumar, and S. Kapur, “Cytochrome P450 Biocatalysts: A Route to Bioremediation,” *International Journal of Pharmaceutical Research & Allied Sciences*, vol. 5, no. 3, pp. 113–123, 2016, [Online]. Available: www.ijpras.com.

[2] A. Ramamoorthy, C. Barnaba, K. Gentry, and N. Sumangala, “The catalytic function of cytochrome P450 is entwined with its membrane-bound nature,” *F1000Research*, vol. 6. pp. 662, May 2017, doi: 10.12688/f1000research.11015.1.

[3] D. W. Nebert, K. Wikvall, and W. L. Miller, “Human cytochromes P450 in health and disease,” *Philosophical Transactions of the Royal Society B: Biological Sciences*, vol. 368, no. 1612. Royal Society, Feb. 2013, doi: 10.1098/rstb.2012.0431.

[4] O. Pelkonen, M. Turpeinen, J. Hakkola, P. Honkakoski, J. Hukkanen, and H. Raunio, “Inhibition and induction of human cytochrome P450 enzymes: Current status,” *Archives of Toxicology*, vol. 82, no. 10. pp. 667–715, Oct. 2008, doi: 10.1007/s00204-008-0332-8.

[5] E. Stavropoulou, G. G. Pircalabioru, and E. Bezirtzoglou, “The role of cytochromes P450 in infection,” *Frontiers in Immunology*, vol. 9, no. JAN. Frontiers Media S.A., Jan. 2018. doi: 10.3389/fimmu.2018.00089.

[6] D. C. Lamb and M. R. Waterman, “Unusual properties of the cytochrome P450 superfamily,” *Philosophical Transactions of the Royal Society B: Biological Sciences*, vol. 368, no. 1612. Royal Society, Feb. 2013, doi: 10.1098/rstb.2012.0434.

[7] P. R. O. de Montellano, “Cytochrome P450-activated prodrugs,” *Future Medicinal Chemistry*, vol. 5, no. 2. pp. 213–228, Feb. 2013. doi: 10.4155/fmc.12.197.

[8] M. Negishi, T. Uno, T. A. Darden, T. Sueyoshi, and L. G. Pedersen, “Structural flexibility and functional versatility of mammalian P450 enzymes,” *The FASEB Journal*, vol. 10, no. 7, pp. 683–689, May 1996, doi: 10.1096/fasebj.10.7.8635685.

[9] C. Xu, C. Yong-Tao Li, and A.-N. Tony Kong, “Induction of Phase I, II and III Drug Metabolism/Transport by Xenobiotics,” 2005, doi: 10.1007/BF02977789.

[10] H. Wang, and E. L. Lecluyse, “Role of Orphan Nuclear Receptors in the Regulation of Drug-Metabolising Enzymes,” *Clinical Pharmacokinetics*, vol. 42, no. 15, pp. 1331-1357, 2003, doi: 10.2165/00003088-200342150-00003.

[11] I. A. Pikuleva, and M. R. Waterman, “Cytochromes P450, drugs, and diseases,” *Journal of Biological Chemistry*, vol. 288, no. 24, pp. 17091-17098, Jun. 2013, doi.org/10.1074/jbc.R112.431916.

[12] D. F. V. Lewis, “P450 structures and oxidative metabolism of xenobiotics,” *Pharmacogenomics,* vol. 4, no. 4. pp. 387-395, Jul. 2003, doi: 10.1517/phgs.4.4.387.22752.

[13] F. Innocenti, C. Grimsley, S. Das, J. Ramirez, C. Cheng, H. Kuttab-Boulos, M. J. Ratain, and A. D. Rienzo, “Haplotype structure of the UDP-glucuronosyltransferase 1A1 promoter in different ethnic groups,” *Pharmacogenetics*, vol. 12, no. 9, pp. 725-733, Dec. 2002, doi: 10.1097/00008571-200212000-00006.

[14] E. Banoglu, “Current Status of the Cytosolic Sulfotransferases in the Metabolic Activation of Promutagens and Procarcinogens,” *Current Drug Metabolism*, vol. 1, no. 1, pp. 1-30, Jul. 2000, doi: 10.2174/1389200003339234.

[15] A. N. Kong, E. Owuor, V. Hebbar, C. Chen, R. Hu, and S. Mandlekar, “Induction of xenobiotic enzymes by the map kinase pathway and the antioxidant or electrophile response element (ARE/EpRE),” *Drug Metabolism Reviews*, vol. 33, no. 3-4, pp. 255-271, Aug-Nov. 2001, doi: 10.1081/dmr-120000652.

[16] T. H. Rushmore, and A-N. T. Kong, “Pharmacogenomics, Regulation and Signaling Pathways of Phase I and II Drug Metabolizing Enzymes,” *Current Drug Metabolism*, vol. 3, no. 5, pp. 481-490, Oct. 2002, doi: 10.2174/1389200023337171.

[17] J. L. Boloton, and M. Chang, “Quinoids as Reactive Intermediates in Estrogen Carcinogenesis,” *Biological Reactive Intermediates VI* , pp 497–507, doi.org/10.1007/978-1-4615-0667-6_75.

[18] N. Shakunthala, “New cytochrome P450 mechanisms: Implications for understanding molecular basis for drug toxicity at the level of the cytochrome,”

Expert Opinion on Drug Metabolism and Toxicology, vol. 6, no. 1. pp. 1–15, Jan. 2010. doi: 10.1517/17425250903329095.

[19] B. P. Sweeney and J. Bromilow, "Liver enzyme induction and inhibition: Implications for anaesthesia," *Anaesthesia*, vol. 61, no. 2. pp. 159–177, Feb. 2006. doi: 10.1111/j.1365-2044.2005.04462.

[20] P. A. H. M. Wijnen, R. A. Op den Buijsch, and M. Drent, P. M. Kuijpers, C. Neef, A. Bast, O. Bekers, G. H. Koek, "Review article: The prevalence and clinical relevance of cytochrome P450 polymorphisms," in *Alimentary Pharmacology and Therapeutics*, vol. 26, no. SUPPL. 2, pp. 211–219, Dec. 2007, doi: 10.1111/j.1365-2036.2007.03490.

[21] L. M. Tompkins and A. D. Wallace, "Mechanisms of Cytochrome P450 Induction," Wiley Periodicals, Inc, 2007. [Online]. Available: www.interscience.wiley.com.

[22] B. T. Burlingham, and T. S. Wildanski,"An Intuitive Look at the Relationship of Ki and IC50 dixon plot: A More General Use for the Dixon Plot". *Journal of Chemical Education,* vol. 80, no. 2, pp. 214, Feb. 2003, https://doi.org/10.1021/ed080p214.

[23] J. M. G. Rodriguez, N. P. Hux, S. J. Philips, and M. H. Towns, "Michaelis-Menten Graphs, Lineweaver-Burk Plots, and Reaction Schemes: Investigating Introductory Biochemistry Students' Conceptions of Representations in Enzyme Kinetics," *Journal of Chemical Education*, vol. 96, no. 9, pp. 1833–1845, Aug. 2019, doi: 10.1021/acs.jchemed.9b00396.

[24] H. Imai, T. Kotegawa, and K. Ohashi, "Duration of drug interactions: Putative time courses after mechanism-based inhibition or induction of CYPs," *Expert Review of Clinical Pharmacology*, vol. 4, no. 4. pp. 409–411, Jul. 2011. doi: 10.1586/ecp.11.30.

[25] J. Strelow, W. Dewe, P. W. Iversen, H. B. Brooks, J. A. Radding, J. McGee, and J. Weidner, "Mechanism of Action Assays for Enzymes," 2012, Assay Guidance Manual [Internet]. Bethesda (MD): Eli Lilly & Company and the National Center for Advancing Translational Sciences; 2004.

[26] M. Srinivas, G. Thirumaleswara, and S. Pratima, "Cytochrome P450 Enzymes, Drug Transporters and their Role in Pharmacokinetic Drug-Drug Interactions of Xenobiotics: A Comprehensive Review," Peertechz Journal of Medicinal Chemistry Research, vol. 3, no. 1, pp. 001–011, Jul. 2017, doi: 10.17352/ojc.000006.

[27] X. Li, Ying Li, W. Gong, M. Y. Yang, Y. Yang, Z. P. Li, Y. L. Wang, and Z. Q. Zhang, "Auto-induction effect of chloroxoquinoline on the cytochrome P450 enzymes of rats associated with CYP 3A and 1A," *PLoS ONE*, vol. 10, no. 9, Sep. 2015, doi: 10.1371/journal.pone.0138875.

[28] E. Higashi, M. Nakajima, M. Katoh, S. Tokudome, and T. Yokoi, "Inhibitory effects of neurotransmitters and steroids on human CYP2A6", *Drug Metabolism and Disposition*, vol. 35, no. 4, pp. 508-514, Apr. 2007, doi: 10.1124/dmd.106.014084.

[29] J. Hakkola, J. Hukkanen, M. Turpeinen, and O. Pelkonen, "Inhibition and induction of CYP enzymes in humans: an update," *Archives of Toxicology*, vol. 94, no. 11. Springer Science and Business Media Deutschland GmbH, pp. 3671–3722, Nov. 01, 2020. doi: 10.1007/s00204-020-02936-7.

[30] R. S. Foti, and D. K. Dalvie, "Cytochrome P450 and non-cytochrome P450 oxidative metabolism: Contributions to the pharmacokinetics, safety, and efficacy of xenobiotics," *Drug Metabolism and Disposition*, vol. 44, no. 8. American Society for Pharmacology and Experimental Therapy, pp. 1229–1245, Aug. 01, 2016. doi: 10.1124/dmd.116.071753.

[31] I. J. Onakpoya, C. J. Heneghan, and J. K. Aronson, "Post-marketing withdrawal of 462 medicinal products because of adverse drug reactions: A systematic review of the world literature," *BMC Medicine*, vol. 14, no. 1, Feb. 2016, doi: 10.1186/s12916-016-0553-2.

[32] J. Huang, C. Niu, C. D. Green, L. Yang, H. Mei, and J. D. J. Han, "Systematic Prediction of Pharmacodynamic Drug-Drug Interactions through Protein-Protein-Interaction Network," *PLoS Computational Biology*, vol. 9, no. 3, 2013, doi: 10.1371/journal.pcbi.1002998.

[33] B. Percha, and R. B. Altman, "Informatics confronts drug-drug interactions," *Trends in Pharmacological Sciences*, vol. 34, no. 3. pp. 178–184, Mar. 2013. doi: 10.1016/j.tips.2013.01.006.

[34] Y. Lu, B. Figler, H. Huang, Y. C. Tu, J. Wang, and F. Cheng, “Characterization of the mechanism of drug-drug interactions from PubMed using MeSH terms,” *PLoS ONE*, vol. 12, no. 4, Apr. 2017, doi: 10.1371/journal.pone.0173548.

[35] C. Hoffelt, and T. Gross, “A review of significant pharmacokinetic drug interactions with antidepressants and their management,” *Mental Health Clinician*, vol. 6, no. 1, pp. 35–41, Jan. 2016, doi: 10.9740/mhc.2016.01.035.

[36] R. Schellander, and J. Donnerer, “Antidepressants: clinically relevant drug interactions to be considered” *Pharmacology*, vol. 86, no. 4, pp. 203-215, Sep. 2010, doi: 10.1159/000319744.

[37] E. Spina, G. Trifiro, and F. Caraci, “Clinically Significant Drug Interactions with Newer Antidepressants,” *CNS Drugs*, vol. 26, no. 1, pp. 39-67, Jan. 2012, doi: 10.2165/11594710-000000000-00000.

[38] R. Boinpally, N. Gad, S. Gupta, and A. Periclou, “Influence of CYP3A4 induction/inhibition on the pharmacokinetics of vilazodone in healthy subjects,” *Clinical Therapeutics*, vol. 36, no. 11, pp. 1638–1649, Nov. 2014, doi: 10.1016/j.clinthera.2014.08.003.

[39] R. Mago, G. Forero, W. M. Greenberg, C. Gommoll, and C. Chen, “Safety and tolerability of levomilnacipran ER in major depressive disorder: Results from an open-label, 48-week extension study,” *Clinical Drug Investigation*, vol. 33, no. 10, pp. 761–771, 2013, doi: 10.1007/s40261-013-0126-5.

[40] S. J. Lee, M. K. Park, D. S. Shin, and M. H. Chun, “Variability of the drug response to nonsteroidal anti-inflammatory drugs according to cyclooxygenase-2 genetic polymorphism,” *Drug Design, Development and Therapy*, vol. 11, pp. 2727–2736, Sep. 2017, doi: 10.2147/DDDT.S143807.

[41] S. Narum, V. Solhaug, K. Myhr, P. W. Johansen, O. Brors, and M. K. Kringen, “Warfarin-associated bleeding events and concomitant use of potentially interacting medicines reported to the Norwegian spontaneous reporting system,” *British Journal of Clinical Pharmacology*, vol. 71, no. 2, pp. 254–262, Feb. 2011, doi: 10.1111/j.1365-2125.2010.03827.

[42] P. K. Ghaswalla, S. E. Harpe, D. Tassone, and P. W. Slattum, “Warfarin–Antibiotic Interactions in Older Adults of an Outpatient Anticoagulation Clinic,” *The American journal of geriatric pharmacotherapy,* vol. 10, no. 6, pp. 352-360, Dec. 2012, doi: 10.1016/j.amjopharm.2012.09.006.

[43] G. Teklay, N. Shiferaw, B. Legesse, and M. L. Bekele, “Drug-drug interactions and risk of bleeding among inpatients on warfarin therapy: A prospective observational study,” *Thrombosis Journal*, vol. 12, no. 1, Sep. 2014, doi: 10.1186/1477-9560-12-20.

[44] S. K. Goswami, S. Jain, H. Chudasama, and D. Santani, “Potential pharmacodynamic drug-drug interaction between concomitantly administered lisinopril and diclofenac sodium: a call for appropriate management in hypertensive osteoarthritic patients” *Drug Metabolism and Drug Interaction*, vol. 26, no. 3, pp. 127-37, 2011, doi: 10.1515/DMDI.2011.020.

[45] J. J. Brugts, and J. W. Deckers, “Statin prescription in men and women at cardiovascular risk: to whom and when” *Current Opinion in Cardiology*, vol. 25, no. 5, pp. 484-489, Sep. 2010, doi: 10.1097/HCO.0b013e32833cd58f.

[46] J. Armitage, “The safety of statins in clinical practice,” *THE LANCET,* vol. 370, pp. 1781-1790, Nov. 2007, doi: 10.1016/S0140-6736(07)60716-8.

[47] E. Bruckert, G. Hayem, S. Dejager, C. Yau, and B. Begaud, “Mild to moderate muscular symptoms with high-dosage statin therapy in hyperlipidemic patients - The PRIMO study,” *Cardiovascular Drugs and Therapy*, vol. 19, no. 6, pp. 403–414, 2005, doi: 10.1007/s10557-005-5686-z.

[48] M. Law, and A. R. Rudnicka, “Statin Safety: A Systematic Review,” *American Journal of Cardiology*, vol. 97, no. 8 SUPPL. 1, Apr. 2006, doi: 10.1016/j.amjcard.2005.12.010.

[49] T. R. Joy, and R. A. Hegele, “Narrative Review: Statin-Related Myopathy” *Annals of Internal Medicine*, vol. 150, no. 12, pp. 858-868, Jun. 2009, doi: 10.7326/0003-4819-150-12-200906160-00009.

[50] D. A. Taha, C. H. de Moor, D. A. Barrett, and P. Gershkovich, “Translational insight into statin-induced muscle toxicity: From cell culture to clinical studies,”

Translational Research, vol. 164, no. 2. Mosby Inc., pp. 85–109, 2014. doi: 10.1016/j.trsl.2014.01.013.

[51] Y. S. Chatzizisis, K. C. Koskinas, G. Misirli, C. Vaklavas, A. Hatzitolios, and G. D. Giannoglou, "Risk Factors and Drug Interactions Predisposing to Statin-Induced Myopathy Implications for Risk Assessment, Prevention and Treatment," *Drug Safety*, vol. 33, no. 3, pp. 171-187, Mar. 2010, doi: 10.2165/11319380-000000000-00000.

[52] A. Bakhai, U. Rigney, S. Hollis, and C. Emmas, "Co-administration of statins with cytochrome P450 3A4 inhibitors in a UK primary care population," *Pharmacoepidemiology and Drug Safety*, vol. 21, no. 5, pp. 485–493, May 2012, doi: 10.1002/pds.2308.

[53] C. Bucsa, A. Farcas, D. Leucuta, C. Mogosan, M. Bojita, and D. L. Dumitrascu, "Drug-drug Interactions of Statins Potentially Leading to Muscle-Related Side Effects in Hospitalized Patients," *Romanian Journal of Internal Medicine*, vol. 53, no. 4, pp. 329-335, Oct-Dec. 2015, doi: 10.1515/rjim-2015-0042.

[54] R. Yuan, S. Madani, X. X. Wei, K. Reynolds, and S. M. Huang, "Evaluation of cytochrome P450 probe substrates commonly used by the pharmaceutical industry to study *in vitro* drug interactions," *Drug Metabolism and Disposition*, vol. 30, no. 12, pp.1311-1319, Dec. 2002, doi: 10.1124/dmd.30.12.1311.

[55] A. Galetin, S. E. Clarke, and J. B. Houston, "Multisite kinetic analysis of interactions between prototypical CYP3A4 subgroup substrates: midazolam, testosterone, and nifedipine," *Drug Metabolism and Disposition*, vol. 31, no. 9, pp. 1108-1116, Sep. 2003, doi: 10.1124/dmd.31.9.1108.

[56] B. A. English, M. Dortch, L. Ereshefsky, and S. Jhee, "Clinically significant psychotropic drug-drug interactions in the primary care setting," *Current Psychiatry Reports*, vol. 14, no. 4, pp. 376–390, Aug. 2012, doi: 10.1007/s11920-012-0284-9.

[57] V. Ozdemir, C. A. Naranjo, N. Herrmaun, K. Reed, E. M. Sellers, and W. Kalow, "Paroxetine potentiates the central nervous system side effects of perphenazine: Contribution of cytochrome P4502D6 inhibition *in vivo*," *Clinical Trial and Therapeutics,* vol. 62, no. 3, pp. 334-347, Sep. 1997.

[58] A. A. El Ela, S. Hartter, U. Schmitt, C. Hiemke, H. Spahn-Langguth, and P. Langguth, "Identification of P-glycoprotein substrates and inhibitors among psychoactive compounds--implications for pharmacokinetics of selected substrates," *The Journal of Pharmacy and Pharmacology*, vol. 56, no. 8, pp. 967-975, Aug. 2004, doi: 10.1211/0022357043969.

[59] S. Kudo, and T. Ishizaki, "Pharmacokinetics of Haloperidol an Update," *Clinical Pharmacokinetics,* vol. 37, no. 6, pp. 435-456, Dec. 1999, doi: 10.2165/00003088-199937060-00001.

[60] S. Zevin, and N. L. Benowitz, "Drug Interactions with Tobacco Smoking an Update," *Clinical Pharmacokinetics*, vol. 36, no. 6, pp. 425-438, Jun. 1999, doi: 10.2165/00003088-199936060-00004.

[61] P. Decina, G. Caracci, R. Sandik, W. Berman, S. Mukherjee, and P. Scapicchio, "Cigarette Smoking and Neuroleptic-Induced Parkinsonism," *Biological Psychiatry*, vol 28, no. 6, pp. 502-508, Sep. 1990, doi.org/10.1016/0006-3223(90)90483-I.

[62] E. Spina, and J. de Leon, "Metabolic Drug Interactions with Newer Antipsychotics: A Comparative Review," *Basic & Clinical Pharmacology & Toxicology*, vol. 100, pp. 4 – 22, 2006, doi.org/10.1111/j.1742-7843.2007.00017.x.

[63] O. V. Olesen, and K. Linnet, "Contributions of Five Human Cytochrome P450 Isoforms to the N-demethylation of Clozapine *In Vitro* at Low and High Concentrations," *Journal of Clinical Pharmacology,* vol. 41, no. 8, pp. 823-832, Aug. 2001, doi: 10.1177/00912700122010717.

[64] M. Gex-Fabry, A. E. Balant-Gorgia, and L. P. Balant, "Therapeutic drug monitoring databases for postmarketing surveillance of drug-drug interactions: evaluation of a paired approach for psychotropic medication," *Therapeutic Drug Monitoring*, vol. 19, no. 1, pp. 1-10, Feb. 1997, doi: 10.1097/00007691-199702000-00001.

[65] E. Skogh, F. Bengtsson, and C. Nordin, "Could discontinuing smoking be hazardous for patients administered clozapine medication? A case report," *Therapeutic Drug Monitoring*, vol. 21, no. 5, pp. 580-582, Oct. 1999, doi: 10.1097/00007691-199910000-00016.

[66] E, Spina, A. Avenoso, G. Facciola, M. G. Scordo, M. Ancione, and A. Madia, “Plasma concentrations of risperidone and 9-hydroxyrisperidone during combined treatment with paroxetine,” *Therapeutic Drug Monitoring*, vol. 23, no. 3, pp. 223-227, Jun. 2001, doi: 10.1097/00007691-200106000-00007

[67] P. K. Gillman, “Tricyclic antidepressant pharmacology and therapeutic drug interactions updated,” *British Journal of Pharmacology*, vol. 151, no. 6. pp. 737–748, Jul. 2007. doi: 10.1038/sj.bjp.0707253.

[68] S. H. Preskorn, and B. Baker, “Fatality associated with combined fluoxetine-amitriptyline therapy,” *JAMA*, vol. 277, no. 21, pp. 1682, Jun. 1997, doi:10.1001/jama.1997.03540450038031.

[69] E. Spina, V. Santoro, and C. D. Arrigo, “Clinically Relevant Pharmacokinetic Drug Interactions with Second-Generation Antidepressants: An Update,” *Clinical Therapeutics*, vol. 30, no. 7, pp. 1206-1227, Jul. 2008, doi: 10.1016/s0149-2918(08)80047-1.

[70] E. Tanaka, “Clinically significant pharmacokinetic drug interactions with benzodiazepines,” *Journal of Clinical Pharmacy and Therapeutics*, vol. 24, pp. 347–355, 1999, doi.org/10.1046/j.1365-2710.1999. 00247.x.

[71] G. Chouinard, K. Lefko-Singh, and E. Teboul, “Metabolism of anxiolytics and hypnotics: benzodiazepines, buspirone, zoplicone, and zolpidem,” *Cell and Molecular Neurobiology*, vol. 19, no. 4, pp. 533-552, Aug. 1999, doi: 10.1023/a:1006943009192.

[72] T. A. Lasher, J. C. Fleishaker, R. C. Steenwyk, and E. J. Antal, “Pharmacokinetic pharmacodynamic evaluation of the combined administration of alprazolam and fluoxetine,” *Psychopharmacology (Berl),* vol. 104, no. 3, pp. 323-327,1991, doi: 10.1007/BF02246031.

[73] Y. Oda, K. Mizutani, I. Hase, T. Nakamoto, N. Hamaoka, and A. Asada, “Fentanyl inhibits metabolism of midazolam: competitive inhibition of CYP3A4 *in vitro*,” *British Journal of Anaesthesia*, vol. 82, no. 6, pp. 900-903, Jun. 1999, doi: 10.1093/bja/82.6.900.

[74] M. E. Morris, and S. Zhang, “Flavonoid-drug interactions: Effects of flavonoids on ABC transporters,” *Life Sciences*, vol. 78, no. 18, pp. 2116–2130, Mar. 2006, doi: 10.1016/j.lfs.2005.12.003.

[75] B. H. Havsteen, “The biochemistry and medical significance of the flavonoids,” *Pharmacology and Therapeutics*, vol. 96, no. 2-3, pp. 67-202, Nov-Dec. 2002, doi: 10.1016/s0163-7258(02)00298-x.

[76] E. Ernst, “Complementary and alternative medicine: What the NHS should be funding?,” *British Journal of General Practice*, vol. 58, no. 548, pp. 208–209, Mar. 2008, doi: 10.3399/bjgp08X279562.

[77] D. A. Kennedy, and D. Seely, “Clinically based evidence of drug–herb interactions: a systematic review,” *Expert Opinion on Drug Safety*, vol. 9, no. 1, pp. 79-124, Jan. 2010, doi: 10.1517/14740330903405593.

[78] A. A. Izzo, “Interactions between herbs and conventional drugs: Overview of the clinical data,” *Medical Principles and Practice*, vol. 21, no. 5. pp. 404–428, Jul. 2012, doi: 10.1159/000334488.

[79] S. P. Borse, D. P. Singh, and M. Nivsarkar, “Understanding the relevance of herb–drug interaction studies with special focus on interplays: a prerequisite for integrative medicine,” *Porto Biomedical Journal*, vol. 4, no. 2, p. e15, Mar. 2019, doi: 10.1016/j.pbj.0000000000000015.

[80] A. R. King, F. S. Russett, J. A. Generali, and D. W. Grauer, “Evaluation and implications of natural product use in preoperative patients: A retrospective review,” *BMC Complementary and Alternative Medicine*, vol. 9, p. 38, Oct. 2009, doi: 10.1186/1472-6882-9-38.

[81] S. Otles, and A. Senturk, “Food and drug interactions: A general review,” *Acta Scientiarum Polonorum, Technologia Alimentaria*, vol. 13, no. 1, pp. 89–102, 2014, doi: 10.17306/J.AFS.2014.1.8.

[82] F. Ibolya, C. M. Dumitru, V. Andrea, J. Iren, and F. Erzsébet, “*In Vitro* Interactions of Diclofenac with Several Types of Food,” *Acta Medica Marisiensis*, vol. 62, no. 3, pp. 334–338, Sep. 2016, doi: 10.1515/amma-2016-0030.

[83] P. Tarighi, S. Eftekhari, M. Chizari, M. Sabernavaei, D. Jafari, and P. Mirzabeigi, “A review of potential suggested drugs for coronavirus disease (COVID-19) treatment,” *European Journal of Pharmacology*, vol. 895. Elsevier B.V., Mar. 2021. doi: 10.1016/j.ejphar.2021.173890.

[84] R. Wu, L. Wang, H. D. Kuo, A. Shannar, R. Peter, P. J. Chou, S. Li, R. Hudlikar, X. Liu, Z. Liu, G. J. Poiani, L. Amorosa, L. Brunetti, and A. N. Kong, “An Update on Current Therapeutic Drugs Treating COVID-19,” *Current Pharmacology Reports*, vol. 6, no. 3. Springer, pp. 56–70, Jun. 2020. doi: 10.1007/s40495-020-00216-7.

[85] A. Carvallo Hector, H. Roberto, F. Maria Eugenia, F. Javier Muniz, and B. Aires, “Safety and Efficacy of the combined use of ivermectin, dexamethasone, enoxaparin and aspirin against COVID-19,” 2022, doi: 10.1101/2020.09.10.20191619.

[86] K. Kragholm, C. Torp-Pedersen, and E. Fosbol, “Non-steroidal anti-inflammatory drug use in COVID-19,” *The Lancet Rheumatology,* vol. 3, no. 7, pp. e465-e466, Jul. 2021, doi:10.1016/S2665-9913(21)00144-2.

[87] I. Cascorbi, “Arzneimittelinteraktionen: Prinzipien, Beispiele und klinische Folgen,” *Deutsches Arzteblatt International*, vol. 109, no. 33–34, pp. 546–556, Aug. 2012, doi: 10.3238/arztebl.2012.0546.

[88] I. Wijaya, R. Andhika, I. Huang, A. Purwiga, and K. Y. Budiman, “The effects of aspirin on the outcome of COVID-19: A systematic review and meta-analysis,” *Clinical Epidemiology and Global Health*, vol. 12, Oct. 2021, doi: 10.1016/j.cegh.2021.100883.

[89] R. Srivastava, and A. Kumar, “Use of aspirin in reduction of mortality of COVID-19 patients: A meta-analysis,” *International Journal of Clinical Practice*, vol. 75, no. 11, Nov. 2021, doi: 10.1111/ijcp.14515.

[90] M. Bojic, C. A. Sedgeman, L. D. Nagy, and F. P. Guengerich, “Aromatic hydroxylation of salicylic acid and aspirin by human cytochromes P450,” *European Journal of Pharmaceutical Sciences*, vol. 73, pp. 49–56, Jun. 2015, doi: 10.1016/j.ejps.2015.03.015.

[91] L. L. Mazaleuskaya, K. N. Theken, L. Gong, C. F. Thorn, G. A. FitzGerald, R. B. Altman, and T. E. Klein, "PharmGKB summary: Ibuprofen pathways," *Pharmacogenetics and Genomics*, vol. 25, no. 2, pp. 96–106, Feb. 2015, doi: 10.1097/FPC.0000000000000113.

[92] M. H. Ahmed, and A. Hassan, "Dexamethasone for the Treatment of Coronavirus Disease (COVID-19): a Review," *SN Comprehensive Clinical Medicine*, vol. 2, no. 12, pp. 2637–2646, Dec. 2020, doi: 10.1007/s42399-020-00610-8.

[93] S. B. Al Rihani, M. Deodhar, P. Dow, J. Turgeon, and V. Michaud, "Is Dexamethasone a Substrate, an Inducer, or a Substrate-Inducer of CYP3As?", *Archives of Pharmacy and Pharmacology Research,* vol. 2, no. 5, Feb. 2020, doi: 10.33552/APPR.2020.02.000546.

[94] B. K. Park, and D. J. Back, "Dexamethasone metabolism by human liver *in vitro*. Metabolite identification and inhibition of 6-hydroxylation," *The Journal of Pharmacology and Experimental Therapeutics,* vol. 277, no. 1, pp. 105-112. Apr.1996, [Online]. Available: https://www.researchgate.net/publication/14586463.

[95] E. S. Tomlinson, D. F. Lewis, J. L. Maggs, H. K. Kroemer, B. K. Park, and D. J. Back, "*In Vitro* Metabolism of Dexamethasone (DEX) in Human Liver and Kidney: The Involvement of CYP3A4 and CYP17 (17,20 LYASE) and Molecular Modelling Studies," *Biochemical Pharmacology*, vol. 54, no. 5, pp. 605-11, Sep. 1997, doi: 10.1016/s0006-2952(97)00166-4.

[96] S. Jain, H. Potschka, P. P. Chandra, M. Tripathi, and D. Vohora, "Management of COVID-19 in patients with seizures: Mechanisms of action of potential COVID-19 drug treatments and consideration for potential drug-drug interactions with anti-seizure medications," *Epilepsy Research*, vol. 174, Aug. 2021, doi: 10.1016/j.eplepsyres.2021.106675.

[97] R. E. Ferner, and J. K. Aronson, "Remdesivir in covid-19," *The BMJ*, vol. 369. BMJ Publishing Group, Apr. 22, 2020. doi: 10.1136/bmj.m1610.

[98] S. Jain, H. Potschka, P. P. Chandra, M. Tripathi, and D. Vohora, "Management of COVID-19 in patients with seizures: Mechanisms of action of potential COVID-19

drug treatments and consideration for potential drug-drug interactions with anti-seizure medications," *Epilepsy Research*, vol. 174, Aug. 2021, doi: 10.1016/j.eplepsyres.2021.106675.

[99] G. A. Diaz, A. B. Christensen, T. Pusch, D. Goulet, S-C, Change, G. L. Grunkemeier, P. A. McKelvey, A. Robicsek *et al.,* "Remdesivir and Mortality in Patients with Coronavirus Disease 2019," *Clinical Infectious Diseases*, Aug. 2021, doi: 10.1093/cid/ciab698.

[100] K. Uzunova, E. Filipova, V. Pavlova, and T. Vekov, "Insights into antiviral mechanisms of remdesivir, lopinavir/ritonavir and chloroquine/hydroxychloroquine affecting the new SARS-CoV-2," *Biomedicine and Pharmacotherapy*, vol. 131. Elsevier Masson SAS, Nov. 01, 2020. doi: 10.1016/j.biopha.2020.110668.

[101] H. Luxenburger, L. Strum, P. Biever, S. Rieg, D. Duerschmied, M. Schultheiss, C. Neumann-Haefelin, R. Thimme, and D. Bettinger, "Treatment with proton pump inhibitors increases the risk of secondary infections and ARDS in hospitalized patients with COVID-19: coincidence or underestimated risk factor?," *Journal of Internal Medicine*, vol. 289, no. 1. Blackwell Publishing Ltd, pp. 121–124, Jan. 01, 2021. doi: 10.1111/joim.13121.

[102] E. J. T. Aguila, and I. H. Y. Cua, "Repurposed GI Drugs in the Treatment of COVID-19," *Digestive Diseases and Sciences*, vol. 65, no. 8. Springer, pp. 2452–2453, Aug. 01, 2020. doi: 10.1007/s10620-020-06430-z.

[103] H. Kanazawa, A. Okada, Y. Matsushima, H. Yokota, S. Okubo, F. Mashige, and K. Nakahara, "Determination of omeprazole and its metabolites in human plasma by liquid chromatography-mass spectrometry," *Journal of Chromatography A*, vol. 949, no. 1-2, pp. 1-9, Mar. 2002, doi: 10.1016/s0021-9673(01)01508-4.

[104] C. S. Stokes, D. A. Volmer, F. Grünhage, and F. Lammert, "Vitamin D in chronic liver disease," *Liver International*, vol. 33, no. 3. pp. 338–352, Mar. 2013. doi: 10.1111/liv.12106.

[105] A. J. Brown, C. S. Ritter, L. S. Holliday, J. C. Knutson, and S. A. Strugnell, "Tissue distribution and activity studies of 1,24-dihydroxyvitamin D 2, a metabolite of

vitamin D_2 with low calcemic activity *in vivo*," *Biochemical Pharmacology*, vol. 68, no. 7, pp. 1289–1296, Oct. 2004, doi: 10.1016/j.bcp.2004.06.015.

[106] H. F. DeLuca, "Overview of general physiologic features and functions of vitamin D," The *American Journal of Clinical Nutrition*, vol. 80, no. 6 Suppl, pp. 1689S-96S, Dec. 2004, doi: 10.1093/ajcn/80.6.1689S.

[107] Z. Wu, Z. Malihi, A. W. Stewart, C. M. M. Lawes, and R. Scragg, "Effect of vitamin D supplementation on pain: A systematic review and meta-analysis," *Pain Physician*, vol. 19, no. 7. American Society of Interventional Pain Physicians, pp. 415–427, Sep. 01, 2016. doi: 10.36076/ppj/2016.19.415.

[108] Y. Ohyama, and T. Yamasaki, "Eight cytochrome P450s catalyze vitamin D metabolism," *Frontiers in Bioscience*, vol. 9, pp. 3007-3018. Sep. 2004, doi: 10.2741/1455.

[109] Y.D. Guo, S. Strugnell, D. W. Back, and G. Jones, "Transfected human liver cytochrome P-450 hydroxylates vitamin D analogs at different side-chain positions," *The Proceedings of the National Academy of Sciences***,** vol. 90, no.18, pp. 8668–8672. Sep. 1993, doi: 10.1073/pnas.90.18.8668.

[110] E. Axen, T. Bergmant, and K. Wikvall, "Purification and characterization of a vitamin D3 25-hydroxylase from pig liver microsomes," *The Biochemical Journal*, vol. 287, no. 3, pp. 725-731, Nov. 1992, doi: 10.1042/bj2870725.

[111] K. Robien, S. J. Oppeneer, J. A. Kelly, and J. M. Hamilton-Reeves, "Drug-vitamin D interactions: A systematic review of the literature," *Nutrition in Clinical Practice*, vol. 28, no. 2. pp. 194–208, Apr. 2013. doi: 10.1177/0884533612467824.

[112] J. Bain, "The many faces of testosterone," *Clinical Interventions in Aging*, vol. 2, no. 4, pp. 567-576, 2007, doi: 10.2147/cia. s1417.

[113] J. Wojcikowski, A. Haduch, and W. A. Daniel, "Effect of antidepressant drugs on cytochrome P450 2C11 (CYP2C11) in rat liver," *Pharmacological Reports*, vol. 65, no. 5, pp. 1247-1255, 2013, doi: 10.1016/s1734-1140(13)71482-8.

[114] J. P. Chovan, S. C. Ring, E. Yu, and J. P. Baldino, "Cytochrome P450 probe substrate metabolism kinetics in Sprague Dawley rats," *Xenobiotica,* vol. 37, no. 5, pp. 459-73, May 2007, doi: 10.1080/00498250701245250.

[115] M. Bilek, and J. Namieśnik, "Chromatographic techniques in pharmaceutical analysis in Poland: History and the presence on the basis of papers published in selected Polish pharmaceutical journals in XX century*." Acta Poloniae Pharmceutica*, vol. 73, no. 3, pp. 605-612, May-Jun. 2016, [Online]. Available: https://www.researchgate.net/publication/306167331.

[116] P. Sharma, "High-performance liquid chromatography: A short review," *Journal of Global Pharma Technology*, vol. 2, no. 5, pp. 22-26, Jun. 2010. [Online]. Available: https://www.researchgate.net/publication/235987484.

[117] O. E. Petrova and K. Sauer, "High-performance liquid chromatography (HPLC)-based detection and quantitation of cellular c-di-GMP." in *Methods in Molecular Biology*, vol. 1657, Humana Press Inc., 2017, pp. 33–43. doi: 10.1007/978-1-4939-7240-1_4.

[118] M. Thammana, "A Review on High Performance Liquid Chromatography (HPLC)," *Journal of Pharmaceutical Analysis*, vol. 5, no. 2, pp. 22-28, Jul-Sep. 2016, [Online]. Available: https://www.rroij.com/open-access/a-review-on-high-performance-liquid-chromatography-hplc-.(rroij.com).

[119] B. Nikolin, B. Imamovic, S. Medanhodzic-Vuk, and M. Sober, "High performance liquid chromatography in pharmaceutical analyses," *Bosnian Journal of Basic Medical Science,* vol. 4, no. 2, pp. 5-9, May 2004, doi: 10.17305/bjbms.2004.3405. PMID: 15629016.

[120] L. Hymoller, and S. K. Jensen, "Vitamin D_2 impairs utilization of vitamin D3 in high-yielding dairy cows in a cross-over supplementation regimen," *Journal of Dairy Science*, vol. 94, no. 7, pp. 3462–3466, Jul. 2011, doi: 10.3168/jds.2010-4111.

[121] G. Sowjanya, S. Ganapaty, and R. Sharma, "In vitro test methods for metabolite identification: A review," *Asian Journal of Pharmacy and Pharmacology*, vol. 5, no. 3, pp. 441–450, 2019, doi: 10.31024/ajpp.2019.5.3.2.

[122] R. Roskar, and T. T. Lusin, "Analytical Methods for Quantification of Drug Metabolites in Biological Samples", In Chromatography - The Most Versatile Method of Chemical Analysis. London, United Kingdom: IntechOpen, 2012 [Online]. Available: https://www.intechopen.com/chapters/40383 doi: 10.5772/51676.

[123] D. Picking, B. Chambers, J. Barker, I. Shah, R. Porter, D. P. Naughton, and R. Delgoda, "Inhibition of cytochrome P450 activities by extracts of hyptis verticillata jacq.: assessment for potential HERB-drug interactions," *Molecules*, vol. 23, no. 2, pp. 430, 2018, doi: 10.3390/molecules23020430.

[124] A. O. T. H. Y. Masubuchi, "Mechanism-based inactivation of CYP2C11 by diclofenac.," *Drug metabolism and disposition*, vol. 29, no. 9, pp. 1190–1195, 2001.

[125] Y. S. Jeong, A. Balla, K. H. Chun, S. J. Chung, and H. J. Maeng, "Physiologically-based pharmacokinetic modeling for drug-drug interactions of procainamide and N-acetylprocainamide with Cimetidine, an inhibitor of rOCT2 and rMATE1, in Rats," *Pharmaceutics*, vol. 11, no. 3, Mar. 2019, doi: 10.3390/pharmaceutics11030108.

[126] Z. Bibi, "Role of cytochrome P450 in drug interactions," *Nutrition and Metabolism*, vol. 5, no. 1, pp. 27, 2008. doi: 10.1186/1743-7075-5-27.

[127] T. Lynch, and A. Price, "The Effect of Cytochrome P450 Metabolism on Drug Response, Interactions, and Adverse Effects," *American Family Physician*, vol. 76, no. 3, pp. 391-396, Aug. 2007, [Online]. Available: www.aafp.org/afp.

[128] J. W. Ko, Z. Desta, N. v Soukhova, T. Tracy, and D. A. Flockhart, "*In vitro* inhibition of the cytochrome P450 (CYP450) system by the antiplatelet drug ticlopidine: potent effect on CYP2C19 and CYP2D6," *British Journal of Clinical Pharmacology*, vol. 49, no. 4, pp. 343-351, Apr. 2000, doi: 10.1046/j.1365-2125.2000.00175. x.

[129] S. O. Nduka, M. J. Okonta, D. L. Ajaghaku, and C. v. Ukwe, "*In vitro* and *in vivo* cytochrome P450 3A enzyme inhibition by Aframomum melegueta and Denniettia tripetala extracts," *Asian Pacific Journal of Tropical Medicine*, vol. 10, no. 6, pp. 576–581, Jun. 2017, doi: 10.1016/j.apjtm.2017.06.006.

[130] A. M. McDonnell, and C. H. Dang, “Basic Review of the Cytochrome P450 System,” *Journal of Advanced Practitioner in Oncology,* vol. 4, no. 4, pp. 263-268, Jul. 2013, doi: 10.6004/jadpro.2013.4.4.7.

[131] A. A. Sprouse, and R. B. van Breemen, “Pharmacokinetic interactions between drugs and botanical dietary supplements,” *Drug Metabolism and Disposition*, vol. 44, no. 2. *American Society for Pharmacology and Experimental Therapy*, pp. 162–171, Feb. 01, 2016. doi: 10.1124/dmd.115.066902.

[132] K. Zurbonsen, F. Bressolle, I. Solassol, P. J. Aragon, S. Culine, and F. Pinguet, “Simultaneous determination of dexamethasone and 6β- hydroxydexamethasone in urine using solid-phase extraction and liquid chromatography: Applications to *in vivo* measurement of cytochrome P450 3A4 activity,” *Journal of Chromatography B: Analytical Technologies in the Biomedical and Life Sciences*, vol. 804, no. 2, pp. 421–429, May 2004, doi: 10.1016/j.jchromb.2004.01.053.

[133] M. H. Ahmed, and A. Hassan, “Dexamethasone for the Treatment of Coronavirus Disease (COVID-19): a Review,” *SN Comprehensive Clinical Medicine*, vol. 2, no. 12, pp. 2637–2646, Dec. 2020, doi: 10.1007/s42399-020-00610-8.

[134] S. B. Al Rihani, M. Deodhar, P. Dow, J. Turgeon, and V. Michaud, “Is Dexamethasone a Substrate, an Inducer, or a Substrate-Inducer of CYP3As?,” *Achieves of Pharmacy and Pharmacology Research,* 2020, doi: 10.33552/APPR.2020.02.000546.

[135] B. K. Park, and D. J. Back, “Dexamethasone metabolism by human liver *in vitro*. Metabolite identification and inhibition of 6-hydroxylation,” *Journal of Pharmacology and Experimental Therapeutics*, vol. 277, no. 1, pp. 105-112, Apr. 1996. [Online]. Available: https://www.researchgate.net/publication/14586463.

[136] E. S. Tomlinson, J. L. Maggs, B. K. Park, and D. J. Back, “Dexamethasone Metabolism in Species Differences,” *The Journal of Steroid Biochemistry and Molecular Biology*, vol. 62, no. 4, pp. 345-352, Jul. 1997, doi.org/10.1016/S0960-0760(97)00038-1.

[137] S. Wang, Y. Dong, K. Su, J. Zhang, L. Wang, A. Han, C. Wen, X. Wang, and Y. He, “Effect of codeine on CYP450 isoform activity of rats,” *Pharmaceutical Biology*, vol. 55, no. 1, pp. 1223–1227, 2017, doi: 10.1080/13880209.2017.1297466.

[138] A. Carvallo Hector, H. Roberto, F. María Eugenia, F. Javier Muniz, and B. Aires, “Safety and efficacy of the combined use of Ivermectin, Dexamethasone, Enoxaparin and Aspirin, against Covid 19”, doi: 10.1101/2020.09.10.20191619.

[139] D. Vukoja, A. Juric, Z. Erkapic, T. Pejic, Z. Zovko, J. Juricic, J. Pejic, and M. Corluka, “Beneficial Treatment Outcomes of Severe COVID-19 Patients Treated Entirely in Primary Care Settings with Dexamethasone Including Regimen—Case Series Report,” *Frontiers in Pharmacology*, vol. 12, Aug. 2021, doi: 10.3389/fphar.2021.684537.

[140] Z. Pan, B. Camara, H. W. Gardner, and R. A. Backhaus, “Aspirin Inhibition and Acetylation of the Plant Cytochrome P450, Allene Oxide Synthase, Resembles that of Animal Prostaglandin Endoperoxide H Synthase,” *Journal of Biological Chemistry*, vol. *273, no.* 29, pp.18139-18145. Jul. 1998. [Online]. Available: http://www.jbc.org/.

[141] A. Ornelas, N. Zacharias-Millward, D. G. Menter, J. S. Davis, L. Lichtenberger, D. Hawke, E. Hawk, E. Vilar, P. Bhattacharya, and S. Millward, “Beyond COX-1: the effects of aspirin on platelet biology and potential mechanisms of chemoprevention,” *Cancer and Metastasis Reviews*, vol. 36, no. 2, pp. 289–303, Jun. 2017, doi: 10.1007/s10555-017-9675-z.

[142] J. R. Vane, and R. M. Botting, “The mechanism of action of aspirin,” in *Thrombosis Research*, vol. 110, no. 5–6, pp. 255–258, Jun. 2003, doi: 10.1016/S0049-3848(03)00379-7.

[143] “International Conference on Harmonisation of Technical Requirements for Registration of Pharmaceuticals for Human Use. *In ICH Harmonised Tripartite Guideline, Validation of Analytical Procedures: Text and Methodology Q2(R1)*; Somatek Inc.: San Diego, CA, USA, 2005.

[144] A. A. Heda, J. M. Kathiriya, D. D. Gadade, and P. K. Puranik, “Development-and-validation-of-rphplc-method-for-simultaneous-determination-of-granisetron-and-dexamethasone,” *Indian Journal of Pharmaceutical Sciences*, vol. 73, no. 6, p.696, 2011.

[145] M. Jafari-Fesharaki, and M. M. Scheinman, “Adverse Effects of Amiodarone,” Pacing and Clinical Electrophysiology, vol. 21, no. 1, pp. 108-120, Jun. 1998.

[146] J. Strelow, W. Dewe, and P. W. Iversen, “Mechanism of Action Assays for Enzymes,” *AGM* 2012. Available online: https://www.ncbi.nlm.nih.gov/books/NBK92001/?report=printable (access ed on 5 January 2022).

[147] L. Liu, Z. Jiang, J. Liu, X. Huang, T. Wang, J. Liu, Y. Zhang, Z. Zhou, J. Guo, and L. Yang, “Sex differences in subacute toxicity and hepatic microsomal metabolism of triptolide in rats,” *Toxicology*, vol. 271, no. 1–2, pp. 57–63, Apr. 2010, doi: 10.1016/j.tox.2010.03.004.

[148] Z. J. Zhang, Z. Y. Xia, J. M. Wang, X. T. Song, J. F. Wei, and W. Y. Kang, “Effects of flavonoids in Lysimachia clethroides duby on the activities of cytochrome P450 CYP2E1 and CYP3A4 in rat liver microsomes,” *Molecules*, vol. 21, no. 6, Jun. 2016, doi: 10.3390/molecules21060738.

[149] Y. Wang, S. Wu, Z. Chen, H. Zhang, and W. Zhao, “Inhibitory effects of cytochrome P450 enzymes CYP1A2, CYP2A6, CYP2E1 and CYP3A4 by extracts and alkaloids of Gelsemium elegans roots,” *Journal of Ethnopharmacology*, vol. 166, pp. 66–73, May 2015, doi: 10.1016/j.jep.2015.03.002.

[150] X. Tao, L. Zheng, L. Qi, Y. Xu, L. Xu, L. Yin, X. Han, K. Liu, and J. Peng, “Inhibitory effects of dioscin on cytochrome P450 enzymes,” *RSC Advances*, vol. 4, no. 96, pp. 54026–54031, 2014, doi: 10.1039/c4ra09160d.

[151] D. W. Nebert, and D. W. Russell, “Clinical importance of the cytochromes P450,” *Lancet*, vol. 360, no. 9340. Elsevier B.V., pp. 1155–1162, Oct. 12, 2002. doi: 10.1016/S0140-6736(02)11203-7.

[152] D. A. Sychev, G. M. Ashraf, A. A. Svistunov, M. L. Maksimov, V. V. Tarasov, V. N. Chubarev, V. A. Otdelenov, N. P. Denisenko, G. E. Barreto, and G. Aliev, “The cytochrome P450 isoenzyme and some new opportunities for the prediction of negative drug interaction *in vivo*,” *Drug Design, Development and Therapy*, vol. 12. Dove Medical Press Ltd., pp. 1147–1156, May 08, 2018. doi: 10.2147/DDDT.S149069.

[153] M. Sun, Y. Tang, T. Ding, M. Liu, and X. Wang, “Inhibitory effects of celastrol on rat liver cytochrome P450 1A2, 2C11, 2D6, 2E1 and 3A2 activity,” *Fitoterapia*, vol. 92, no. 1, pp. 1–8, Jan. 2014, doi: 10.1016/j.fitote.2013.10.004.

[154] A. Shayeganpour, A. O. S. El-Kadi, and D. R. Brocks, “Determination of the enzyme(s) involved in the metabolism of amiodarone in liver and intestine of rat: the contribution of cytochrome P450 3A isoforms,” *Drug Metabolism and Disposition,* **vol.** *34*, no. 1, pp. 43–50, Jan. 2006, doi: 10.1124/dmd.105.006742.

[155] A. Chen, X. Zhou, S. Tang, M. Liu, and X. Wang, “Evaluation of the inhibition potential of plumbagin against cytochrome P450 using LC-MS/MS and cocktail approach,” *Scientific Reports*, vol. 6, Jun. 2016, doi: 10.1038/srep28482.

[156] F. Puisset, E. Chatelut, A. Sparreboom, J. P. Delord, D. Berchery, T. Lochon, T. Lafont, and H. Roche, “Dexamethasone as a probe for CYP3A4 metabolism: Evidence of gender effect,” *Cancer Chemotherapy and Pharmacology*, vol. 60, no. 2, pp. 305–308, Jul. 2007, doi: 10.1007/s00280-006-0385-4.

[157] P. L. I. J P Desjardins, “Inhibition of the rat cytochrome P450 3A2 by an antisense phosphorothioate oligodeoxynucleotide *in vivo*,” *Journal of Pharmacology and Experimental Therapeutics*, vol. 275, no. 3, pp. 1608–13, Dec. 1995.

[158] L. Li, Z. Li, C. Deng, M. Ning, H. Li, S. Bi, T. Zhou, and W. Lu, “A mechanism-based pharmacokinetic/pharmacodynamic model for CYP3A1/2 induction by dexamethasone in rats,” *Acta Pharmacologica Sinica*, vol. 33, no. 1, pp. 127–136, Jan. 2012, doi: 10.1038/aps.2011.161.

[159] S. Lehrer, and P. Rheinstein, “Common drugs, vitamins, nutritional supplements and COVID-19 mortality,” *International Journal of Functional Nutrition*, vol. 2, no. 1, Mar. 2021, doi: 10.3892/ijfn.2021.14.

[160] E. J. T. Aguila, and I. H. Y. Cua, “Repurposed GI Drugs in the Treatment of COVID-19,” *Digestive Diseases and Sciences*, vol. 65, no. 8. Springer, pp. 2452–2453, Aug. 01, 2020. doi: 10.1007/s10620-020-06430-z.

[161] Y. Jo, L. Jamieson, I. Edoka, L. Long, S. Silal, J. R. C. Pulliam, H. Moultire, I. Sanne, G. Meyer-Rath, and B. E. Nichols, “Cost-effectiveness of Remdesivir and

Dexamethasone for COVID-19 Treatment in South Africa," *Open Forum Infectious Diseases*, vol. 8, no. 3, Mar. 2021, doi: 10.1093/ofid/ofab040.

[162] T. M. Drake, C. J. Fairfield, R. Pius, S. R. Knight, L. Norman, M. Girvan, H. E. Hardwick, A. B. Docherty, R. S. Thwaites, and P. J. M. Openshaw, "Non-steroidal anti-inflammatory drug use and outcomes of COVID-19 in the ISARIC Clinical Characterisation Protocol UK cohort: a matched, prospective cohort study," *The Lancet Rheumatology*, vol. 3, no. 7, pp. e498–e506, Jul. 2021, doi: 10.1016/S2665-9913(21)00104-1.

[163] A. Hussain, D. P. Naughton, and J. Barker, "Development and Validation of a Novel HPLC Method to Analyse Metabolic Reaction Products Catalysed by the CYP3A2 Isoform: *In Vitro* Inhibition of CYP3A2 Enzyme Activity by Aspirin (Drugs Often Used Together in COVID-19 Treatment)," *Molecules*, vol. 27, no. 3, Feb. 2022, doi: 10.3390/molecules27030927.

[164] A. Burenheide, T. Kunze, and B. Clement, "Inhibitory effects on cytochrome P450 enzymes of pentamidine and its amidoxime pro-drug," *Basic and Clinical Pharmacology and Toxicology*, vol. 103, no. 1, pp. 61–65, Jul. 2008, doi: 10.1111/j.1742-7843.2008.00236. x.

[165] B. Russell, C. Moss, G. George, A. Santaolalla, A. Cope, S. Papa, and M. V. Hemelrijck, "Associations between immune-suppressive and stimulating drugs and novel COVID-19 - A systematic review of current evidence," *ecancermedicalscience*, vol. 14. ecancer Global Foundation, Mar. 27, 2020. doi: 10.3332/ecancer.2020.1022.

[166] E. Rinott, E. Kozer, Y. Shapira, A. Bar-Haim, and I. Youngster, "Ibuprofen use and clinical outcomes in COVID-19 patients," *Clinical Microbiology and Infection*, vol. 26, no. 9, pp. 1259.e5-1259.e7, Sep. 2020, doi: 10.1016/j.cmi.2020.06.003.

[167] L. L. Mazaleuskaya, K. N. Theken, L. Gong, C. F. Thorn, G. A. FitzGerald, R. B. Altman, and T. E. Klein, "PharmGKB summary: Ibuprofen pathways," *Pharmacogenetics and Genomics*, vol. 25, no. 2, pp. 96–106, Feb. 2015, doi: 10.1097/FPC.0000000000000113.

[168] G. Liu, S. Chen, A. Hu, L. Zhang, W. Sun, J. Chen, W. Tang, H. Zhang, C. Liu, and C. Ke, "The Establishment and Validation of the Human U937 Cell Line as a Cellular Model

to Screen Immunomodulatory Agents Regulating Cytokine Release Induced by Influenza Virus Infection," *Virologica Sinica*, vol. 34, no. 6, pp. 648–661, Dec. 2019, doi: 10.1007/s12250-019-00145-w.

[169] J. Karlsson, and C. J. Fowler, "Inhibition of endocannabinoid metabolism by the metabolites of ibuprofen and flurbiprofen," *PLoS ONE*, vol. 9, no. 7, Jul. 2014, doi: 10.1371/journal.pone.0103589.

[170] V. S. P. P. P. P. M. V. P Karttunen, "Pharmacokinetics of ibuprofen in man: a single-dose comparison of two over-the-counter, 200 mg preparations," *International Journal of Clinical Pharmacology, Therapy, and Toxicology*, vol. 28, no. 6, pp. 251–5, Jun. 1990.

[171] S. K. K. O. Y. K. H. Y. E Tanaka, "The effects of short-term administration of ibuprofen on trimethadione metabolism and antipyrine metabolite formation in the rat," *Research Communications in Chemical Pathology and Pharmacology*, vol. 48, no. 2, pp. 317–20, May 1985.

[172] S. Deb, A. A. Reeves, R. Hopefl, and R. Bejusca, "ADME and pharmacokinetic properties of remdesivir: Its drug interaction potential," *Pharmaceuticals*, vol. 14, no. 7. MDPI, Jul. 01, 2021. doi: 10.3390/ph14070655.

[173] K. Yang, "What Do We Know About Remdesivir Drug Interactions?," *Clinical and Translational Science*, vol. 13, no. 5. Blackwell Publishing Ltd, pp. 842–844, Sep. 01, 2020. doi: 10.1111/cts.12815.

[174] D. J. Keeling, C. Fallowfield, K. J. Milliner, S. K. Tingley, R. J. Ife, and A. H. Underwood, "Studies on the mechanism of action of omeprazole," *Biochemical Pharmacology*, vol. 34, no. 15, pp. 2967-73, Aug.1985.

[175] D. Groenendaal-van de Meent, M. D. Adel, J. V. Dijk, B. Barroso-Fernandez, R. E. Galta, G. Golor, and M. Schaddelee, "Effect of Multiple Doses of Omeprazole on the Pharmacokinetics, Safety, and Tolerability of Roxadustat in Healthy Subjects," *European Journal of Drug Metabolism and Pharmacokinetics*, vol. 43, no. 6, pp. 685–692, Dec. 2018, doi: 10.1007/s13318-018-0480-z.

[176] X.Q. Li, T. B. Andersson, M. Ahlstrom, and L. Weidolf, “Comparison of inhibitory effects of the proton pump-inhibiting drugs omeprazole, esomeprazole, lansoprazole, pantoprazole, and rabeprazole on human cytochrome P450 activities,” *Drug Metabolism and Deposition*, vol. 32, no. 8, pp. 821-827, Aug. 2004.

[177] M. R. Haussler, C. Haussler, P. Jurutka, and P. Thompson, “The vitamin D hormone and its nuclear receptor: Molecular actions and disease states,” *The Journal of Endocrinology*, vol. 154, pp. S57-53, 1997, DOI:10.1677/JOE.0.154S057.

[178] E. al Qadi, and A. H. Battah, “Development of high-performance liquid chromatographic method for vitamin D3 analysis in pharmaceutical preparation,” *Jordan Journal of Pharmaceutical Sciences,* vol. 3, no. 2, pp. 78-86, 2010.

[179] D. D. Bikle, “Vitamin D metabolism, mechanism of action, and clinical applications,” *Chemistry and Biology*, vol. 21, no. 3. Cell Press, pp. 319–329, Mar. 20, 2014. doi: 10.1016/j.chembiol.2013.12.016.

[180] Jacekkwojcikowski, “Effect of antidepressant drugs on cytochrome P450 2C11 (CYP2C11) in rat liver,” *Pharmacological Reports*, vol. 65, no. 5, pp. 1247-1255, Oct. 2013.

[181] Z. Wang, Y. S. Lin, X. E. Zheng, T. Senn, T. Hashizume, M. Scian, L. J. Dickmann, S. D. Nelson, T. A. Baillie, M. F. Hebert, D. Blough, C. L. Davis, and K. E. Thummel,“An inducible cytochrome P450 3A4-dependent vitamin D catabolic pathway,” *Molecular Pharmacology*, vol. 81, no. 4, pp. 498–509, Apr. 2012, doi: 10.1124/mol.111.076356.

[182] D. Lycans, E. Salloum, M. K. Wingate, and T. Melvin, “Vitamin D Deficiency: ‘At Risk’ Patient Populations and Potential Drug Interactions,” *Marshall J Med*, vol. 2, no. 1, p. 11, doi: 10.18590/mjm.2016.vol2.iss1.11.

[183] U. Grober and K. Kisters, “Influence of drugs on vitamin D and calcium metabolism,” *Dermato-Endocrinology*, vol. 4, no. 2. pp. 158–166, Apr. 2012. doi: 10.4161/derm.20731.

[184] B. H. Ng, and K. H. Yuen, “Determination of plasma testosterone using a simple liquid chromatographic method,” *Journal of Chromatography B: Analytical Technologies in*

the Biomedical and Life Sciences, vol. 793, no. 2, pp. 421–426, Aug. 2003, doi: 10.1016/S1570-0232(03)00326-X.

[185] T. Yamasaki, S. Izumi, H. Ide, and Y. Ohyama, "Identification of a novel rat microsomal vitamin D3 25-hydroxylase," *Journal of Biological Chemistry*, vol. 279, no. 22, pp. 22848–22856, May 2004, doi: 10.1074/jbc.M311346200.

[186] R. C. Tuckey, E. K. Y. Tang, S. R. Maresse, and D. S. Delaney, "Catalytic properties of 25-hydroxyvitamin D3 3-epimerase in rat and human liver microsomes," *Archives of Biochemistry and Biophysics*, vol. 666, pp. 16–21, May 2019, doi: 10.1016/j.abb.2019.03.010.

[187] J. M. T. Wong, P. A. Malec, O. S. Mabrouk, J. Ro, M. Dus, and R. T. Kennedy, "Benzoyl chloride derivatization with liquid chromatography-mass spectrometry for targeted metabolomics of neurochemicals in biological samples," *Journal of Chromatography A*, vol. 1446, pp. 78–90, May 2016, doi: 10.1016/j.chroma.2016.04.006.

[188] R. Shinkyo, T. Sakaki, M. Kamakura, M. Ohta, and K. Inouye, "Metabolism of vitamin D by human microsomal CYP2R1," *Biochemical and Biophysical Research Communications*, vol. 324, no. 1, pp. 451–457, Nov. 2004, doi: 10.1016/j.bbrc.2004.09.073.

[189] C. Robertson, R. A. Lucas, and A. le Gresley, "Scope and limitations of nuclear magnetic resonance techniques for characterisation and quantitation of vitamin D in complex mixtures," *Skin Research and Technology*, vol. 26, no. 1, pp. 112–120, Jan. 2020, doi: 10.1111/srt.12773.

[190] L. Hymoller, and S. K. Jensen, "Vitamin D analysis in plasma by high performance liquid chromatography (HPLC) with C30 reversed phase column and UV detection - Easy and acetonitrile-free," *Journal of Chromatography A*, vol. 1218, no. 14, pp. 1835–1841, Apr. 2011, doi: 10.1016/j.chroma.2011.02.004.

[191] P. Zakeri-Milani, M. Nemati, S. Ghanbarzadeh, H. Hamishehkar, and H. Valizadeh, "Fasted state bioavailability of two delayed release formulations of divalproex sodium in healthy Iranian volunteers," *Randomized Controlled Trial*, vol. 61, no. 8, pp. 439043, 2011, doi: 10.1055/s-0031-1296225.

[192] E. Souri, H. Jalalizadeh, and S. Saremi, “Development and Validation of a Simple and Rapid HPLC method for determination of pioglitazone in human plasma and its application to a pharmacokinetic study,” *Journal of Chromatographic Science*, vol. 46, no. 9, pp. 809-12, Oct. 2008, doi: 10.1093/chromsci/46.9.809.

[193] J. Bhatt, A. Jangid, G. Venkatesh, G. Subbaiah, and S. Singh, “Liquid chromatography-tandem mass spectrometry (LC-MS-MS) method for simultaneous determination of venlafaxine and its active metabolite O-desmethyl venlafaxine in human plasma,” *Journal of Chromatography B: Analytical Technologies in the Biomedical and Life Sciences*, vol. 829, no. 1–2, pp. 75–81, Dec. 2005, doi: 10.1016/j.jchromb.2005.09.034.

[194] R. C. Tuckey, C. Y. S. Cheng, and A. T. Slominski, “The serum vitamin D metabolome: What we know and what is still to discover,” *Journal of Steroid Biochemistry and Molecular Biology*, vol. 186. Elsevier Ltd, pp. 4–21, Feb. 2019. doi: 10.1016/j.jsbmb.2018.09.003.

[195] J. Luque-Garcıa and L. de Castró, “Extraction of fat-soluble vitamins,” *Journal of Chromatography. A*, vol. 935, no. 1-2, pp. 3-11. Nov. 2001, doi: 10.1016/s0021-9673(01)01118-9.

[196] B. Widner, M. C. Kido Soule, F. X. Ferrer-González, M. A. Moran, and E. B. Kujawinski, “Quantification of Amine- And Alcohol-Containing Metabolites in Saline Samples Using Pre-Extraction Benzoyl Chloride Derivatization and Ultrahigh Performance Liquid Chromatography Tandem Mass Spectrometry (UHPLC MS/MS),” *Analytical Chemistry*, vol. 93, no. 11, pp. 4809–4817, Mar. 2021, doi: 10.1021/acs.analchem.0c03769.

[197] I. Shah, R. James, J. Barker, A. Petroczi, and D. P. Naughton, “Misleading measures in Vitamin D analysis: A novel LC-MS/MS assay to account for epimers and isobars,” *Nutrition Journal*, vol. 10, no. 1, 2011, doi: 10.1186/1475-2891-10-46.

[198] S. Zelzer, W. Goessler, and M. Herrmann, “Measurement of vitamin D metabolites by mass spectrometry, an analytical challenge,” *Journal of Laboratory and Precision Medicine*, vol. 3, pp. 99–99, Dec. 2018, doi: 10.21037/jlpm.2018.11.06.

[199] C. J. Hedman, D. A. Wiebe, S. Dey, J. Plath, J. W. Kemnitz, and T. E. Ziegler, “Development of a sensitive LC/MS/MS method for vitamin D metabolites: 1,25 Dihydroxyvitamin D2&3 measurement using a novel derivatization agent,” *Journal of Chromatography B: Analytical Technologies in the Biomedical and Life Sciences*, vol. 953–954, no. 1, pp. 62–67, Mar. 2014, doi: 10.1016/j.jchromb.2014.01.045. [200]

[202] R. Sabourian, S. Z. Mirjalili, N. Namini, F. Chavoshy, M. Hajimahmoodi, and M. Safavi, “HPLC methods for quantifying anticancer drugs in human samples: A systematic review,” *Analytical Biochemistry*, vol. 610. Academic Press Inc., Dec. 2020, doi: 10.1016/j.ab.2020.113891.

[201] T. D. Bjornsson, J. T. Callaghan, H. J. Einolf, V. Ficher, L. Gan, S. Grimm, J. Kao, S. P. King, G. Miwa, L. Ni, G. Kumar, J. McLeod, S. R. Obach, S. Roberts, A. Roe, A. Shah, F. Snikeris, J. T. Sullivan, D. Tweedie, J. M. Vega, J. Wash, and S. A. Wrighton, “The conduct of in vitro and in vivo drug-drug interaction studies: A PhRMA perspective,” *Journal of Clinical Pharmacology*, vol. 43, no. 5. SAGE Publications Inc., pp. 443–469, May. 2003, doi: 10.1177/0091270003252519.